U.S. DEPARTMENT OF COMMERCE
National Oceanic and Atmospheric Administration
Environmental Research Laboratories

NOAA Technical Memorandum ERL NSSL-54

MODEL OF PRECIPITATION AND VERTICAL AIR CURRENTS

Edwin Kessler
William C. Bumgarner

National Severe Storms Laboratory
Norman, Oklahoma
June 1971

TABLE OF CONTENTS

TABLE OF CONTENTS (Cont'd.)

LIST OF FIGURES

LIST OF FIGURES (Cont'd.)

LIST OF FIGURES (Cont'd.)

LIST OF TABLES

LIST OF PRINCIPAL SYMBOLS

$\mathcal{A}$ - acceleration identified with the thermal component of buoyancy (m/sec^2).

A - total acceleration identified with buoyancy.

D - diameter of an updraft column; raindrop diameter.

D_c - diameter of an updraft column, at the threshold of sustained convection.

F_1 - parameter proportional to the condensation rate (evaporation rate) in a rising (descending) air column; unity when the air column is cloudy at all altitudes.

G - condensation function, usually represented by C_4+C_5z.

H - assumed height of an updraft or downdraft column.

k_5 - assumed mixing rate for heat, momentum, and water substance associated with mixing in the horizontal plane.

k_6 - coefficient that converts the evaporation rate to a rate of buoyancy change [$k_6 \approx 0.1 (m/sec^2)/(gm\ H_2O/m^3)$].

k_7 - see ρ below.

k_8 - coefficient that converts condensed water to an equivalent buoyancy [$k_8 \approx 0.01 (m/sec^2)/(gm/m^3)$].

$\mathcal{L}$ - average density of <u>condensate</u> in the vertical column of depth H ($\mathcal{L}=\overline{M+m}$).

m - when positive, the cloud content; when negative, the saturation deficit.

m_o,
m(z,o) - environmental moisture.

M - precipitation content of air.

N_o - precipitation particle size-distribution parameter.

ρ - air density often enters as a vertical logarithimic gradient taken as a constant ($k_7 = -\partial \ln\rho/\partial z$).

LIST OF PRINCIPAL SYMBOLS (Contd.)

S_d - average thermal buoyancy approached as a dry air column sinks without mixing with its environment.

S_m - average thermal buoyancy approached as a moist air column rises without mixing with its environment.

t - time coordinate.

u - horizontal wind.

V - fall speed of precipitation relative to the air.

w - vertical wind.

z - vertical coordinate.

MODEL OF PRECIPITATION AND VERTICAL AIR CURRENTS

Edwin Kessler and William C. Bumgarner

ABSTRACT

Time-dependent moist columnar convection is numerically modelled as an extension of Priestley's 1953 study of buoyant dry elements in a turbulent environment. Solutions are given of simultaneous equations for the vertical velocity, buoyancy, and cloud and precipitation content, in an air column moving under buoyancy and subject to continuous mixing of heat, momentum and moisture at a constant rate with its stationary environment. Thus, an upward acceleration of air tends to be reduced by thermal diffusion and exchange of momentum with the ambient quiet atmosphere, but tends to be increased by the release of latent heat of condensation. When the cloud content exceeds a prescribed threshold, a parametized autoconversion process produces some precipitation which is subsequently augmented by collection of cloud. The weight of condensation products, the cooling by evaporation of cloud in entrained unsaturated air, and the cooling that accompanies evaporation of precipitation in the subcloud layer, all tend to produce negative buoyancy.

The distinctive velocity regimes characteristic of the model and akin to those discussed by Priestley, may be classified in terms of environmental lapse rate, moisture content, and the size and amplitude of the initiating and following disturbance. Damped Brunt-Vaisala oscillations occur in a stable dry atmosphere, or in a conditionally unstable, moderately moist atmosphere when the starting perturbation is weak. A stronger perturbation or more moisture produces cloud and precipitation, followed by a shower and downdraft, and then by damped B-V oscillations. Weak static instability is associated with sustained updrafts if the mixing rate is sufficiently small, but for mixing rates above a threshold that depends on the environmental lapse rate and moisture content, the starting perturbation and resultant updraft are restored asymptotically to zero.

Several types of conditions develop in conditionally unstable cases: a strong steady updraft may develop without precipitation beneath but with precipitation outside an implied area of strong updraft, when there is a strong starting perturbation, small mixing rate, an elevated condensation level, and a steep lapse rate. If these conditions are insufficiently pronounced, however, steady updrafts ultimately present in the model may be only moderate or weak, with precipitation beneath; or damped condensation oscillations or B-V oscillations may preface restoration of the disturbed model atmosphere to zero motion in conditionally unstable cases. Great changes of the solutions, from one type to another, occur as one or more of the controlling parameters cross thresholds determined by values of the other parameters.

The model suggests that a critical horizontal size and critical perturbation buoyancy must be exceeded in nature if sustained moist convection is to result in any given conditionally unstable lapse rate and moisture condition. A suggested upper bound to updraft diameter is identified with a critical Layer Richardson Number in the associated horizontal, vertically shearing flow. The diurnal variation of energy-absorbing boundary-layer qualities is discussed in relation to the geographical and diurnal variability of thunderstorms, and a number of studies are suggested to evaluate and improve the theory.

NOTE

The moist instability parameter, S_m, for a typical summer troposphere is about 0.8 m/sec^2 when the lapse rate is dry adiabatic rather than 0.4 m/sec^2 as indicated on pages 9 and 38 and elsewhere. The latter value applies to a cooler atmosphere and should be used with a condensation function of smaller magnitude than is employed here. Some revisions are therefore indicated, but essential features of this paper are uneffected by the corresponding adjustments of numerical values. The authors thank Mr. Pieter Feteris for discovering this error.

MODEL OF PRECIPITATION AND VERTICAL AIR CURRENTS[1]

Edwin Kessler and William Bumgarner

1. INTRODUCTION

This study of a vertical, time-dependent, relatively simple numerical model of atmospheric moist convection represents an attempt to gain an appreciation of probable working relationships among important parameters. We here use much of the approach of Priestley (1953), who considered the motion and temperature of a parcel of dry air moving under its own buoyancy, and subject to the turbulent transfer of heat and momentum with an unchanging environment at rest. The three modes of motion he derived depend largely on the scale of motion and not at all on the amplitude of an initiating disturbance. In his asymptotic mode, the scale of motion is small, and the mixing rates for heat and momentum are correspondingly large, and an initiating disturbance is damped even though the lapse rate is unstable. Related results for fluid motions controlled by molecular conduction and viscosity were first discussed by Rayleigh (1916). The other modes treated by Priestley are oscillatory with stable lapse rates, and absolute buoyancy with sufficiently unstable lapse rates and small mixing rates. The remarkable natural phenomenology, which we are seeking to model numerically, has been lucidly discussed by Scorer and Ludlam (1953), and by Ludlam (1963), among others.

Our model uses continuity equations for air and water substance with an equation, somewhat similar to one of Priestley's, that describes the variation of vertical air velocity in terms of thermal buoyancy, the load of condensation products, and entrainment of stationary environmental air. Another equation, analogous to another of Priestley's, relates variations of thermal buoyancy to vertical velocity, to the lapse rate and moisture content of the environment, and to the heat transferred during condensation or evaporation of cloud and precipitation. Our model may be regarded as an extension of Priestley's study to moist conditionally unstable cases, and in such cases, the amplitude of an initiating

---

[1]Developed version of a paper first presented at the International Meteorological Conference at Tel Aviv, Israel, Nov. 30 - Dec. 4, 1970.

disturbance appears as an important determinant of the form of following events.

The use of a fixed profile of vertical velocity, vertical averaging where practical, and of approximate representations of some rather complex processes, produces relatively simple equations and facilitates comprehension while emphasizing some gross aspects of model atmosphere behavior. The solutions explicitly refer to conditions in vertical columns, but an application of the Richardson Number with constraints joining horizontal to vertical velocities provides a basis for estimating relationships between dimensional and distributional features of cellular atmospheric convection and environmental parameters. These proposed relationships suggest forecasting rules, and observational projects to test and improve the theory.

2. MODELLING EQUATIONS

The conservation and continuity of water substance in a vertical column are given by

$$\frac{\partial M}{\partial t} = -(V+w)\frac{\partial M}{\partial z} - M\frac{\partial V}{\partial z} - Mw\frac{\partial \ln \rho}{\partial z} + AC + CC - EP - k_5 M, \qquad (1)$$

$$\frac{\partial m}{\partial t} = -w\frac{\partial m}{\partial z} + wG + mw\frac{\partial \ln \rho}{\partial z} - AC - CC + EP - k_5(m-m_o) \ . \qquad (2)$$

Here M, always positive or zero, is the precipitation content of air; m when positive is the cloud content, and when negative is the saturation deficit; V, always a negative quantity, represents the terminal velocity of precipitation relative to the air; w is the vertical velocity of air, ρ is the air density, and G is a condensation function. The terms on the right-hand side of the precipitation equation model, in order, the vertical advection of precipitation, an effect of the divergence of the precipitation fall speed, an effect of the compressibility of air, the spontaneous creation of precipitation from cloud (autoconversion, AC), the growth of precipitation by collection of cloud (CC), the evaporation of precipitation in dry air (EP)[2], and the depletion of cloud and

[2]As shown in table 1, the term AC is applied only where m exceeds the autoconversion threshold a, usually 1 gm/m^3; the term CC is applied only where m is positive, i.e., where there is cloud; and the term EP is applied only where m is negative, i.e., where the air is not saturated.

Table 1. Mathematical Models of Microphysical Parameters.

Microphysical Process or Parameter	Mathematical Representation
Condensation and evaporation of cloud ($gm\ m^{-3}\ sec^{-1}$)	$wG = \frac{4w_{max}}{H}\left(z - \frac{z^2}{H}\right)(C_4 + C_5 z)$
Drop-size distribution parameter (m^{-4})	N_o
Autoconversion of cloud, AC ($gm\ m^{-3}\ sec^{-1}$)	$k_1(m-a)$ (for $m>a$ only)
Collection of cloud, CC	$k_2 E N_o^{.125} m M^{.875} \exp(k_7 z/2)$ (for $m>0$ only)
Evaporation of precipitation EP ($gm\ m^{-3}\ sec^{-1}$)	$k_3 N_o^{.35} m M^{.65}$ (for $m<0$ only)
Terminal velocity of precipitation ($m\ sec^{-1}$)	$V = -38.8 N_o^{-.125} M^{.125} \exp(k_7 z/2)$

Main Factors Used in This Study
(m-g-s units)

$H = 10^4$	$N_o = 10^7$	$k_1 = 10^{-4}$
$C_4 = 3 \times 10^{-3}$	$a = 1$	$k_2 = 6.96 \times 10^{-4}$
$C_5 = -3 \times 10^{-7}$	$E = 1$	$k_3 = 1.93 \times 10^{-6}$
		$k_7 = 10^{-4}$ ($k_7 = -\partial \ln\rho/\partial z$)

precipitation through a mixing of cloudy air with environmental air whose saturation deficit is given by m_o. Details of the terms in (1) and (2) that account for microphysical processes are given in table 1.

Equations (1) and (2) define the distributions of vapor, cloud, and precipitation density when microphysical parameters and the vertical profile of the vertical air velocity are given. The derivation of these equations and the nature of their solutions have been discussed in depth by Kessler (1969).

The components of a model for the vertical velocity in 1-dimensional space have, so far, always involved several rather arbitrary features (Warner, 1970), partly because some important characteristics of cloud behavior are still not well understood, and because there is no proper basis for introducing the regulatory dynamic pressure without an explicit treatment of the columnar environment. In the models of Das (1964), Srivastava (1967), and Weinstein (1970), in a column of assumed height, the vertical velocity everywhere approximates a simple response to advection of vertical velocity and to the resultant of forces identified with local thermal buoyancy, water load, and drag or entrainment. We have chosen to simplify our problem by assuming that the vertical velocity has a parabolic vertical profile, and that its tendency is determined by an average value of buoyancy and other forces in the column of interest.

This approach contrasts also with jet models of Mason and Emig (1961) and of Squires and Turner (1962), and as well with the bubble model described by Scorer and Ludlam (1953), treated as a marching problem by Simpson and Wiggert (1969).[3]

We write not of the growth of a cloud tower, but more of the development of an average condition. Thus, we assume that

$$w = \frac{4w_{max}}{H}\left(z - \frac{z^2}{H}\right) , \tag{3}$$

[3]This is obviously not a comprehensive review of other's treatments of moist convection but the reader may also wish to refer to the two-dimensional moist models of Arnason, et al., (1969), Murray (1971), Orville (1971), and Takeda (1971).

and

$$\frac{\partial \bar{w}}{\partial t} = \frac{2}{3} \frac{\partial w_{max}}{\partial t} = (A-k_8L) - \frac{|A-k_8L|^{\frac{1}{2}}}{H^{\frac{1}{2}}} w_{max} - k_5\bar{w} ,$$

i.e.,

$$\frac{\partial w_{max}}{\partial t} = 1.5\left[A-k_8L - \frac{|A-k_8L|^{\frac{1}{2}}}{H^{\frac{1}{2}}} w_{max}\right] - k_5 w_{max} . \tag{4a}$$

Here H, 10^4m in this paper, is the assumed height of the updraft column (or downdraft column, when w_{max} is negative), A is the average acceleration associated with thermal buoyancy[4], in an implied upper or lower half layer of depth H/2, L is the average density of cloud plus precipitation in the vertical column, and $k_8=0.01 \approx g/\rho$ is a factor to convert L to an equivalent acceleration.

The coefficient k_5, , held constant over the model cloud lifetime in the present treatment, has been called the mixing rate by Priestley (1953). While we recognize that the mixing rate, in nature, certainly varies in both space and time, and is partly self-determined during the evolution of a cloud or storm, we look here for insight from the calculated behavior of updraft columns whose uniform mixing rate is prescribed. The reader may consult more comprehensive discussions on this important matter by Priestley (1953), by Scorer and Ludlam (1953), and by Turner (1963), who has provided a model whose solution, including element size, is related to an assigned turbulent velocity in the surroundings.

While (4a) makes an allowance for the presence of condensate, it also differs from Priestley's similar equation in the presence of the second term on the right-hand side. This somewhat simulates drag, but its essential effect is to make the value of w_{max} always drift toward that attained by an air parcel at z=H/2 following its upward (downward) drift from z=0 (z=H) according to the equation

$$\frac{dw}{dt} = A - k_5 w, \tag{4b}$$

---

[4] In customary notation, $A = \frac{T-T_o}{T} g \approx \frac{T'}{T} g$. The shape of the vertical profile implies that oppositely directed forces act in the upper and lower parts of the buoyant column. This shape also crudely simulates the role of the stratosphere and lower solid boundary, respectively.

where A = $\mathcal{A}-k_8\mathcal{L}$. When drag is absent, the e-folding time in (4a) is $[H/(\mathcal{A}-k_8\mathcal{L}]^{\frac{1}{2}}$, just the time required for a parcel to ascend from 0 to H/2 under the acceleration $\mathcal{A}-k_8\mathcal{L}$. When $k_5=0$, the reader can easily verify that both (4a) and (4b) assign the value $w(H/2)=(|A|H)^{\frac{1}{2}}x(\text{sign } A)$ to w_{max} under steady state conditions. When k_5 is as large as 10^{-3} sec^{-1}, the steady state values defined by (4a) and illustrated in figure 1, may be the lower by about 10 percent in practical cases. Finally, in this connection, we observe that the magnitude of $\mathcal{L}$ in (4a) must be given by solutions of (1) and (2) and that another equation is required to define $\mathcal{A}$ in (4a).

A thermal buoyancy force develops as an air parcel is displaced from its equilibrium level in an atmosphere not neutrally stratified. In the case of continuing rising motion in a column extending upward from the surface, the entire column would eventually be composed of parcels originating near the

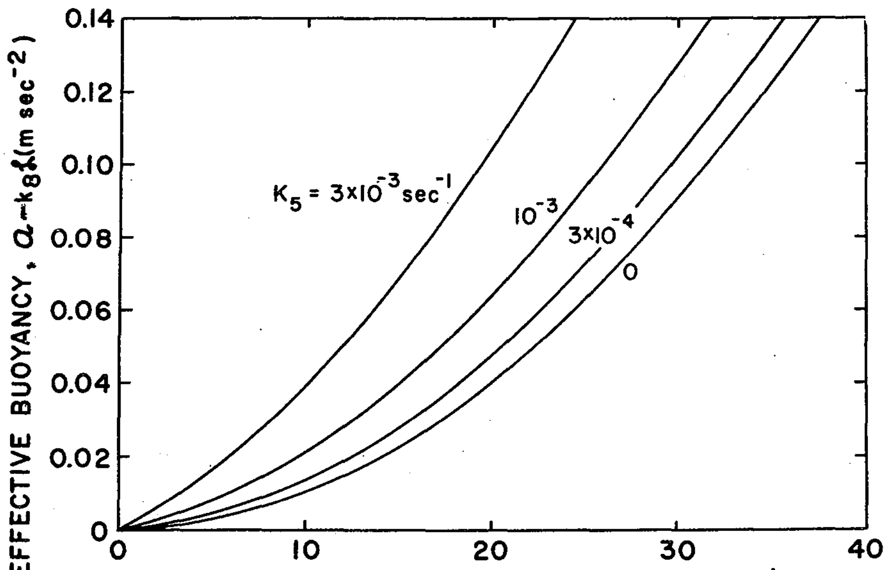

Figure 1. Steady state maxima of vertical velocity in relation to effective buoyancy, as defined by equation (4a) in the text, for several values of the momentum mixing rate k_5, and a height of the updraft column equal to 10^4m.

surface, and modified by processes of precipitation development and entrainment during ascent. An analogous statement applies to continuing descent of air with the downdraft originating near a great height H. The magnitude of thermal buoyancy developed depends on the environmental lapse rate, the gain of latent heat during condensation, the loss of sensible heat during evaporation of mixed cloud, and the dilution of buoyancy that accompanies mixing of air in the convective column with outside air. The assumption embodied in (3) is consistent with the simple implicit representation of these processes in the following equation:

$$\frac{\partial A}{\partial t} = \frac{w_{max}}{H} \left[F_1 S_m - (1-F_1)\, S_d - A \times \mathrm{sign}\, w\right] - k_5 A - k_6 \left\{ \varepsilon_M - k_5 \frac{1}{n} \sum_{m<0} [m(z,0)] \right\} . \qquad (5)$$

In (5), F_1 is the fraction of grid points where cloud exists ($m>0$), weighted according to their relative contribution to the condensation rate.[5] Thus, in completely cloudy rising air, $F_1=1$ and the bracketed term with its coefficient tends to cause the buoyancy to drift (with an e-folding time of w_{max}/H) toward S_m, a parameter that depends on the static stability in the environment. S_m is the acceleration identified with the average temperature difference between the environmental sounding and the temperature profile associated with moist adiabatic ascent of saturated surface air; S_m is positive when the lapse rate exceeds the moist adiabatic rate.

Examination of typical soundings in tropical atmospheres, or in a summer atmosphere in the temperate zones, suggests that $S_m=0.4$ m/sec^2 (corresponding to an average temperature excess of about 10C) is a representative value for moist ascent through an environment (of typical tropospheric depth) with a dry adiabatic lapse rate. Since, with downward saturated motion, the bracketed expression tends to cause A to approach $-S_m$, the tendency of the bracketed term in unstable moist air is to amplify weak velocities of either sign.

S_d is also positive in a conditionally unstable atmosphere. It is the value of thermal buoyancy approached during dry descending motion, with dry ascending motion causing the thermal buoyancy to drift toward $-S_d$. Thus, the bracketed term on the right-hand side of (5) simulates restoring forces during

---

[5]See Appendix A.

upward or downward motion of dry air in a conditionally unstable atmosphere.

S_m and S_d are always chosen so that their sum is 0.4 m/sec^2; this corresponds to a condition of the summer troposphere. When both are 0.2, for example, the implied tropospheric lapse rate is midway between moist and dry adiabatic values. During marching calculations, S_m is reduced slightly and S_d is correspondingly increased, when the subcloud layer is moistened by evaporation of precipitation. This feature, detailed in Appendix B, accounts for a loss of average buoyancy owing to sensible cooling of the subcloud layer.

The term $-k_5 A$ represents the dilution of thermal buoyancy, owing to mixing with the environment; we have chosen the same mixing rate for heat as for momentum at this stage of the investigation.[6]

The last two terms in brackets account for cooling effects of evaporation. The average rate of evaporation of precipitation, ε_M, is calculated from grid-point values of the term EP in (1) and (2). The evaporation of precipitation is effective only in unsaturated air.

The second term within the last brackets represents the rate of cloud evaporation, calculated where m<0 and averaged over the depth H. This term can be understood when compared with an equation that represents both dilution and evaporation of cloud. Thus, at any point, we have entrainment's contribution to depletion represented in (1) as

$$\frac{\delta m(z,t)}{\delta t} = - k_5 [m(z,t) - m(z,0)] \quad , \tag{6}$$

where m(z,0) is the initial and ambient condition in the model. The term, $-k_5 m(z,t)$, represents the mixing of cloud with saturated cloud-free air, and the term, $k_5 m(z,0)$, obviously represents the added contribution to depletion that occurs because of evaporation in unsaturated entrained air (where m is negative).

---

[6] In his 1953 paper, Priestley discusses solutions with unequal mixing rates for heat and momentum.

The coefficient, $k_6 \approx .1 (m/sec^2)/(gmH_2O/m^3)$, converts the rate of evaporation to the equivalent rate of change of acceleration attributable to evaporative cooling.[7]

3. SOME ELEMENTARY PROPERTIES OF THE MODEL

Some properties of the mathematical model defined by (1) through (5) can be quickly learned by examination of simplified equations.

3.1 Steady State Relationships Among Updraft Speed, Condensed Water Load, and Buoyancy.

First we should know how the condensed water load, L, tends to vary with the updraft speed, w_{max}, and what values of A would tend to exist in the model with associated values of L and w_{max}. In order to develop this knowledge, we have solved steady state approximations to (1) and (2) by a Runge-Kutta method that can be used whenever $(w+V)$ is everywhere negative.[8] Vertically averaged precipitation and cloud content in relation to updraft speeds and values of k_5 are plotted in figure 2.

The rapid increase of water load with updraft speed indicated in figure 2 implies that in a moist atmosphere, the effective buoyancy and updraft should increase only slowly with increasing thermal component of buoyancy. In figure 3, for cases with $k_5=0$, we show explicitly how w_{max} depends on the thermal component of buoyancy in a dry model atmosphere and in a saturated updraft model whose condensed moisture content is illustrated in figure 2. It is evident that in

---

[7] $k_6 = Lg/C_p T\rho$, where L is the latent heat of evaporation, C_p is the specific heat at constant pressure, and ρ is the air density. A comparison of (4a) and (5) with Priestley's velocity and buoyancy equations is given in App. C.

[8] Of course, this problem can be solved under more general conditions with marching calculations continued until a steady state is reached -- then the complete eqs. (1), (2), and (3), with w_{max} fixed can be used. The steady state conditions are closely approached after the longer of the times H/w_{max} and $H/(v+w_{max})$. See Kessler (1969, pp. 72 and 80).

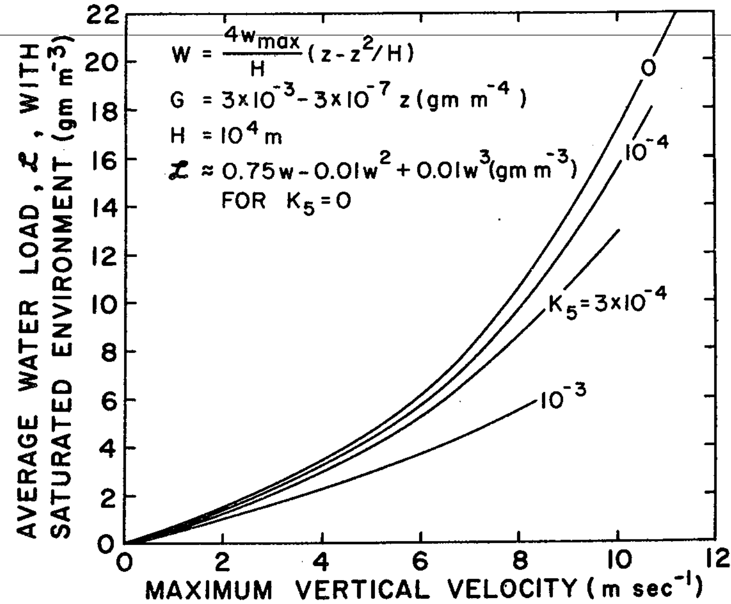

Figure 2. Average density of cloud + precipitation in a vertical column 10 km high, in relation to the maximum vertical air speed and mixing rate k_5. The diagram applies to steady state conditions in saturated model updraft columns in saturated environments.

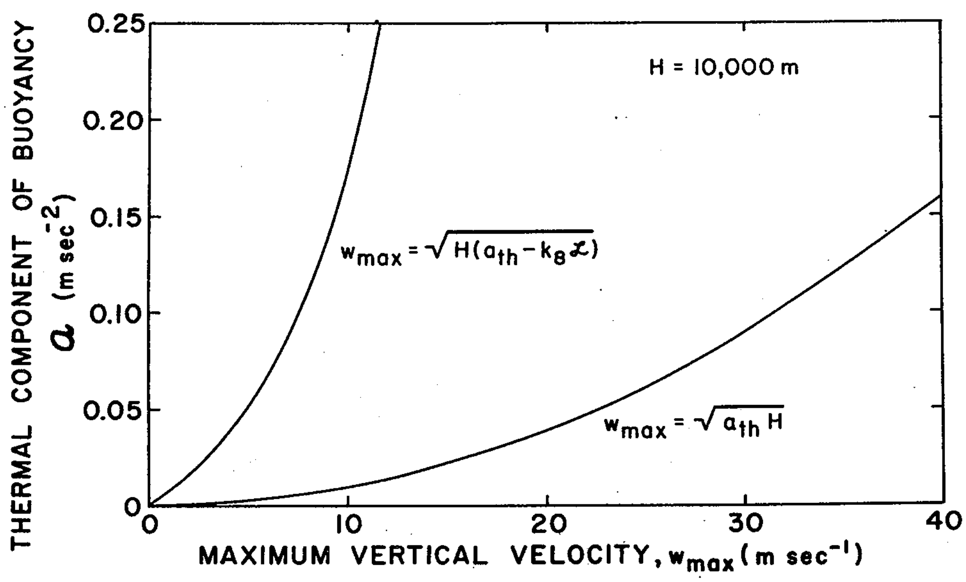

Figure 3. Thermal component of buoyancy in relation to steady maximum vertical velocity in moist and dry atmospheres with no mixing.

the moist case, additional buoyancy is utilized in supporting a relatively large increase in condensation products accompanying a relatively small increase in updraft speed.

It is very important to note that in a model atmosphere with an elevated condensation level, there are two families of solutions accompanying strong updrafts. In one of these the condensed water load is essentially independent of the updraft speed, and neither precipitation nor cloud extend to the ground beneath the updraft column. This family is represented by the dashed lines in figure 4, applicable to an updraft column 6 km high. In these cases, the model average water load is well defined by the height of the condensation level, with the average temperature or condensation function G, and the mixing rate k_5.

3.2 Some Properties of the Buoyancy Equation

It is immediately obvious that the primary control of vertical velocity and hydrometeor development resides in the buoyancy equation, (5).

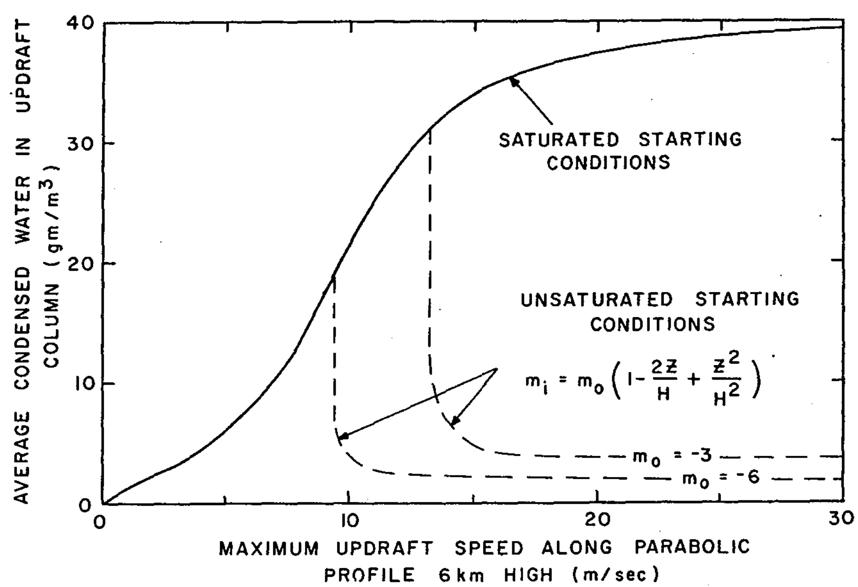

Figure 4. Vertically averaged steady state condensed water content in relation to maximum updraft speed and initial (ambient) moisture profile, without horizontal mixing (from Kessler, 1969, p. 71).

Inspection of (5) shows that there is only one source for buoyancy increases in a conditionally unstable atmosphere, viz., rising motion of cloudy air. Momentum mixing reduces buoyant effects and evaporation of cloud contributes to negative buoyancy, and both of the processes are independent of the updraft speed in this model. It is apparent then that buoyancy can be sustained in cloudy air only if the vertical velocity and associated condensation rate exceed some threshold. A similar conclusion may be surmised from consideration of our mixing law and Austin's work (1951), which shows how much colder than its dry environment initially cloudy air becomes as it mixes with environmental air and as the cloud evaporates.

We now explore the associations among k_5, S_m, w_{max}, and m_o, which determine whether the thermal buoyancy A increases, decreases, or remains steady. As a preliminary to numerical calculations based on the complete equations, we use the following simplified form of (5), applicable to rising cloudy air in an environment whose average saturation deficit is $\overline{m_0}$ (a negative quantity):

$$\frac{\partial A}{\partial t} = \frac{w_{max}}{H} (S_m - A) - k_5 A + 0.1 k_5 \overline{m_o} \quad . \tag{5a}$$

We supplement this with

$$A = \frac{w^2_{max}}{H} + k_8 L \quad , \tag{4c}$$

where the effects of mixing of momentum in the rising current are neglected. Relationships between L and w are of two kinds:

$$L = .75 w_{max} - .01 w^2_{max} + .01 w^3_{max} \quad , \tag{7a}$$

$$L = 5 \tag{7b}$$

The first corresponds to a curve shown in figure 2, and the second is a rough approximation for high-speed updraft cases such as illustrated by dashed lines in figure 4 (Kessler, 1969)

Although there are inconsistencies in this treatment, they are not large enough to deceive us with respect to implications of the solutions of (5a) illustrated in figures 5 and 6. For parameter values specified by a plotted curve in these figures, $\partial A/\partial t > 0$ in the region bounded by the curve and the ordinate $\overline{m_o} = 0$; $\partial A/\partial t = 0$ along a curve, and is negative to its left. This means of course, that the steady condition that is implicit in our use of (4c) is consistent with this analysis only along the curves.

In figure 5, where the model environmental lapse rate is everywhere midway between dry and moist adiabatic values, consider environmental moisture $\overline{m}_o = -10$. With an average condensed water load of 5 gm/m^3, the thermal buoyancy identified with the updraft velocity and water load alone, would decrease with time owing to effects of diffusion of buoyancy and evaporation of cloud, unless condensation were produced in an updraft column whose maximum were 7 m/sec or more. If the updraft were a little stronger than 7 m/sec, $\partial A/\partial t$ would be positive, and both A and w_{max} would increase until the speed of about 34 m/sec were attained. Thus, with other parameters fixed, the magnitude of the initiating disturbance in this conditionally unstable case determines whether the subsequent airflow will decline (as a damped oscillation) or become the steady updraft condition analogous to Priestley's absolute buoyancy.

The curves for various values of k_5 may be related to the horizontal dimension of disturbances (see sec. 5) and they reflect the storage of latent instability in a conditionally unstable atmosphere. They suggest that stronger amplitudes are required with smaller scale disturbances to produce persistent updrafts in conditionally unstable cases. For a specified environmental lapse rate, stronger amplitudes of an initiating disturbance are also required in drier atmospheres. The curves also indicate that for each condition of environmental moisture and lapse rate, there is a size of disturbance below which no perturbation, however large, can produce a persistent updraft.

In figure 6, the plots are for various values of the lapse rate, with the mixing rate or size of the disturbance held constant. These lead also to inferences like those discussed above, and support the concept that the amplitude of disturbances necessary for sustained convection should increase as the lapse rate stabilizes.

We should note that the role of the amplitude of an initiating disturbance as a strong determinant of the form of following events, is a feature peculiar to the conditionally unstable cases. In cases of absolute stability ($\gamma > \gamma_m$) or instability ($\gamma < \gamma_d$), the form of the model solution after a long time depends only on the scale of the phenomenon, and

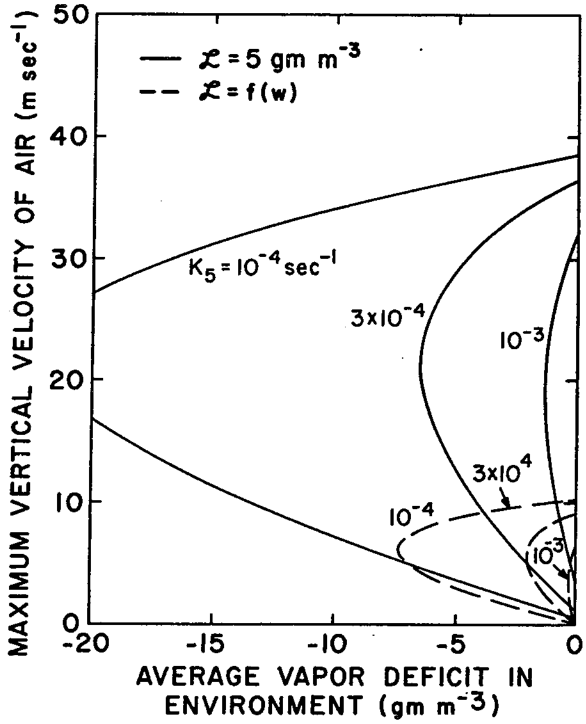

Figure 5. Loci of $\partial A/\partial t=0$ in relation to mixing rate, the speed of rising air currents, and environmental moisture, with effects of evaporation of precipitation neglected. The family of curves for L=5 simulates the cases of high speed updrafts without precipitation beneath; the other simulates updrafts with precipitation at the ground and correspondingly large water loads. The lapse rate in the model environment is midway between moist- and dry-adiabatic values.

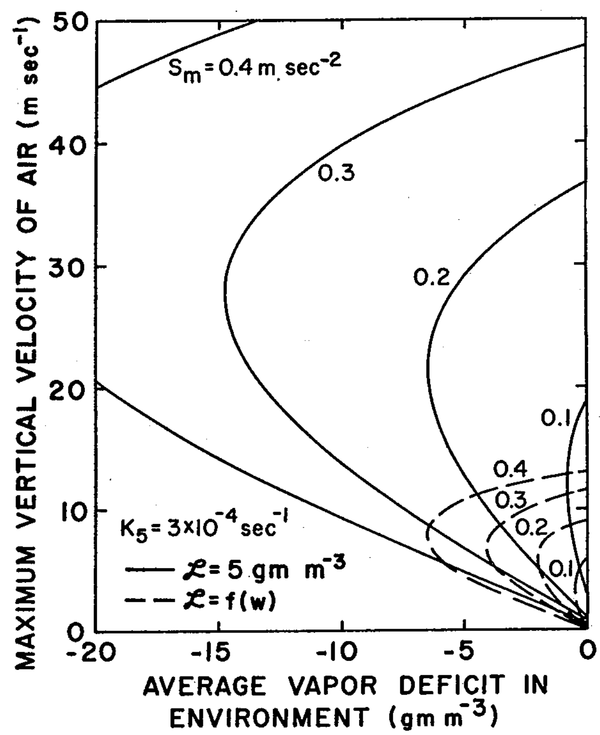

Figure 6. Loci of $\partial A/\partial t=0$ in relation to environmental lapse rate, the speed of rising currents and environment moisture. The mixing rate is $3\text{x}10^{-4}$ sec^{-1} in all cases. S_m=0.4 m/sec represents a dry adiabatic lapse rate in the environment and S_m=0 represents a moist adiabatic lapse rate.

the amplitude of an initiating disturbance, as discussed by Priestley.[9]

Of course, forecasters have long thought that strong disturbances, e.g., cold fronts, have an important role in the initiation of local storms, so this is not a new concept. It is also embodied in others' numerical models. For example, Squire's and Turner's model updraft (1962) is sustained only when the upward flux of air at cloud base exceeds a critical threshold.

We should bear in mind that these results are rather critically dependent on the form of the mixing law incorporated into the models. Eventually, we must have models in which the mixing rate is a dependent parameter.

3.3 Relationships Among Updraft, Water Load and Rainfall Rate During Updraft Oscillations

We now turn to fundamental properties of the oscillations involving updraft, condensed water load, and rainfall rate. Byers and Braham (1949) discussed such oscillations in terms of observational data gathered during the Thunderstorm Project, and solutions of various numerical models have since included such oscillations. Kessler (1969, pp. 72-73) obtained condensation oscillations as solutions to a simple analytic model based on inferences from his kinematic study. When such oscillations occur, their approximate period may be

$$T = 2\pi/\left(k_8 G - \frac{(k_5 - C_3)^2}{4}\right)^{\frac{1}{2}}, \tag{8}$$

where C_3 has the magnitude $|V/H|$ or about 10^{-3}. We must note that these condensation oscillations do not occur in the model when the water load is independent of the updraft speed. Such independence may occur with high-speed updrafts and an elevated condensation level (see fig. 4), and the updraft then monotonically approaches a positive value representing equilibrium among forces of buoyancy, water load, and drag.

In the present numerical context, we first examine the coupled oscillations with $k_5 = 0$, with (1), (2), and (3)

---

9 This statement may be modified for a narrow range of unlikely moist cases in which $\gamma<\gamma_d$ and the mixing rate is large.

otherwise unchanged, and with (4) and (5) simplified as below:

$$\frac{\partial w_{max}}{\partial t} = A - k_8 L \ , \quad A = \text{constant.}$$

With the simplest case of a saturated model atmosphere, the time variations of w_{max}, surface rainfall rate R_o, and L for the case where $A=.04 m/sec^2$, are shown in figure 7. The average period of 1650 sec, shown in figure 7, is very close to that defined by (8).[10]

We may also note the excessive rainfall defined by these marching calculations. In light of earlier discussion, it is clear that our combinations of a very moist environment with substantial thermal buoyancy are unrealistic, since an indefinitely small perturbation would be amplified and sustained and heat would be transferred upward in a nearly saturated real atmosphere before the implied static instability becomes so large.

3.4 Role of Buoyancy in Updraft Oscillations

Figure 8 shows time variations of w_{max} for various values of A, with all other parameters held fixed. In accordance with the analytic theory, the periods and phases are practical unaffected by changes of A. For very large values of A, however, there is a phase shift associated with the nonlinear relationship between updraft speed and water storage. As the updraft speed tends to exceed about 10 m/sec, the locus of maximum water storage is displaced upward to the upper half of the convective column, whence a longer time is required for descent to the ground after the updraft decreases. The updraft speeds and average water loads (not shown) with each value of A are close to values along the uppermost curve in figure 2.

3.5 Magnitude of the Condensation Function in Relation to Updraft Oscillations

Figure 9 shows the effect of varying the condensation function in this simple numerical model. The period of condensation oscillations increases with $1/\sqrt{G}$, as indicated by

---

[10] With $k_8=10^{-2}$ and $G=1.5x10^{-3}$, (8) yields T=1636 sec when $k_5=0$ and $C_3=10^{-3}$. This agreement is at least partly fortuitous, because C_3 cannot be precisely related to the more general problem.

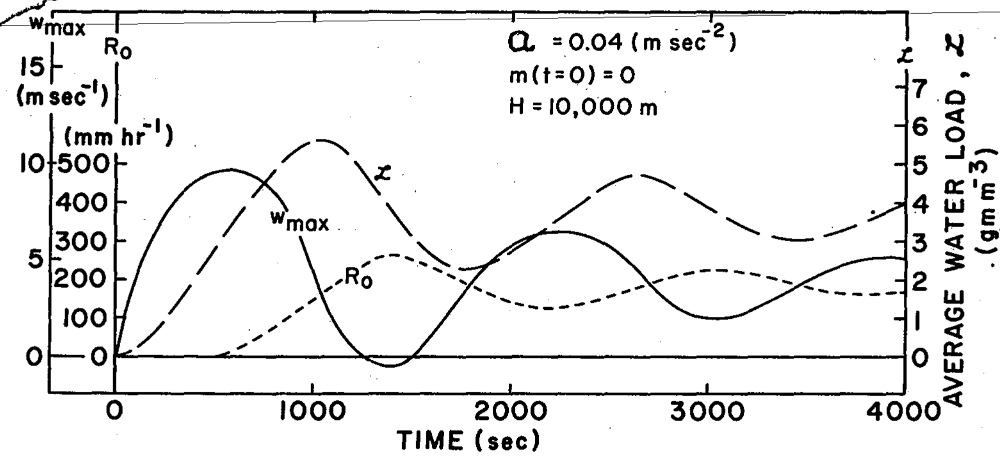

Figure 7. Mutually dependent oscillations of updraft speed, average water load, and precipitation rate, in a model saturated atmosphere with constant thermal buoyancy and no horizontal mixing.

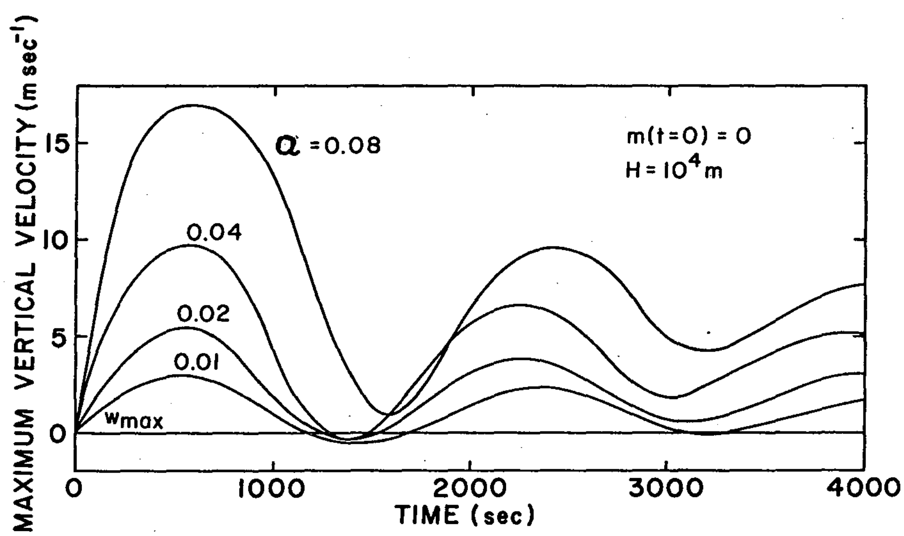

Figure 8. Updraft oscillations in relation to constant thermal buoyancy in a model saturated atmosphere without horizontal mixing.

the results of analytic theory, (8). It would be interes- to test this result by comparing the periods of shower deve- ment in warm and cold air masses, as revealed by radar echoes

3.6 Role of the Height of the Condensation Level in Updraft Oscillations

Figure 10 shows the effect of varying the initial moisture content when the thermal buoyancy is great enough to produce an updraft speed larger than the fall speed of precipitation. As the moisture content decreases, the condensation level rises, and the updraft develops longer initially in the longer absence of a substantial water load. (This does not wholly correspond to the more general model discussed in sec. 4 below, where delay of condensation has adverse effects on buoyancy.) The regime of high-speed steady updrafts occurs when an updraft strong enough to hold precipitation aloft develops before significant precipitation forms from cloud. Such high-speed updraft cases have been discussed by Kessler (1969, p. 73).

3.7 Simple Oscillations

The numerical model has simple oscillations (Brunt, 1927) as solutions, as well as condensation oscillations. The forme correspond to the oscillatory mode discussed by Priestley.

In the case where condensation and mixing are absent and vertical displacements and buoyancy forces are small, (4) becomes

$$\frac{\partial w_{max}}{\partial t} \approx 1.5A = \frac{d^2 z}{dt^2} \text{ (near } z=H/2) \quad ,$$

and (5) becomes

$$\frac{\partial A}{\partial t} \approx -\frac{w_{max} S_d}{H} \quad .$$

The second equation, when integrated, becomes

$$A = -\frac{S_d}{H}(z - z_o) \quad ,$$

and substitution of this expression for A into the first equation yields

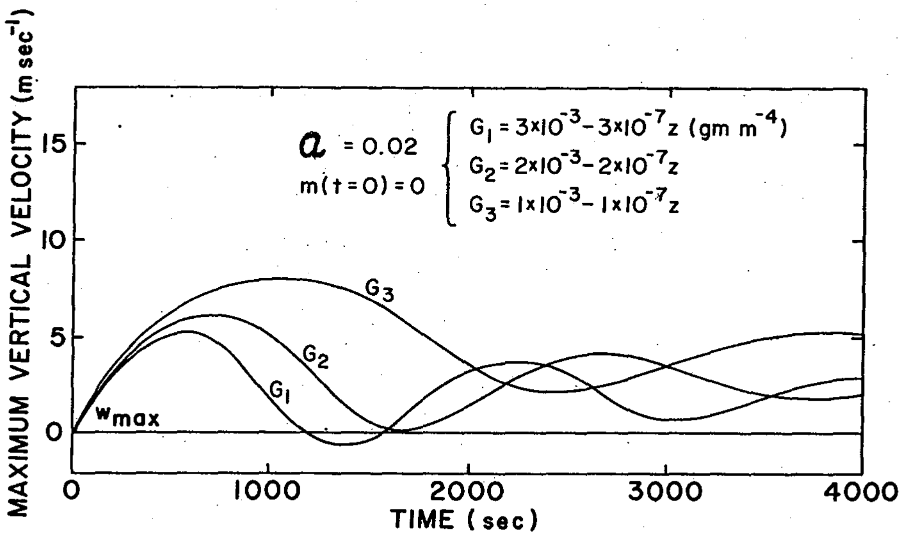

Figure 9. Updraft oscillations in relation to the condensation function, in a model saturated atmosphere with constant thermal components of buoyancy and no mixing. The period is very nearly proportional to $1/\sqrt{G}$.

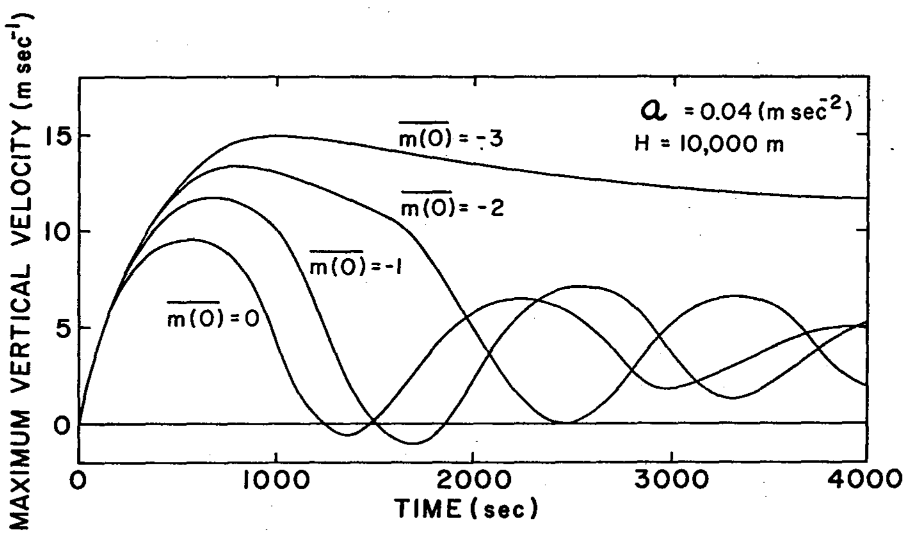

Figure 10. Updraft development in relation to environmental moisture or height of the condensation level in a model atmosphere with a constant thermal component of buoyancy and no horizontal mixing. Steady updrafts tend to develop as the condensation level rises, provided that the thermal component of buoyancy is sufficiently large.

$$\frac{d^2z}{dt^2} = -\frac{1.5S_d}{H}(z-z_o) \quad .$$

In the stable case, $S_d>0$, and the height of a parcel and all other variables then oscillate with the common period $\tau = 2\pi/\sqrt{1.5S_d/H}$, tabulated in table 2. Corresponding results of the numerical model discussed in section 4, lie within 10 sec of the tabulated values, suggesting the adequacy of the finite difference scheme.[11]

Table 2. Period τ of Simple Undamped Oscillations in Relation to Buoyancy Parameter S_d.

S_d(m/sec^2)	Equiv. Lapse Rate γ *	τ(sec)
0	γ_d	∞
.1	$0.25\ (3\gamma_d + \gamma_m)$	1620
.2	$0.50\ (\gamma_d + \gamma_m)$	1148
.3	$0.25\ (\gamma_d + 3\gamma_m)$	936
.4	γ_m	811
2.0	0	363

*Based on an assumed mean environmental temperature of 250 K, and depth $H=10^4$ m. See also App. C.

3.8 Further Discussion of Asymptotic Cases and Absolute Buoyancy

Priestley denoted the asymptotic case as that where, although the lapse rate is unstable, an initiating perturbatio is monotonically reduced to zero. This trend responds to effects of mixing, analogous to the effects of molecular viscosity and conduction treated in classical papers. Our equations admit similar solutions.

[11] When mixing is present the period is $\tau=2\pi/[(1.5S_d/H)-k_5^2/4]^{\frac{1}{2}}$ and so is essentially unaffected by values of k_5 much smaller than those associated witl critical damping.

Consider (4) and (5) in relation to updrafts in a dry atmosphere, i.e., $w \geq 0$ and L, F_1, ε_M and ε_m all identically zero. Then we have

$$\frac{\partial w_{max}}{\partial t} = 1.5 \left[A - \left|\frac{A}{H}\right|^{\frac{1}{2}} w_{max}\right] - k_5 w_{max} , \tag{9}$$

$$\frac{\partial A}{\partial t} = \frac{w_{max}}{H} (S_d + A) - k_5 A \quad . \tag{10}$$

With $\frac{\partial w_{max}}{\partial t} = \frac{\partial A}{\partial t} = 0$, steady state relationships are defined, viz.,

$$S_d = -k_5 \; [(AH)^{\frac{1}{2}} + \frac{2}{3} k_5 H] - A \quad , \tag{11}$$

and

$$w_{max} = -\frac{k_5 H A}{S_d + A} \quad . \tag{12}$$

The limiting value of S_d for steady upward motion is given by (11) with $A = 0$. Thus, steady states with vertical motion occur when $S_d < -\frac{2}{3} k_5{}^2 H$. Magnitudes of S_d larger than the indicated threshold are associated with the monotonic growth of any disturbance, however small, toward an asymptote of vertical velocity defined by (11) and (12). Equation (11) is not satisfied by smaller magnitudes of S_d, and smaller negative values are associated with reduction of disturbances to zero. The motion resulting when $S_d < -\frac{2}{3} k_5{}^2 H$ corresponds to Priestley's absolute buoyancy, and when $-(2k_5^2 H/3) \leq S_d \leq 0$, we have cases like those denoted as asymptotic by Priestley. In the present treatment, of course, both modes of motion develop monotonically toward an asymptote after the effects of an initiating disturbance have been manifested, but we will retain Priestley's concept of the asymptotic case as that where the trend is toward zero velocity.

Figure 11, an extension of table 1 in Priestley's paper, illustrates solutions of (11) and (12) at the asymptotic boundary and in the region of absolute buoyancy. Inspection

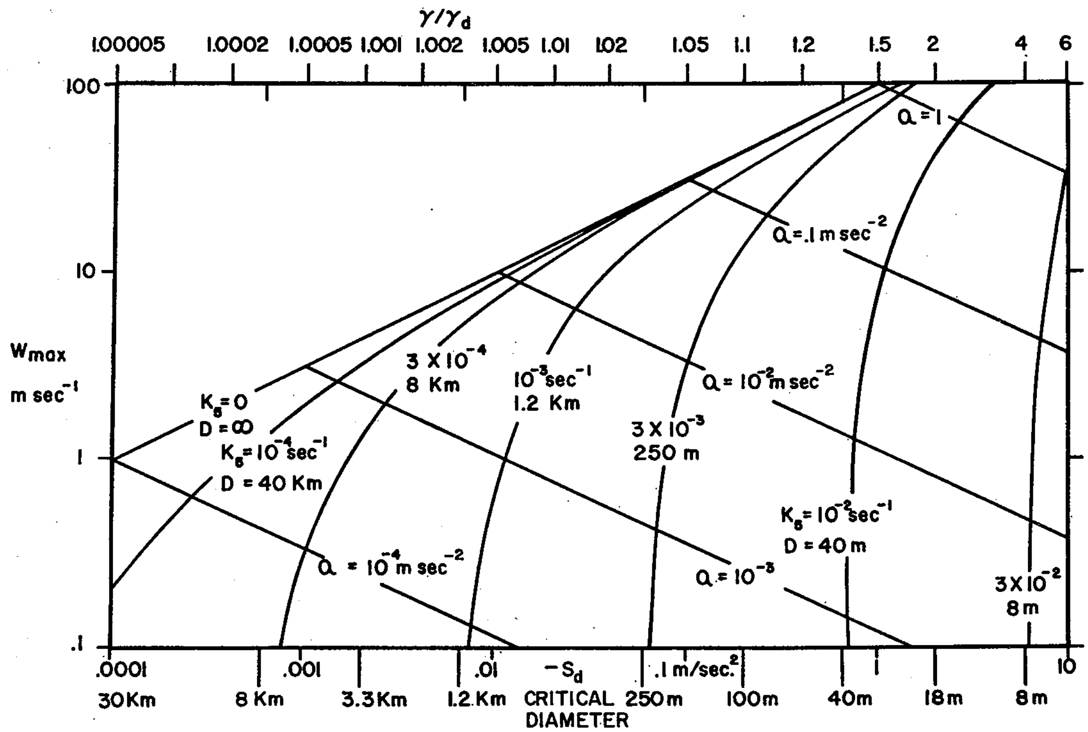

Figure 11. Steady state relationships in the absolutely buoyant region corresponding to $S_d < -\frac{2}{3} k_5^2 H$, with $H=10^4$ m, as defined by (9)-(12) in the text. Sloping curves are labeled with values of mixing rate and the associated size of a cylindrical element, as suggested by Priestley and Richardson (1926), (eq.(13) in our text). The average thermal buoyancy for a particular element size and superadiabatic lapse rate shown on the abscissa is shown by the straight lines sloping downward from left to right. Any ordinate value may be regarded as the approximate speed attained by an element in a cylindrical column of indicated size, rising from zero to 5000 m in an environment with indicated lapse rate. (See also Appendix C.)

(4) and (5) shows that asymptotic cases should also occur in a saturated atmosphere whose lapse rate exceeds the moist adiabatic; since the water load is closely related to updraft speed when updrafts are weak, the solutions will be altered by condensation oscillations from the monotonic behavior expected in the dry case. Also, since the water load opposes positive buoyancy, we expect the asymptotic boundary to lie further from $S_m=0$ in the moist case than from $S_d=0$ in the dry case. Because of the great complexity of the moist equations, we have not attempted a detailed analytic study of the moist asymptotic family, but a numerical solution is illustrated in section 4.

4. SOLUTIONS OF THE COMPLETE NUMERICAL MODEL

4.1 General Comments

Finite difference calculations based on the complete model ((1) through (5)) have been made with many values of the regulating parameters and a 41 grid-point column. The computer program presented in detail in appendix E uses forward time differences and centered space differences and is simply an expanded version of the program described by Newburg and Kessler (Kessler, 1969, p. 80).

The following discussion deals exclusively with cases where the updraft is initiated by a starting perturbation buoyancy, i.e., an initial assigned value of A. Subsequent development in model conditionally unstable situations may depend greatly on the magnitude of this input parameter for reasons discussed in section 3.2.

We describe five types of solutions given by the model, viz., (a) in stable dry cases, simple damped oscillations; (b) in moist stable or conditionally unstable cases, cloud and precipitation development which may lead to a shower (a kind of condensation oscillation), followed by damped simple oscillations; (c) an updraft that becomes steady, and is accompanied by steady rain at the ground; (d) an updraft that becomes steady and strong (15-40 m/sec) without precipitation beneath, but, in a moist atmosphere, with precipitation implied outside the area beneath the strongest updraft; and (e) with weak absolute instability, disturbances restored monotonically and asymptotically to zero when the mixing rate is sufficiently large. With larger absolute instability than type (e), steady updrafts with cloud and precipitation (types (c) and (d)) develop in a moist model, or sustained updrafts without cloud develop in a dry model.

The types of solution, somewhat arbitrarily defined, to drift from (a) toward (d) as the environmental lapse rate and the perturbation buoyancy increase, and as the mixing rate decreases, i.e., as the implied horizontal dimension of the updraft area increases. With a given conditionally unstable lapse rate, solution (b) is less favored when the moisture content of the environment is high, but solution (d) is most favored by less-than-saturated moisture conditions, i.e., by a somewhat elevated condensation level, or by a large threshold for cloud conversion (large value of a in the autoconversion term AC in (1) and (2)). The transitions between solution types (b) and (c) and between (d) and (e) appear to be discontinuous for small changes of input parameters across thresholds, as suggested by the discussion in section 3.2. Types (a) and (b) correspond to Priestley's oscillatory solutions and (c) and (d) to his "absolute buoyancy". Type (e), in a dry atmosphere, is quite analogous to Priestley's asymptotic case, but in a saturated atmosphere, for example, with the lapse rate slightly more unstable than the moist adiabatic, updraft behavior following a starting perturbation may be described as an asymptotic decline of the mean with superimposed condensation oscillations.

4.2 Sample Solutions

Solution types (a), (b), and (d), are represented in figures 12 and 13. Among the parameters used in the calculations, only the starting perturbation buoyancy is different in these two cases. Other parameters are as listed in table 1 and as follows: mixing rate $k_5 = 3 \times 10^{-4}$ sec^{-1}; environmental and starting moisture $m_o = -4 + 8 \times 10^{-4} z - 4 \times 10^{-8} z^2$) gm/m The perturbation buoyancies corresponding to figures 12 and 13 are 0.025 m/sec^2 and 0.05 m/sec^2, respectively, and are equivalent to average starting temperature excesses of approximately 0.7 and 1.4°C.

At the top of figure 12 is a time-height portrayal of the development of cloud, precipitation, and vapor distributions in the weak perturbation case. Beneath that, on the same time scale, the magnitudes of the maximum updraft, average condensed water load, and rainfall rate at the ground are plotted with the thermal component of buoyancy. The third series of plots illustrates terms contributing to $\partial A/\partial t$. The plot of δA_m represents $(w_{max}/H)[F_1 S_m - A \times \text{sign } w]$ in (5), or the effect of vertically moving cloudy air. The plot of δA_d represents $-(w_{max}/H[(1-F_1)(S_d) + A \times \text{sign } w]$ or the effect of vertically moving unsaturated air. The contribution of vertically averaged evaporation of precipitation and cloud represented by ε_M and ε_m, respectively. The fourth plot presents $\partial A/\partial t$ or the sum of all the contributions to change of thermal buoyancy, including small values of $-k_5 A$ not separately depicted.

In physical terms, the development of updrafts and hydrometeors in the complete model shown in figure 12 is regulated as follows: An upward air current develops immediately after the start in response to the input perturbation thermal buoyancy. The thermal buoyancy immediately starts to decline, partly as a result of mixing of updraft air with environmental air ($-k_5 A$), but more because the enviromental lapse rate is stable for vertical motions of dry air (δA_d). As saturation is attained, condensation occurs. Then the term δA_d decreases and δA_m becomes a prominent contributor to positive buoyancy in the examples given since an appreciable vertical velocity accompanies condensation. The thermal buoyancy then declines less rapidly and, indeed, the thermal component increases again after 300 sec. The increase corresponds to a more rapid addition of heat of condensation, than the rate of combined losses of sensible heat associated with mixing of ambient and environmental air, and evaporation of cloud.

Meanwhile, however, condensation products are accumulating in the updraft column, and since the effective buoyancy is related to both its thermal component and water load, this increase of condensation products has an important effect on the updraft. In figure 12, the rate of increase of condensation products combined with the rate of increase of thermal buoyancy results in a decline of the effective buoyancy ($A-k_8 L$), and a reduction of the updraft speed after 300 sec. By now, substantial amounts of precipitation have formed in the updraft column, and descent of precipitation toward the ground is hastened as the updraft weakens. When precipitation falls into the subcloud layer, its partial evaporation there produces a substantial contribution toward negative thermal buoyancy. The downdraft in figure 12 starting at about 1600 sec is attributable to dominant effects of the water load, in the presence of a residual small positive thermal buoyancy.

As precipitation falls rapidly out of the descending air column and the cloud evaporates, we have the case of descending dry motion in a stable environment, and a restoring upward buoyancy increases. The subsequent record is that of a simple oscillation.

The early developments illustrated in figure 13 are similar to those in figure 12. Because of the stronger starting thermal perturbation, however, the vertical velocity

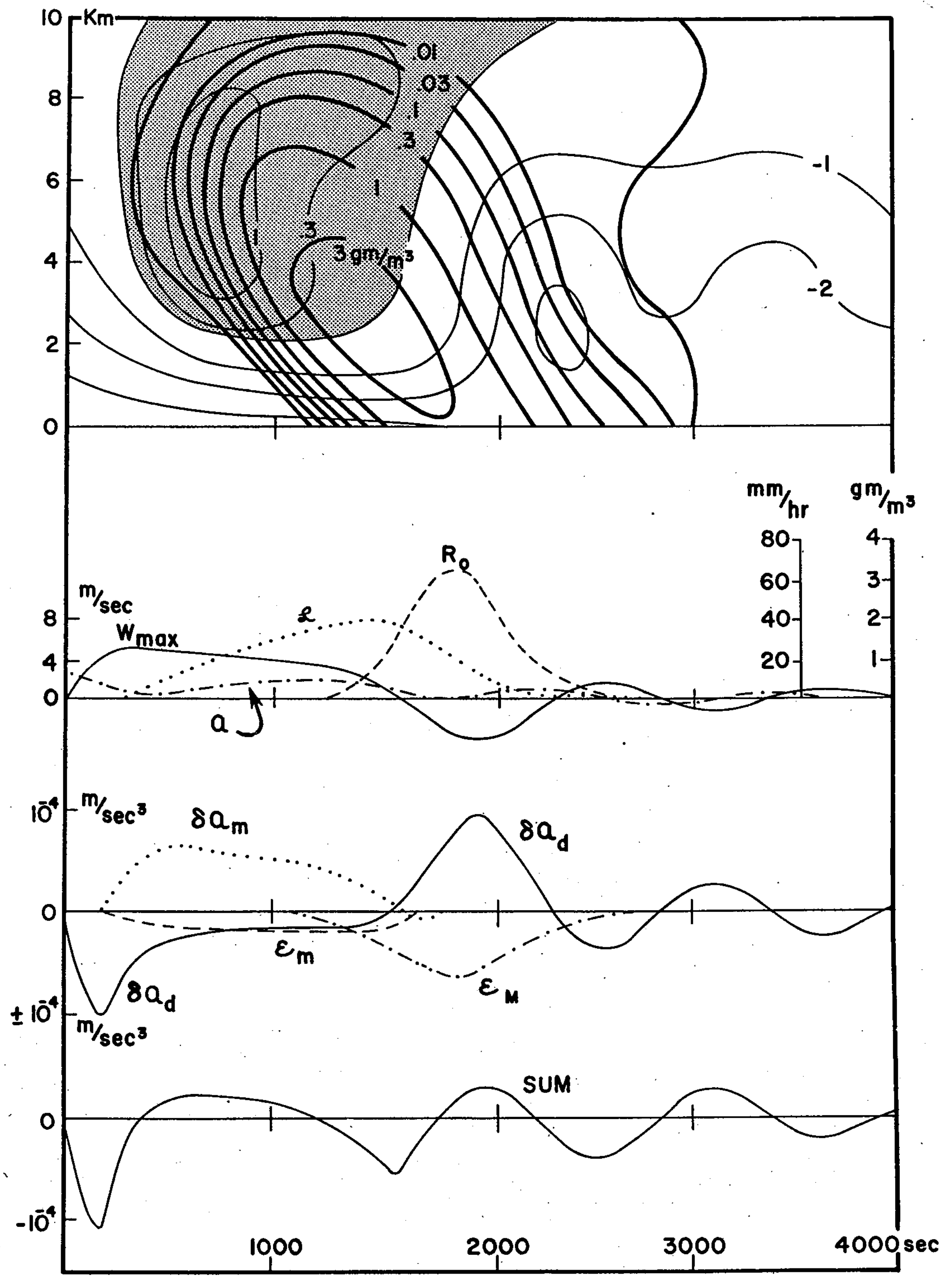

Figure 12. Development of cloud, precipitation, buoyancy, and updraft speed in a weakly perturbed model atmosphere. The text includes a detailed discussion.

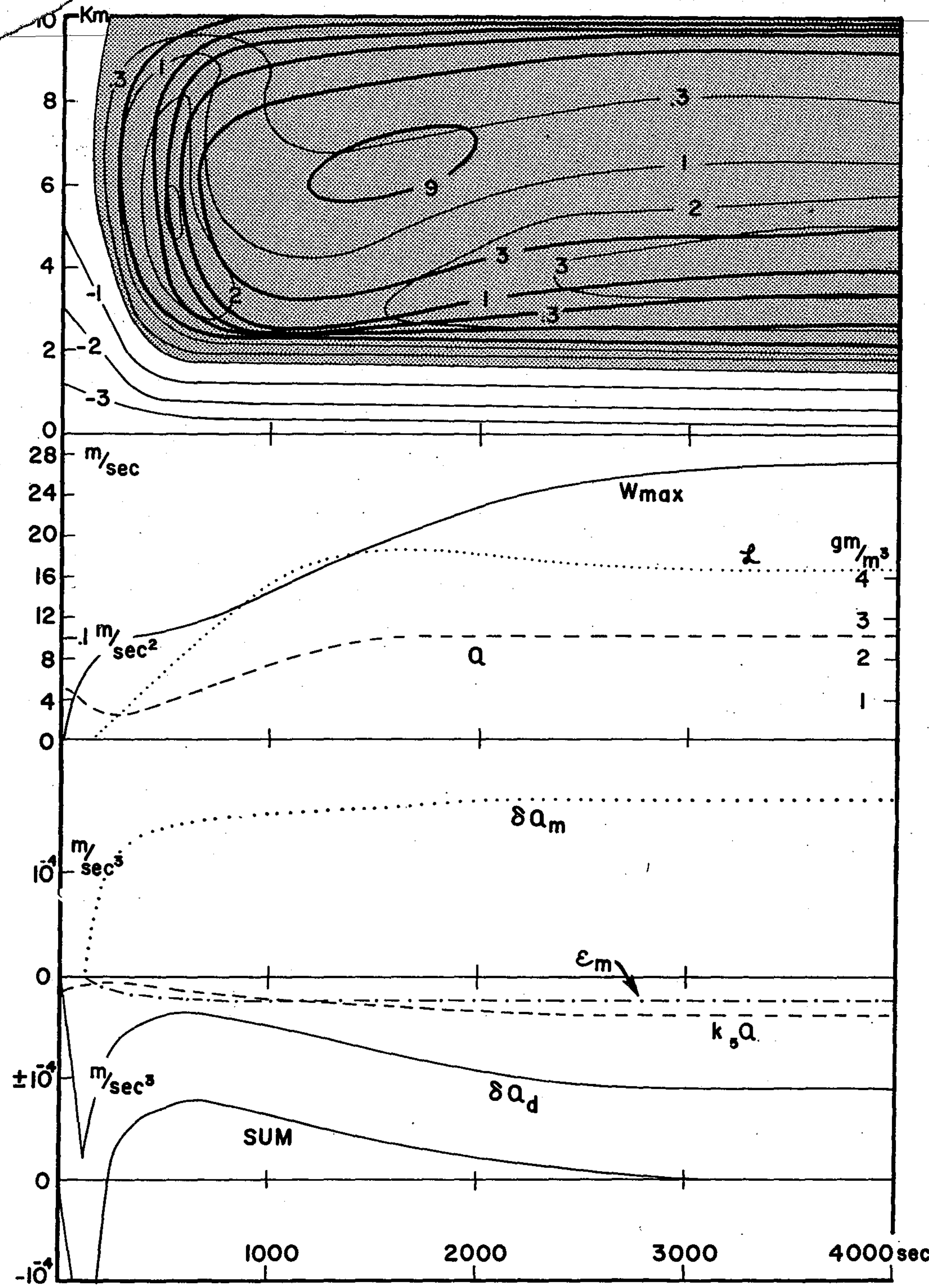

Figure 13. Development of hydrometeors, buoyancy and updraft speed in a model atmosphere with a starting thermal perturbation twice as large as illustrated in figure 12. The text gives detailed discussion.

is larger in figure 13 when condensation begins. This produces a more rapid recovery of the thermal buoyancy, whose rate of increase exceeds the contrary tendency of the increasing water load. Therefore, the updraft continues to increase, precipitation is held aloft, and the high-speed steady updraft case develops. The precipitation aloft diverges there, and descent toward the ground is implied in adjacent regions where the updraft is not so strong.

Numerical examples with weak absolute instability are shown in figures 14 and 15. Figure 14, based on a dry case, illustrates the dependence of the ultimate steady state solution on the environmental stability parameter S_d, and its independence of the starting thermal perturbation A_o. Thus, with $k_5 = 10^{-3}$ sec^{-1}, $S_d = -.01$ m sec^{-2}, the updraft tends with time toward 0.75 m/sec, whether or not the starting perturbation produces a starting transient in excess of that value. For all values of S_d between zero and -6.66×10^{-3}, the only steady state is zero vertical velocity, and trends toward zero are shown for the same two starting perturbations used to illustrate the absolutely buoyant cases.

Figure 15 illustrates the numerical solution of a moist absolutely unstable case. Here the environment is completely saturated and S_m=+0.025 m sec^{-2}, corresponding to a maximum attainable average excess temperature in the ascending column of about 0.6C. With a starting perturbation A_o=.01 m sec^{-2} and a mixing rate of $3\times10^{-4} sec^{-1}$, updrafts attain a maximum value near 3.5m/sec, and a rainfall rate of 55 mm/hr occurs; then these and associated parameters decrease to negligible values in about 3 hours. Total rainfall beneath the model updraft column in this example is about 22 mm. When the model instability S_m is sufficiently increased, or the mixing rate k_5 reduced while a saturated environment is maintained updrafts and other parameters drift through the regime of damped condensation oscillations toward the type (c) steady condition. This development of rain at the ground may also depend on microphysical processes so active, or updraft development so slow that the formation of precipitation from cloud occurs when the updraft speed has not yet attained the fall speed characteristic of precipitation. With faster updraft development or slower cloud-conversion processes, the end result tends toward high-speed updrafts without precipitation beneath, when instability is great.

Because we have not accounted for a stabilization of the atmosphere necessarily associated with the rapid ascent of part of it, the examples given may be thought to exaggerate the intensity and duration of events. Thus, the perturbation buoyancy used for figure 12 may lead to little or no rain in

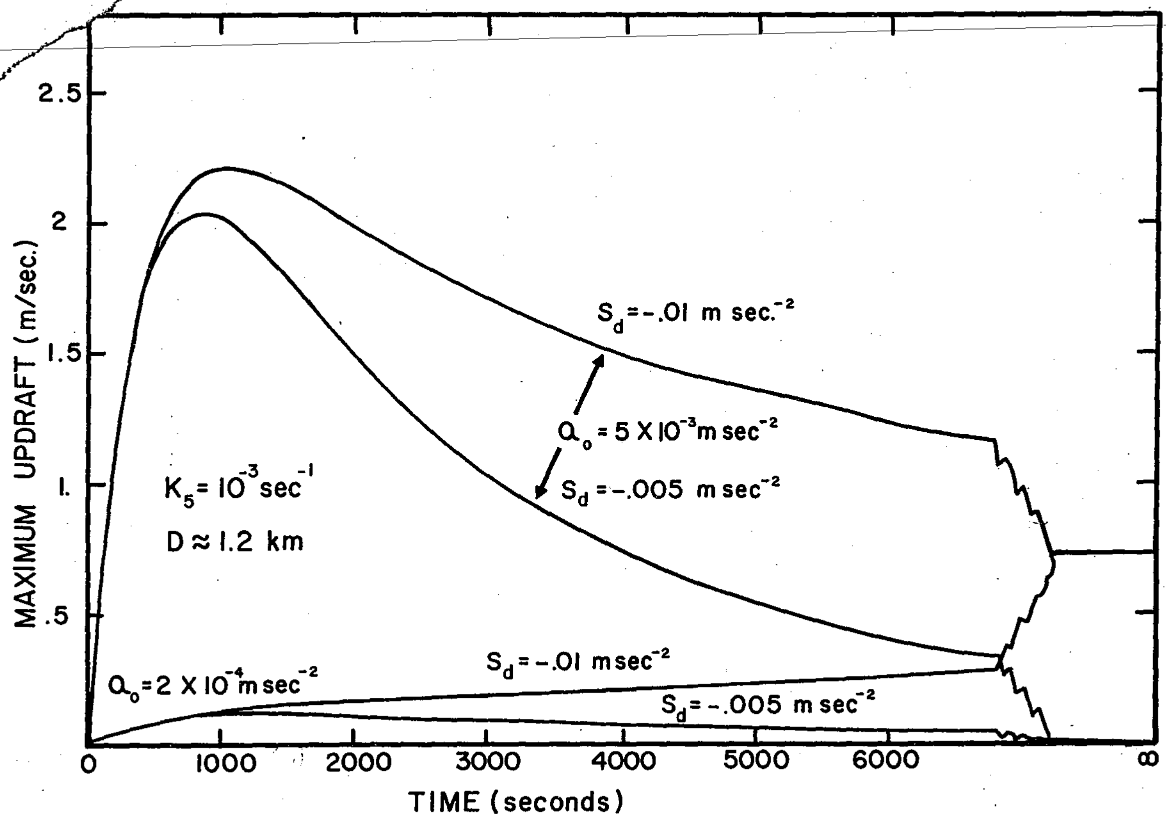

Figure 14. Development of vertical velocity with time, with two absolutely unstable lapse rates, and two starting disturbances. With $k_5=10^{-3}$ sec, updrafts approach 0.75 m/sec when $S_d=-.01$ m sec^{-2}, and approach zéro asymptotically when $S_d \geq -6.66\times10^{-3}$m sec^{-2}.

a more comprehensive model, and figure 13 would more logically portray vertical motion of limited duration. Nevertheless, an implication of this study of perturbation buoyancy effects may still be valid. The weaker perturbations would tend to be damped, and the duration of events established by the stronger perturbations should depend on the strength of sources of fresh air similar to that overturned in the convective process.

4.3 Distribution of Solution Types in Relation to Model Input Parameters.

The distribution of solution types shown in figure 16 corresponds fairly to our expectations based on section 3.2. Along the abscissa is the initial and environmental moisture content at z=0, i.e., the magnitude of C_o in the equation

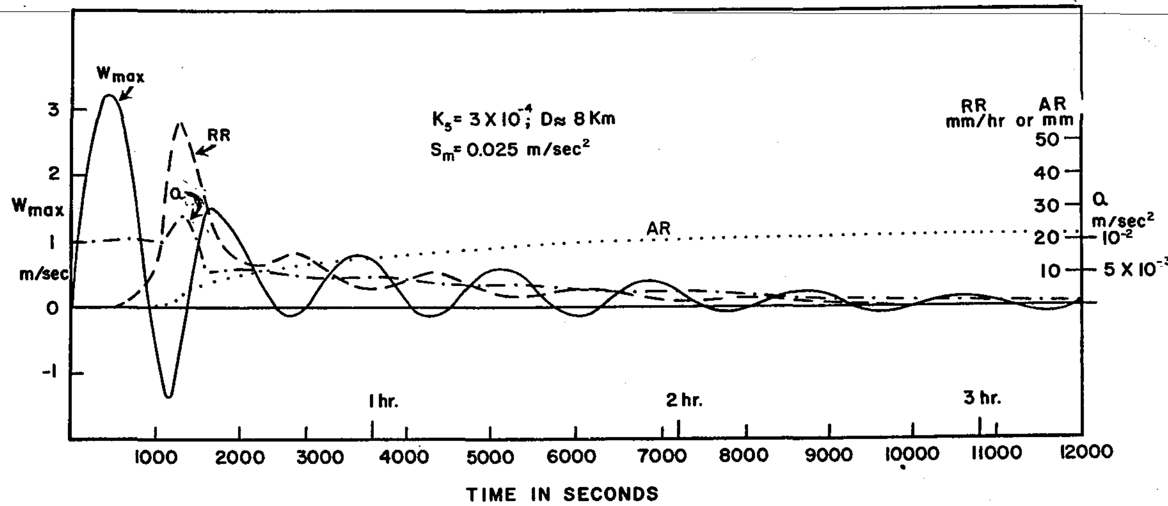

Figure 15. Updrafts, thermal component of buoyancy, precipitation rate at the ground, and accumulated precipitation in relation to time in a saturated model atmosphere with a super-moist adiabatic lapse rate. The decline of updrafts to zero, analogous to Priestley's asymptotic cases, is accompanied by condensation oscillations in the moist model.

$m = C_o - (2C_o/H)z + (C_o/H^2)z^2$. The starting perturbation is plotted along the ordinate. Interior lines show the loci of the solution types referred to in section 4.1, when all parameters except those indicated on the ordinate and abscissa are as given in section 4.2.

As the mixing rate k_5 declines, the area occupied by type d solutions in a diagram like figure 16 increases, as suggested by figure 5. Increasing the autoconversion threshold has a similar effect, since this reduces the accumulation of condensation products and increases the effective buoyancy.

An alternate presentation of solution types is illustrated in figure 17. This diagram represents the development with time of vertical velocity for conditions depicted by an ordinate value $A_o = 0.025$ in figure 16. The upper shaded area in figure 17 represents the condition of continuing precipitation at the ground, and the lower shaded area of figure 17 falls in figure 16's region of showers. Between these two lie cases of high-speed updrafts without precipitation at the ground beneath the strongest updraft. Below the shower area, the air motion is fairly described by the theory of simple oscillations

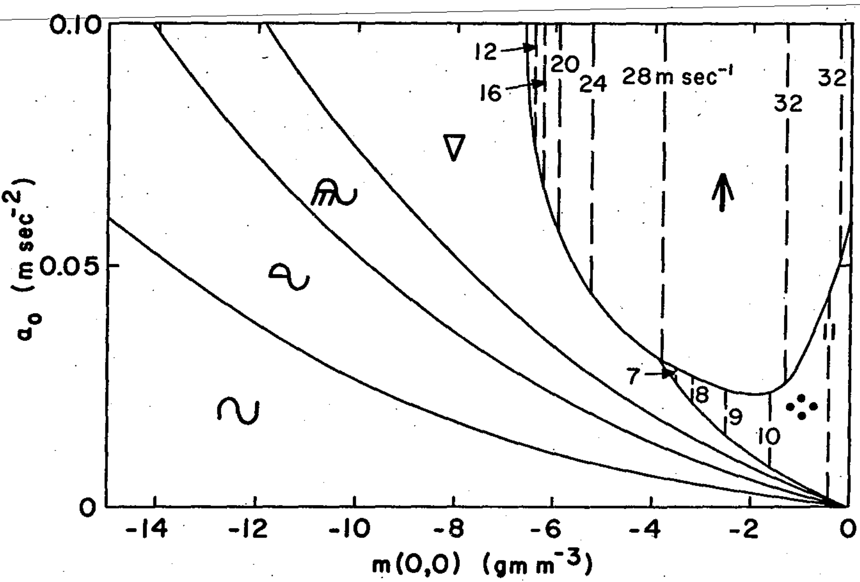

Figure 16. Types of solutions of the complete numerical model in relation to environmental moisture and starting thermal perturbation. Simple oscillations (Type a) appear at lower left, solitary showers (Type b) are indicated by a triangle, high-speed updrafts without precipitation beneath (Type d) are indicated by an arrow, and continuous precipitation at the ground (Type c) is represented at the lower right. Isopleths in the right side of the figure indicate the steady values of maximum vertical velocity ultimately attained with solution Types c and d. All of the illustrated solutions way between moist and dry adiabatic values and for mixing rate $k_5 = 3x10^{-4}$ sec^{-1}.

We again emphasize that these results are quite dependent on the form of mixing law we have somewhat arbitrarily chosen; the further theoretical development of mixing models applicable to large cumulus clouds, and the testing and refinement of this aspect of cloud models should be matters of high priority.

As one of many possible analyses involving the microphysical parameters, we illustrate the effect on the distribution of solution types, of change of the particle-size distribution. If N_o were $10^5 m^{-4}$ instead of $10^7 m^{-4}$ as in figure 16, the particle sizes would be increased by a factor $100^{.25} = 3.162$, for the same water content. Other factors would also change, however. The faster fall speeds of the

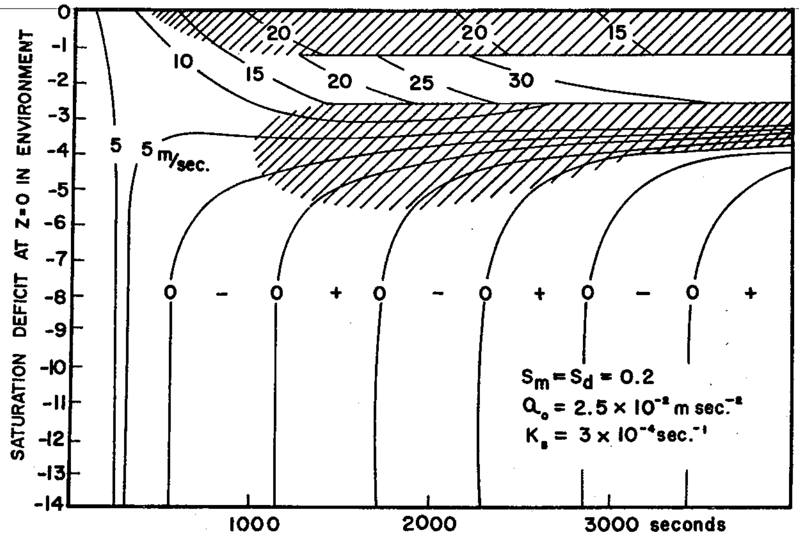

Figure 17. Development of vertical velocity and precipitation at the ground (shaded areas) in relation to time, for example, with a starting perturbation A_o=0.025, and in relation to environmental moisture content. Ordinate values represent C_0 in the equation $m_0=C_0-2C_0 x10^{-4}\ z+C_0\ x10^{-8}z^2$.

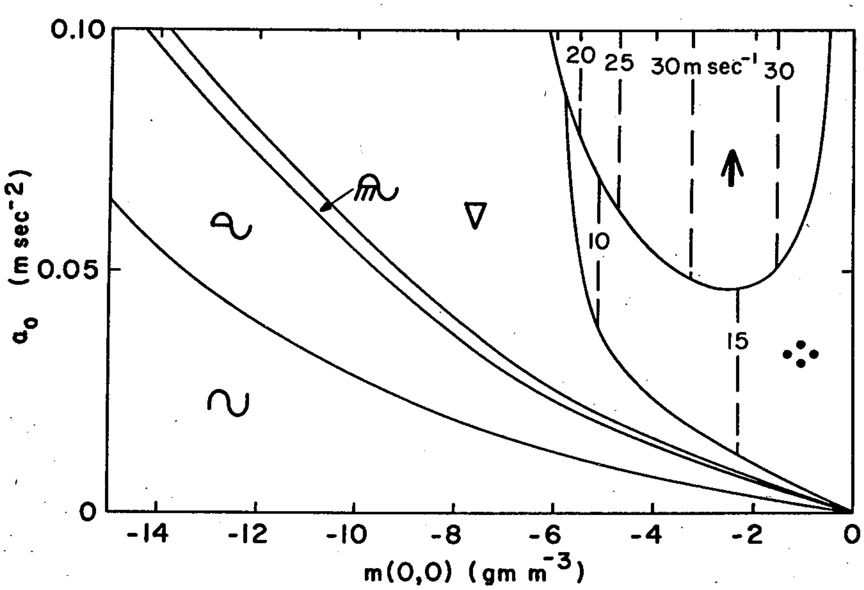

Figure 18. Same as figure 16, except the drop-size distribution parameter is 10^5, and the precipitation formed aloft corresponds in size, fall speed, and some other characteristics to small hail.

larger particles ($V \propto N_o^{-.125}$) would be associated with a greater fallout, and diminished precipitation content M. On the other hand, the accretion rate of precipitation for cloud would be smaller ($AC \propto N_o^{.125}$) because of the less numerous particles; cloud density m would rise and the net decline of L would be less than that of M. For cases where precipitation falls into the subcloud layer with either value of N_o, the rate of evaporation of precipitation in that layer would be reduced since $EP \propto N_o^{.35}$, but it is obvious that the effects of EP on the buoyancy would be larger if some evaporation occurred where there had been none before. The complicated interactions of these and some other model processes are automatically accounted for when calculations are made with the changed value of N_o. The result of about 30 such sets of calculations have been the basis for figure 18, which shows a larger area of steady precipitation and a smaller area of high-speed updrafts than in figure 16. There are implications in figures 16 and 18 of possible significance for those who strive to reduce the incidence of damaging hail. Further development of models should help to clarify whether hail formation affects the intensity of updrafts and, for example, surface winds in real storms.

5. COMMENTS ON THE SIZE OF THUNDERSTORMS AND EFFECTS OF THE PLANETARY BOUNDARY LAYER ON STORM DEVELOPMENT

5.1 Size in Relation to Mixing Rate

The parameter k_5 can be related to the size of the updraft column. Following Priestley (1953), this appears worthwhile, although before much further study, the authors expect to indicate size to an accuracy of little better than an order of magnitude. The equation Priestley used becomes in mgs units

$$k_5 = .117\ D^{-2/3}\ \text{sec}^{-1}\ , \tag{13}$$

$$D = 0.04\ k_5^{-3/2}\ \text{meters}\ ,$$

where D is the diameter of a cylindrical column. This relationship is plotted in figure 19.

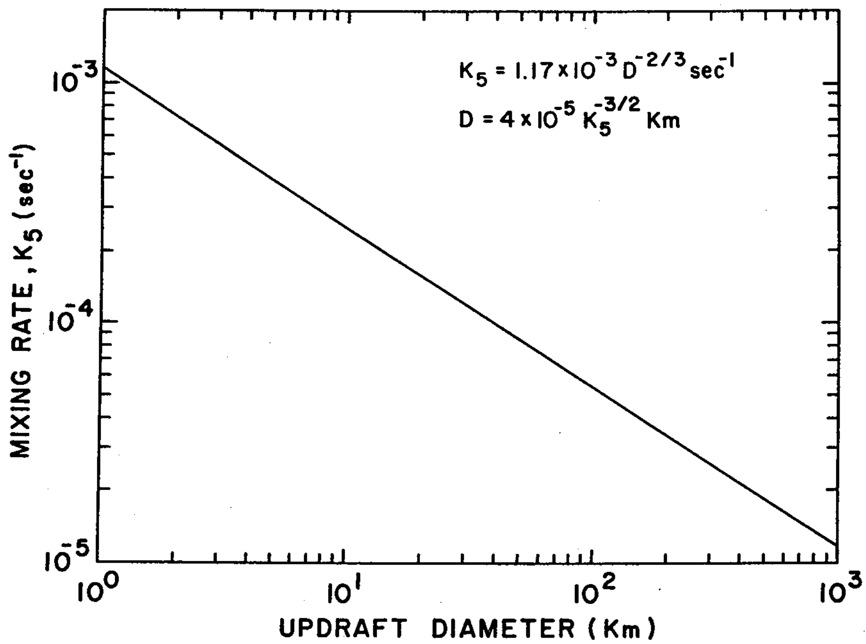

Figure 19. Horizontal extent of a rising column vs. mixing rate, according to an equation used by Priestley (1953).

5.2 A Critical Richardson Number in Relation to Storm Size and Intensity

We have discussed in sections 3.2 and 4, the concepts of a critical size and buoyancy required to initiate sustained up drafts. We need also to inquire into criteria for a maximum size and in this connection it seems that an effect of a circulation on itself may be significant. A vertical current is associated with inflow below and outflow above, hence with a vertical shear of the horizontal winds, and Richardson (1920) has given us a criterion for the breakdown of a vertically shearing current.

Consider a cylindrical column of radius R and height H. At the height H/2, we assume that the updraft is w_{max}. The flux through the level H/2 is thus $\pi R^2 \rho_m w_{max}$ and continuity requires that this be matched by an inward flux of air below the level H/2. Then

$$\pi R^2 \rho_m w_{max} = 2\pi R \frac{H}{2} \rho_b \overline{u_i} \quad ,$$

and

$$\bar{u}_i = \frac{Rw_{max}}{H},$$

if we neglect the difference between ρ_m and ρ_b. Above the level $H/2$, an equal outward flux is associated with the wind speed $\bar{u}_o$. Then the average shear of the horizontal wind is

$$\frac{\Delta u}{\Delta z} \approx \frac{\bar{u}_o - u_i}{H/2} = \frac{2Dw_{max}}{H^2} \quad , \tag{14}$$

and a Richardson Number involving mean quantities is

$$R_i = \frac{\frac{g}{\bar{\Theta}} \frac{\Delta \Theta}{\Delta z}}{(\Delta u/\Delta z)^2} = \frac{g\ H^3 \Delta \Theta}{4 \bar{\Theta} D^2 w^2_{max}} \quad , \tag{15}$$

where $\Delta\theta$ is the difference of potential temperatures between height z=H and z=0, and D is the diameter of the updraft column. We have neglected the vertical variation of air density in this part of the analysis; it can readily be included, but although the variation through a great depth is substantial, the effect of this variation of air density on the shear calculation is quite small.

Richardson proposed the value $R_i=1$ as the criterion for an increase of a turbulent perturbation although we now recognize that parameters other than R_i are important with respect to the growth and spread of turbulence (Pao and Goldburg, 1969). Atmospheric turbulence seems usually to be initiated with $R_i \approx 0.25$; the value unity is treated here because real circulations are associated with substantial irregularities. In the depth $H=10^4$ m of a typical summer troposphere, we have also $\bar{\theta} \approx 320$ K, and $\Delta\theta \approx 50$ K when the lapse rate is moist adiabatic.

The discussion of (4b) suggests that when mixing is weak or absent, the vertical velocity at a specified height is approximately proportional to the square root of the effective buoyancy. Approximate relationships involving the water load, maximum updraft speed and thermal component of buoyancy are illustrated in figure 3, whence we suggest, for a column 10^4 m high,

$$w_{max} \approx .25\ (A\ H)^{\frac{1}{2}} \quad \text{(high estimate of water load included)} \tag{16a}$$

or

$$w_{max} \approx (AH)^{\frac{1}{2}} \qquad \text{(no water load)} \ . \qquad (16b)$$

Examination of a tephigram shows that, in the absence of diffusion, $\Delta\theta$ and the mean thermal component of buoyancy, A, are approximately related in a cloudy updraft, representative of tropical conditions, by

$$A \approx \left(\frac{.4H}{10^4} - 8x10^{-3}\ \Delta\Theta\right) \ , \qquad (17)$$

whence

$$w^2_{max} \approx 5x10^{-4}\ [5x10^{-3}\ H-\Delta\theta]H\ [\text{high } H_2O] \ , \qquad (18a)$$

$$w^2_{max} \approx 8x10^{-3}\ [5x10^{-3}\ H-\Delta\theta]H\ [\text{no } H_2O] \ . \qquad (18b)$$

Then

$$\frac{D^2}{H^2} \approx \frac{g\ \Delta\theta}{\overline{4\theta}\ R_i\ [8x10^{-3}\ (5x10^{-3}H - \Delta\theta)]} \qquad (19)$$

when there is no condensed water, or four times this quantity when there is a high water load. If the environmental lapse rate is nearly moist adiabatic, i.e., $\Delta\theta \approx 5x10^{-3}H$ in a tropical atmosphere, the updraft is very weak, and D^2/H^2 is very large. When the lapse rate is midway between moist and dry adiabatic, i.e., $\Delta\theta \approx 2.5x10^{-3}H$, we have $\frac{D^2}{H^2}$ near unity for small water loads, or about 4 when the water load corresponds to that accompanying precipitation at the ground. Thus with environmental average lapse rates intermediate between moist and dry adiabatic values, we expect storms to range in breadth from a dimension about the same as their height (low water load), to about twice that broad when the water load is high.[12]

Figure 20 shows the diameter of cylindrical updraft columns 10 km high at whose edge the layer Richardson Number is unity, in relation to the lapse rate and maximum updraft speed. Thus, isopleths sloping downward from left to right are loci of estimated maximum size in relation to lapse rate and updraft speed, larger horizontal sizes being quite prone to disruption by turbulence of their own making. The two curves plotted in figure 20 rising from left to right, represent W_{max} as defined by (18 a and b). The region between may be thought of as a probable locus of maximum storm sizes. When a vertical perturbation is large enough to be amplified by the buoyancy it produces, its velocity may grow toward the upper bound initially, because the water load is initially small. If the horizontal size of the perturbation is larger than the dimensions indicated along the upper curve, it should break down into circulations of smaller sizes. After the disturbance becomes a storm, the water load increases; then the updraft may decrease and the maximum size may drift toward a larger value indicated along the lower curve. If the storm size were strongly regulated by the maximum updraft that occurs at any time during development, the maximum sizes would be better indicated by the upper curve (smaller sizes).

Of course, this Richardson criterion is only suggestive of maximum storm sizes. With Scorer and Ludlam (1953), we believe that the entrainment of environmental air and the conditioning of environmental air by towers are factors encouraging growth but we know too little of these processes. We note that a cell must be limited by the availability of unstable air, exhausted in proportion to wD^2. A very large uncertainty is associated with our use of $\Delta\theta$ in (15). To the extent that $\Delta\theta_w$ is more appropriate, for example, our theory would define smaller sizes. Furthermore, the vertical shear in a storm's environment may tend to add on a storm's downshear

---

[12] When storms form in a line, we suggest that low-level convergence and high-level divergence occur in the direction normal to the line. The magnitude of the associated shear is then twice that given in (14) and the factor 16 appears in place of 4 in the denominators of (15) and (19). Thus, we look for the width of long storm lines to be perhaps half the diameter of cylindrically shaped storms. The factors favoring lines or cylinders may affect size also, of course, in still unknown ways.

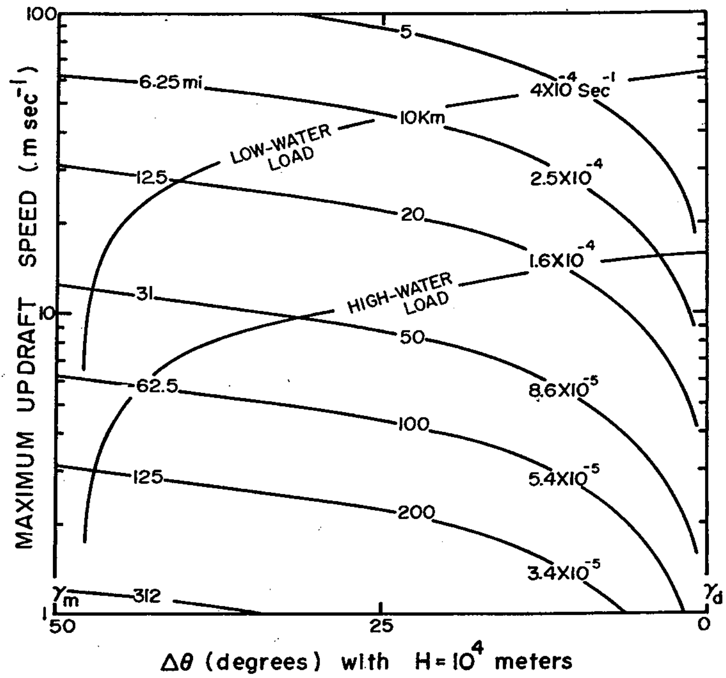

Figure 20. The maximum diameter of model updraft columns not prone to breakdown by turbulence of their own making. The limiting criterion is defined in this chart with R_i unity, and an updraft column 10^4 m high. The relationship between $\Delta\theta$ and moist and dry adiabatic lapse rates shown on the abscissa applies with a surface temperature and dewpoint of about +24C, corresponding to a summer thundery atmosphere in temperate latitudes.

side to the shear of the storm circulation itself, thus, adding to the factors tending to limit a storm's growth.[13]

The foregoing analysis has not utilized all elements of our theory, which could be used more carefully to define the sizes of convective elements large enough to be sustained in the presence of horizontal diffusion and small enough not to be the cause of their own turbulent breakdown. For example, we might examine an array of figures like figure 16 prepared

[13] And, possibly, contributing to the development of new storms on the downshear side of old ones. (See sec.5.3.

for different values of the environmental lapse rate and k_5, along with figures 19 and 20. It seems, however, that an effort involved in this refinement would be better directed at this stage toward further examination of the theory's premises. It is encouraging though, to note that the range of storm diameters (5-25 km) suggested by this simple theory is similar to that observed (see fig. 21, but we need also to be mindful that the radar echo boundaries are not identical with updraft boundaries).

5.3 Inferences for Storm Behavior and Empirical Tests

We give here a rather speculative topical commentary on thunderstorm behavior as it is or may be, in light of the theory.

(1) Role of Perturbations. Perturbations are emphasized in this theory. Unless their horizontal dimension and amplitude are above a critical size that depends on environmental parameters, sustained model convection does not occur. We are, therefore, led in forecasting to renew our surveillance of possible perturbation sources, and to examine data obtained by experimental observational networks that can shed more light on the connection between starting perturbations and real thunderstorms.

(2) Diurnal and Geographical Variations of Storm Behavior. The maximum frequency of thunderstorms and tornadoes over most of the United States occurs during the evening hours rather than during the hottest part of the day at the ground (Flora, 1954; Rasmussen, 1970); some of Rasmussen's data is illustrated here as figure 22. Consider that during the early afternoon, the horizontal dimensions of disturbances in the planetary boundary layer (PBL) are apt to be small because of a steep lapse rate in that layer. Then we expect towering clouds that develop to be small in proportion to their roots, and to suffer correspondingly large losses of buoyant energy by entrainment of ambient air. During the evening and at night, however, the boundary layer becomes internally stable, while often retaining its essential warmth with respect to higher layers. Then larger convergence areas can exist in the PBL without breakdown, and the PBL should also then admit gravity waves whose propagation and superposition may be significant for the initiation of sustained deep convection. We also note a related effect in the PBL which may contribute to

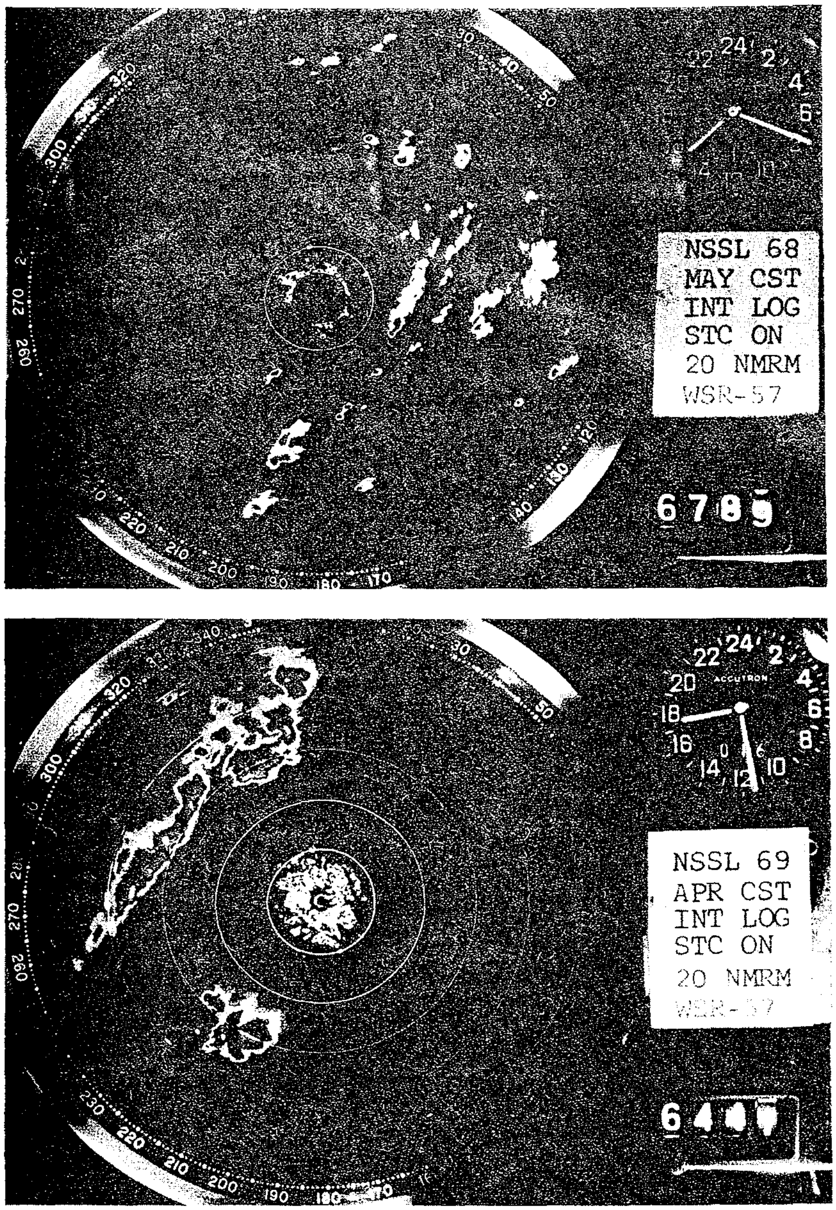

Figure 21. Photographs of the PPI display of the NSSL WSR-57 radar, May 13, 1968 (top) and April 16, 1969. Range marks are at intervals of 20 nmi. The size of cells within a group may be associated with a moist conditioning of air by the cells themselves, requiring an approximation to $\Delta\theta_w$ in equation (15) in place of $\Delta\theta$. Cell sizes and intensities appear to be characteristic of the occasion, and presumably, the air mass.

the observed diurnal variation of convective storms; the stronger coupling of a deep air layer with terrain at midday should inhibit the involvement in deep convection of the boundary layer air, the principal reservoir of vigorous storms' energy and moisture.[14]

Figure 22 shows that early afternoon storms are prominent along the Gulf Coast, in the Rocky Mountains, and in the Appalachian Mountains. We may expect mountain topography to provide strong local heat sources that would promote overturning during the hottest part of the day at the ground, on the scale of topographical irregularities. With regard to the afternoon maximum of thunderstorm activity along the Gulf Coast, indicated in Rasmussen's data, we note that our theory indicates that smaller scale convection can be sustained in moister atmospheres. Thus, the smaller scale of convection inferred for the unstable boundary layer characteristic of midday, may give rise to absolute buoyancy when the air is sufficiently moist. The early maxima along the Gulf Coast should also be promoted by the sea breeze, and in Florida by peninsula-induced convergence (Frank, et al., 1967).

(3) The Highly Turbulent Nation of Thunderstorms. Our application of Richardson's theory suggests a fresh view of storm turbulence. The air in the environment of a storm may be nonturbulent in the presence of its own vertical shear because it is only conditionally unstable. When this air is sufficiently lifted by the storm circulation, however, it becomes cloudy and its Richardson Number becomes zero or negative. Then its vertical shear would contribute to the amplification of ubiquitous small disturbances. The shear of the environment would also act to induce some shear in the column of warm air rising from low altitudes in the storm core, with promotion of the multi-turreted boiling appearance so characteristic of storms.

---

[14] We also propose that the rapid changes of cloud forms, commonly witnessed in late afternoon over land areas, are associated with a rapid transition at this time of the boundary layer from an unstable layer strongly coupled to terrain, to a thin stable layer overlain by a deep, warm, and moist decoupled layer.

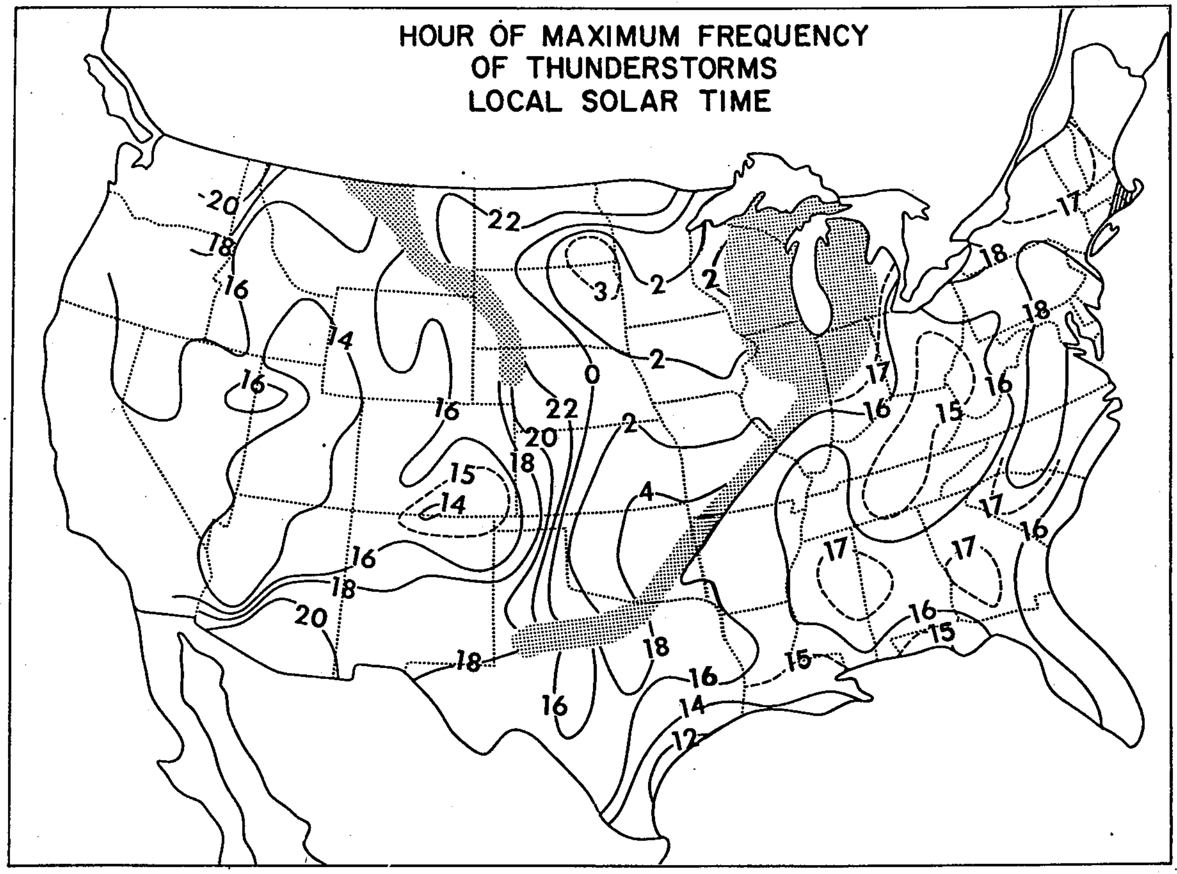

Figure 22. Local solar time of maximum thunderstorm frequency over the United States.

We might use aircraft and Doppler radar to investigate the turbulence within storms in relation to vertical shear in the storm environment.

(4) Right- and Left-Moving Storms, and Storms That Split. Severe storms commonly move markedly to the right or to the left of the mean-layer winds, right-movers being more frequent. Explanations have involved availability of atmospheric moisture and dynamic effects including effects of storm rotation (Newton, 1960; Fujita, 1968; Charba and Sasaki, 1968; Kuo, 1970). We particularly note Fankhauser's report (1971) which includes discussion of one of the class of storms that move with the wind while not severe, and to the right of the wind while severe. During a nonsevere period, we expect the

horizontal momentum of storm air to adjust more nearly to the average in the environment because its slower ascent gives it more time to do so. During a severe period, however, the more rapid replacement of storm air by fresh low-level air would be associated with a greater difference between the horizontal motion of storm air and environmental air, and more of a barrier effect. Then the air at mid-levels would tend more to flow around the storm with its speed enhanced by the Bernoulli effect as shown in figure 23. Then the greatest vertical shear would be in areas on the southeast and northwest sides of the storm, and local disturbances that are always present would be most prone to grow in these areas. Investigators have noted that the right- and left-moving storms are actually associated with new cell development on their southeast and northwest sides, respectively.

This explanation of the motion of severe storms is quite incomplete, but along with the other proposed explanations, it seems deserving of further investigation, including, of course, study of the factors that may favor development on one or the other of the southeast or northwest sides.

Radar observations of storms often shows a splitting into right- and left-moving parts (see Fankhauser, 1971, fig. 20). The storms that split and their fragments are often large and intense. Perhaps the splitting is an effect of the circulation on itself, as suggested in section 5.2.

(5) Propagation of Storms. Severe storms and showers sometimes move ahead of the cold front often identified as their primary cause, while on other occasions, the storms may remain along the causal front. In terms of our theory, the latter condition would be identified with disturbances which are, in some sense, of subcritical size and/or amplitude.

In a nearly homogeneous conditionally unstable air mass, the largest disturbances ahead of a storm line may be produced by the already existing storms. In addition to the well-advertised effect of cold air underrunning, we may consider the effect of the storm circulation in changing the vertical shear of the horizontal wind near the storms. Then the propagation of storms, i.e., the

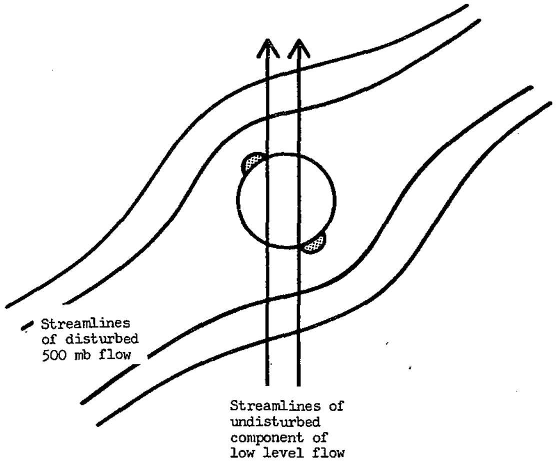

Figure 23. To the extent that a severe storm acts as a barrier in potential flow, the speed of a typical southwesterly flow aloft would be most increased in the shaded areas on northwest and southeast sides of the storm. The intensified vertical shear near these areas might then provide a source of energy for the amplification of small vertical disturbances to a magnitude where conditional buoyant energy would become available. The resultant motion of the whole storm complex would correspond to left- and right-moving storm cases when new development is favored in northwest or southeast areas, respectively (Hammond, 1967; Haglund, 1969; Fankhauser, 1971, esp. his figures 6B and 16).

direction of development of new storms, may be toward the place where the vertical shear is locally enhanced, and the pace of storm propagation should depend on the environment's instability and already existing shear. It seems worthwhile to investigate the Richardson Number as a forecasting parameter.

6. CONCLUDING REMARKS

The principal results of this work are discussed in the Abstract and Introduction, and in sections 4 and 5. The forms of model convection given by the theory are summarized in figure 24.

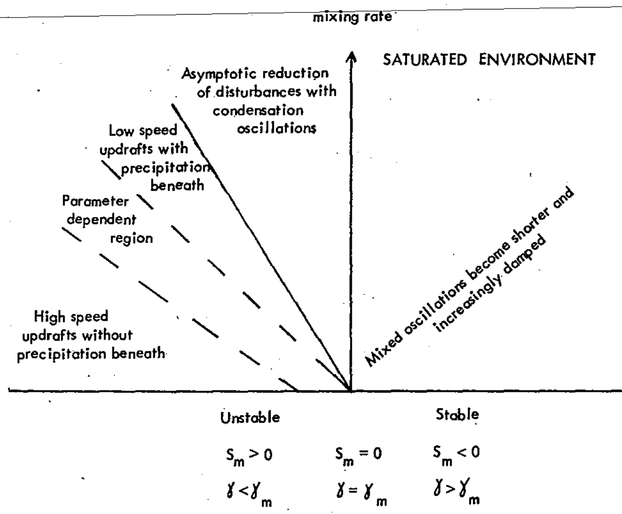

Figure 24. Modes of model air motion in relation to lapse rate and mixing rate in dry and saturated model environments. The location of boundaries of the parameter-dependent region depends on the amplitude of model disturbances and microphysical processes. The more complicated conditionally unstable cases are discussed in section 4.3.

Our model emphasizes the importance of substantial perturbations for initiation of sustained convection in conditionally unstable cases. Thus, we sense a confirmation of the widely held belief that more accurate forecasting of convection will depend greatly on more detailed observations of percursor phenomena. The practical importance of improved theories should lie in their indication of the types of weather data that should be obtained and processed for application to storm-forecasting operations.

It may be worthwhile to test some features of the model further. For example, solutions might be obtained with various shapes of the environmental moisture profiles, but with the total vapor content held constant in order to estimate the effect of the vapor distribution on the occurrence and intensity of convection. The atmosphere's ability to store its instability against the occurrence of a disturbance of sufficient amplitude and horizontal size might be evaluated further by use of the model. Atmospheric data might be studied to evaluate the role of environmental shear on the propagation of real storms, and the development of storms in real cases might be investigated in light of combined effects of large-scale disturbances and boundary layer effects discussed in section 5. Perhaps some useful new forecasting parameters or rules could be discovered.

The reader may have already considered several ways by which the present model could be improved. For example, hail could be treated more realistically by requiring that the drop-size parameter N_o increase during descent of precipitation through a melting level. Or, with the aid of some carefully designed constraints, the parabolic vertical velocity profile might be replaced by a distribution more reflective of local, rather than average, buoyancy. We judge the first modification would probably not change the conclusions substantially, nor significantly enlarge their scope. The second would probably affect the answers considerably, but one wonders how far to carry a model, as simplified as this one is with respect to entrainment processes and environmental effects on the vertical gradient of pressure. We note also that features such as these are already present in other models.

Perhaps more important at this stage than ad hoc improvements to our model, are further theoretical and experimental examinations of entrainment mechanisms, of the turbulent breakdown or growth of organized disturbances, of energy dissipation in the boundary layer, and of the coupling between the boundary layer and higher layers. These processes and relationships must be critical ingredients of a realistic numerical model of time-dependent deep moist convection in a two- or three-dimensional space.

Finally, we emphasize that a great virtue of a numerical model is its susceptibility to improvement based on empirical tests and theoretical reasoning. Especially where facilities are available, as at the NSSL, to observe phenomena on the scale of thunderstorms, contemporaneous study of storm models and observational data can provide much valuable guidance and more rapid evolution of new knowledge.

7. ACKNOWLEDGMENTS

Dr. Rex Inman of Oklahoma University noted the relationship of two of the basic equations in this paper with Priestley's earlier model, at an intermediate stage of our investigation. Dr. Edward A. Newburg of Virginia Commonwealth University, provided guidance to the solution of differential equations by finite differences. Various helpful suggestions were also provided by Prof. Frank H. Ludlam of Imperial College, London; Prof. Fred Sanders of MIT, Cambridge, Mass., and by several of the staff at the National Severe Storms Laboratory.

8. REFERENCES

Arnason, G., R.S. Greenfield, and E.A. Newburg (1968), A numerical experiment in dry and moist convection including the rain state, J. Atmos. Sci. 25, No. 3, 405-415.

Browning, K.A. (1964), Airflow and precipitation trajectories within severe local storms which travel to the right of the winds, J. Atmos. Sci. 21, No. 6, 634-639.

Brunt, D. (1927), The period of simple vertical oscillations in the atmosphere, Quart. J. Roy. Meteorol. Soc. 53, 30-32.

Byers, H.R., and R.R. Braham (1949), The Thunderstorm, U.S. Government Printing Office, Washington, D.C., 287 pp.

Charba, J., and Y. Sasaki (1968), Structure and movement of the severe thunderstorms of 3 April 1964 as revealed from radar and surface mesonetwork data analysis, NSSL Tech. Memo. No. 41, 47 pp.

Das, P. (1964), Role of condensed water in the life cycle of a convective cloud, J. Atmos. Sci. 21, No. 4, 404-418.

Fankhauser, J.C. (1971), Thunderstorm-environment interactions determined from aircraft and radar observations, Monthly Weather Rev. 99, No. 3, 171-192.

Flora, S. (1953), Tornadoes of the United States, (Univ. of Okla. Press, Norman, Okla.), (see pp. 56-57).

Frank, N.L., P.L. Moore, and G.E. Fisher (1967), Summer shower distribution over the Florida Peninsula as deduced from digitized radar data, J. Appl. Meteorol. 6, No. 2, 309-316.

Fujita, T., and H.Grandoso (1969), Split of thunderstorm into anticyclonic and cyclonic storms and their motion as determined from numerical model experiments, J. Atmos. Sci. 25, No. 3, 416-439.

Haglund, G.T. (1969), A study of a severe local storm of 16 April 1967, NSSL Tech. Memo. No. 44.

Hammond, G.R. (1967), Study of a left-moving thunderstorm of 23 April 1967, NSSL Tech. Memo. No. 31.

Kessler, E. (1969), On the continuity of water substance in atmospheric circulations, Meteorol. Monographs 10, No. 32.

Kuo, H.L. (1969), Motions of vortices and circulating cylinder in shear flow with friction, J. Atmos. Sci. 26, No. 3, 390-398.

Ludlam, F.H. (1963), Severe local storms: A review, Meteorol. Monographs 5, No. 27, 1-30.

Mason, B.J., and R. Emig (1961), Calculations of the ascent of saturated buoyant parcel with mixing, Quart. J. Roy. Meteorol. Soc. 87, No. 372, 212-222.

Murray, F. (1970), Numerical models of a tropical cumulus cloud with bilateral and axial symmetry, Monthly Weather Rev. 98, No. 1, 14-28.

Newton, C.W. (1960), Hydrodynamic interactions with ambient wind field as a factor in cumulus development, Cumulus Dynamics, ed. C.E. Anderson, 135-143 (Pergamon Press, New York, N.Y.).

NBS (1964), Handbook of mathematical functions, Applied Math. Series No. 55, ed. M. Abramowitz and I.A. Stegun (U.S. Government Printing Office, Washington, D.C.).

Orville, H.D., and L. J. Sloan (1970), A numerical simulation of the life history of a rainstorm, J. Atmos. Sci. 27, No. 8, 1148-1159.

Pao, Y-H, and A. Goldburg, eds. (1969), Clear Air Turbulence and Its Detection (Plenum Press, New York, N.Y.).

Priestley, C.H.B. (1953), Buoyant motions in a turbulent environment, Australian J. Phys. 6, No. 3, 279-290.

Rasmussen, E. (1970), Diurnal variability of thunderstorms by months for 300 U.S. stations (unpublished).

Richardson, L.F. (1920), The supply of energy from and to atmospheric eddies, Proc. Roy. Soc. London, Ser. A 97, 354-373.

Richardson, L.F. (1926), Atmospheric diffusion shown on a distance-neighbor graph, Proc. Roy. Soc. London, Ser. A 110, 709-737.

Scorer, R.S., and F.H. Ludlam (1953), Bubble theory of penetrative convection, Quart. J. Roy. Meteorol. 79, No. 1, 94-103.

Simpson, P., and J.S. Turner (1962), An entraining jet model for cumulus-nimbus updrafts, Tellus XIV, No. 4, 422-435.

Srivastava, R.C. (1967), A study of the effect of precipitation on cumulus dynamics, J. Atmos. Sci. 24, No. 1, 36-45.

Takeda, Y. (1971), Numerical simulation of a precipitating convective cloud, The Formation of a Long Lasting Cloud, J. Atmos. Sci. 28, No. ,

Turner, J.S. (1963), The motion of buoyant elements in turbulent surroundings, J. Fluid Mech. 16, Pt. I, 1-16.

Warner, J. (1970), Steady state one-dimensional models of cumulus convection, J. Atmos. Sci. 27, No. 7, 1035-1940.

Weinstein, A.I. (1970), A numerical model of cumulus dynamics and microphysics, J. Atmos. Sci. 27, No. 2, 246-255.

APPENDIX A

THE CONDENSATION PARAMETER F_1

The condensation parameter F_1 is proportional to the rate of evaporation of cloud throughout the vertical air column. It accounts for the variable rate of condensation or evaporation of cloud with altitude.

The parameter F_1 is given by the sum of weighting functions calculated at each grid point where $m>o$, i.e., where cloud exists. The individual weights are proportional to the product of the condensation function with the vertical velocity at the grid point. The sum of the separate weights yields the number F_1 proportional to the rate at which cloud is condensed (or evaporated) throughout the updraft column in rising (or descending) cloud-containing air. As applied in (5), F_1 provides a rough accounting of the latent heat exchanged during the condensation and evaporation accompanying vertical motion of cloudy air; when cloud is absent everywhere, $F_1=0$.

The condensation function C.F. as given in table 1, is

$$\text{C. F.} = \frac{4w_{max}}{H} \left(z-\frac{z^2}{H}\right)(C_4 + C_5\, z), \qquad \text{(A-1)}$$

where C_5 is a negative quantity. A normalized weighting function is obtained when (A-1) is divided by its average value in the depth H times the number of grid points $\frac{H}{h}$. Thus, our weighting function, W.F., is

$$\text{W. F.} = \frac{6}{H} \; \frac{\left(z-\frac{z^2}{H}\right)(C_4 + C_5 z)}{\left(C_4 + C_5\, \frac{H}{2}\right)\ \left(\frac{H}{h}\right)} \quad . \qquad \text{(A-2)}$$

When cloud exists at every grid point, the sum of the weights, F_1, is $\frac{n^2-1}{n^2}$, i.e., very nearly unity.

The above discussion applies in cases where $H \leq - C_4/C_5$. When $H > - C_4/C_5$, the condensation function is set to zero where $z > -C_4/C_5$, and the weighting function is calculated on the basis of a revised equation that considers the moisture content only in the lower part of the updraft column.

The condensation parameter F_1 is plotted in figure A-1 in relation to the height of the base of a cloud that extends downward from a height H=10 km.

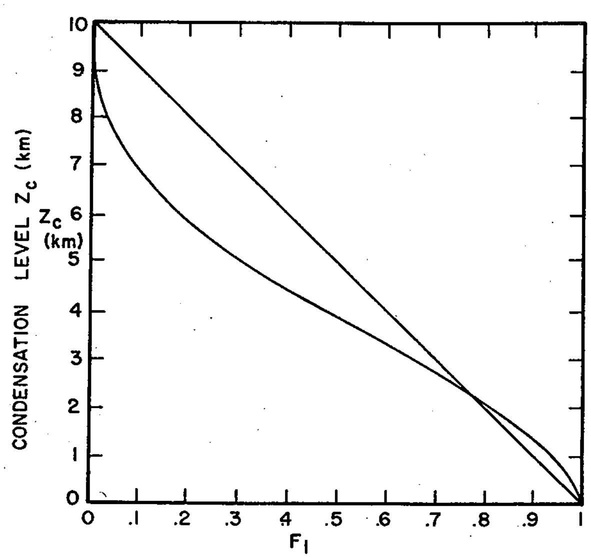

Figure A-1. The curved line is the condensation rate parameter F_1 in relation to the height of the base of a cloud extending downward from 10 km.

APPENDIX B

ADJUSTMENT OF S_m AND S_d DURING EVAPORATION IN THE SUBCLOUD LAYER

The following adds a detail to section 4 of the main text:

Specific values of the assigned parameter S_m and S_d are associated with a specific class of combinations of model environmental moisture and lapse rate conditions. The environmental conditions are, in turn, associated with a model condensation level and an average temperature excess or deficit following the motion of moist and dry parcels. Thus, S_m and S_d are related to the space-averaged thermal buoyancy of a non-entraining parcel which rises dry adiabatically to the convective condensation level and moist adiabatically thereafter.

When rain falls into the subcloud layer, that layer is moistened and cooled by evaporation. A tendency to change the buoyancy during this process is roughly accounted for by the term ε_M in (5). We need also to account for the change that has occurred when evaporation of precipitation has proceeded to some limit with corresponding cooling of the subcloud layer. The average buoyancy is then less than in the case of parcel ascent without precipitation, implied in the original choice of S_m.

The effect on buoyancy of a lowering condensation level is roughly represented by a change in S_m based on the change in surface moisture represented by $m_{o,t}$. The value, $m_{o,t}$ determines the (steady state) height of the corresponding convective condensation level (z_c). With mixing neglected, the relationship between z_c and the saturation deficit at time t, at the ground, m(o,t), is

$$m_{o,t} = \exp(-k_7 z_c) \left\{ \frac{1}{k_7} \left[\frac{C_5}{k_7} + C_4 + C_5 z_c \right] \right\} - \frac{1}{k_7} \left[\frac{C_5}{k_7} + C_4 \right] \quad \text{(B-1)}$$

where $k_7 = -\frac{\partial \ln \rho}{\partial z}$ and $C_4 + C_5 z$ is the assumed condensation function (see table 1, page 5 of main text). For small values of z_c, (B-1) is closely approximated by

$$z_c = -3.3 \times 10^2 m_{o,+} \text{ meters} \quad , \tag{B-2}$$

when $C_4 = 3\times10^{-3}$ and $C_5 = -3\times10^{-7}$.

The computer program uses the value of m at z=0 to estimate the amount by which the moisture content has been changed in the subcloud layer as follows:

(a) The starting convective condensation level $z_{c,o}$ is calculated with (B-2).

(b) The average saturation deficit $\overline{m}_d$ applicable to the layer $0<z<z_c$ is calculated from the initial (environmental) moisture profile in that depth, as weighted by the factor z_c/H.

(c) At every time step, the computer changes S_m according to the implied average cooling of the lower level indicated by the current value of $m_{o,t}$ according to the equation:

$$S_m = S_m(\text{input}) - 0.1\ \overline{m}_d\ \frac{m_{o,t} - m_{o,o}}{m_{o,o}} \tag{B-3}$$

where the factor 0.1 has the same basis as the coefficient for the evaporation term in (5).

As an example, suppose that input S_m=0.2, corresponding to a lapse rate intermediate between the moist and dry adiabatic rates, and suppose that the environmental moisture is given by

$$m_{z,o} = -3+6\times10^{-4}\ z - 3\times10^{-8}\ z^2 \quad , \tag{B-4}$$

then $z_c = 10^3$ meters and $\overline{m}_d = -.27$. When evaporation of precipitation has increased surface moisture to $m_{o,t} = -1.5$, for example, we have

$$S_m = 0.2 - 0.1\times(-0.27)\left[\frac{-1.5+3.0}{-3.0}\right]$$

$$= .1865 \quad .$$

The parameter S_d is simultaneously altered so that the equality $S_m+S_d=0.4$ continues to be satisfied (see page 10).

It seems that a correction to the term for evaporation of cloud should also be given in a cloud layer beneath the original CCL. A more comprehensive approach would facilitate the desired use of more rigorous arguments.

APPENDIX C

COMPARISON OF VERTICAL VELOCITY AND BUOYANCY EQUATIONS WITH THOSE OF PRIESTLEY'S MODEL

Here we compare Priestley's thermodynamical equations with those of this paper as specialized for application to a dry atmosphere. Priestley's equations [(7) and (8) in his 1953 paper], applicable to parcels, are

$$\frac{dw}{dt} = \frac{gT'}{T_e} - k_1 w \quad , \tag{C-1}$$

$$\frac{dT'}{dt} = \left(w \, \frac{\partial T_e}{\partial z} + \Gamma \right) - k_2 T' \quad , \tag{C-2}$$

where $\partial T_e/\partial z$ is the lapse rate in the environment, Γ is the magnitude of the dry adiabatic lapse rate, T' is the temperature difference between the parcel and its environment, and k_1 and k_2 are mixing rates for momentum and heat, respectively.

Our dry equations, as presented in section 3.8, are

$$\frac{\partial w_{max}}{\partial t} = 1.5 \left[A - \left|\frac{A}{H}\right|^{\frac{1}{2}} w_{max} \right] - k_5 \, w_{max} \quad , \tag{9}$$

$$\frac{\partial A}{\partial t} = \frac{w_{max}}{H} \left[S_d + A \right] - k_5 A \tag{10}$$

In Priestley's notation, the thermal buoyancy A_{th} is represented by $\frac{gT'}{T_e}$,and our potential thermal buoyancy S_d is defined by $\frac{gH}{2T_e}\left(\frac{\partial T_e}{\partial z} + \Gamma\right)$. In other words, S_d is the average value of the acceleration that would act on an air column lifted from the surface to level H with individual temperature changes $-\Gamma$, in an environment whose lapse rate is $\partial T_e/\partial z$. In our equations, we have equated the mixing rates for heat and momentum, and denoted them as k_5. With these comparisons, we rewrite Priestley's equations in our notation:

$$\frac{dw}{dt} = A - k_5 w \quad , \tag{C-1a}$$

$$\frac{dA}{dt} = -\frac{2w}{H} S_d - k_5 A \quad . \tag{C-2a}$$

As discussed in section 3.8, (9) and (10) define steady state relationships

$$S_d = k_5 \left[(AH)^{\frac{1}{2}} + \frac{2}{3} k_5 H \right] - A \ , \tag{11}$$

and

$$w_{max} = \frac{k_5 HA}{S_d + A} \quad . \tag{12}$$

For values of $S_d < -\frac{2}{3} k_5^2 H$, solutions of (9) and (10) drift asymptotically toward values of w, S_d and A defined by the simultaneous solutions of (11) and (12). The solutions, corresponding to Priestley's absolute buoyancy, are plotted in figure 11, page 24 of main text. When $-\frac{2}{3} k_5^2 H < S_d \leq 0$, corresponding to the region called asymptotic by Priestley, (11) is not satisfied by any positive or negative value of A and the only steady state solution of (9) and (10) is zero vertical velocity, also approached asymptotically from any disturbed starting state. When $S_d > 0$, a statically stable model condition, a disturbance is followed by damped oscillations as discussed by Priestley and in section 3.7.

In our notation, Priestley's absolutely buoyant region is defined by (C-1a) and (C-2a) where $S_d < -0.5\ k_5^2 H$. Priestley's asymptotic region in his model exists when $-.5k_5^2 H < S_d \leq 0$.

It is interesting to compare the critical diameters, D_c, that define the boundary between absolute buoyancy and the asymptotic region, as defined by Priestley's model and by this one as specialized for the dry case. By combining the thresholds defined above with the relationship (13) in the text, we obtain for our theory

$$D_c = -\ 0.03 \left(\frac{H}{S_d}\right)^{3/4} \text{ meters} \tag{C-3}$$

and

$$D_c = -\ 0.025\ \left(\frac{H}{S_d}\right)^{3/4}\ \text{meters} \qquad \text{(C-4)}$$

for Priestley's. Equation (C-3) has been applied to determine some of the relationships illustrated in figure 11. The difference between (C-3) and (C-4) is, of course, much smaller than the uncertainty in our knowledge of the applicability of our mixing rate concept.

APPENDIX D

CALCULATION OF STEADY STATE VERTICAL PROFILES OF PRECIPITATION IN STEADY VERTICAL AIR CURRENTS

In order to investigate certain features of steady state solutions without resorting to extended marching computations, the equations for cloud and precipitation [(1) and (2)] are added together

$$\frac{\partial (M+m)}{\partial t} = -(w+V)\frac{\partial M}{\partial z} - w\frac{\partial m}{\partial t} + wG + (m+M)w\frac{\partial \ln\rho}{\partial z} - M\frac{\partial V}{\partial z}$$

$$- k_5 M - k_5 (m - m_0) . \qquad \text{(D-1)}$$

In the steady state, the time derivative is zero, and with w and V of the same order in a moist atmosphere, we neglect m since usually m<<M in such cases. Then (D-1) becomes

$$0 = -(w+V)\frac{\partial M}{\partial z} + wG + Mw\frac{\partial \ln\rho}{\partial z} - M\frac{\partial V}{\partial z} - k_5 M . \qquad \text{(D-2)}$$

Note (table 1, page 5) that V may be given as

$$V = k_o M^{1/8} \exp(k_7 z/2) . \qquad \text{(D-3)}$$

Then

$$\frac{\partial V}{\partial z} = \frac{V}{8M}\frac{\partial M}{\partial z} + \frac{k_7}{2} V . \qquad \text{(D-4)}$$

Substitution for $\frac{\partial V}{\partial z}$ and solution for $\frac{\partial M}{\partial z}$ yields

$$\frac{\partial M}{\partial z} = \frac{w(G + M\frac{\partial \ln p}{\partial z}) - M(\frac{k_7}{2} V + k_5)}{w + 1.125V} . \qquad \text{(D-5)}$$

This equation is solved numerically by a fourth order Runge-Kutta method for the first three points and a faster Milne predictor-corrector method for the remaining points (see NBS, 1964, p. 896). Physically, the upper boundary condition is $M_H=0$. With that condition, however, $\frac{\partial M}{\partial z}$ at z=H is also zero and the numerical technique fails. Therefore, a starting value $M=10^{-7}$ at z=H is used.

The integration proceeds from z=H downward. If w+1.125V remains negative throughout the integration, the solution is realistic. In other cases, the problem as given is inadequately posed.

Figure D-1 lists a representative calculated M-profile. A small computer such as the IBM 1620 yields such a profile with the program listed in figures D-2 a,b,c in about 5 min of calculation time.

WMAX= 5.00M/SEC
NO= .10000000E+08
MO= .10000000E-06GM/M**3
DH= -50.000M
K5= .00000000E-50

Z	M	DM/DZ	W	V	W+1.125*V
10000.0	.000000	-.44444E-11	-.00000	-1.13170	-1.27317
9750.0	.000969	-.10561E-04	.48750	-3.52085	-3.47346
9500.0	.006478	-.35740E-04	.95000	-4.40870	-4.00979
9250.0	.019927	-.73992E-04	1.38750	-5.01049	-4.24930
9000.0	.044532	-.12494E-03	1.80000	-5.47147	-4.35540
8750.0	.083436	-.18835E-03	2.18750	-5.84468	-4.38776
8500.0	.139721	-.26392E-03	2.55000	-6.15631	-4.37584
8250.0	.216371	-.35117E-03	2.88750	-6.42146	-4.33664
8000.0	.316226	-.44941E-03	3.20000	-6.64974	-4.28096
7750.0	.441917	-.55767E-03	3.48750	-6.84768	-4.21615
7500.0	.595794	-.67467E-03	3.75000	-7.01996	-4.14745
7250.0	.779854	-.79884E-03	3.98750	-7.17002	-4.07877
7000.0	.995655	-.92827E-03	4.20000	-7.30052	-4.01308
6750.0	1.244252	-.10608E-02	4.38750	-7.41353	-3.95272
6500.0	1.526121	-.11940E-02	4.55000	-7.51072	-3.89956
6250.0	1.841113	-.13253E-02	4.68750	-7.59345	-3.85513
6000.0	2.188417	-.14520E-02	4.80000	-7.66287	-3.82073
5750.0	2.566549	-.15715E-02	4.88750	-7.71997	-3.79746
5500.0	2.973361	-.16811E-02	4.95000	-7.76558	-3.78628
5250.0	3.406085	-.17784E-02	4.98750	-7.80048	-3.78804
5000.0	3.861393	-.18614E-02	5.00000	-7.82535	-3.80352
4750.0	4.335484	-.19284E-02	4.98750	-7.84082	-3.83343
4500.0	4.824191	-.19782E-02	4.95000	-7.84750	-3.87844
4250.0	5.323091	-.20099E-02	4.88750	-7.84594	-3.93919
4000.0	5.827629	-.20233E-02	4.80000	-7.83669	-4.01627
3750.0	6.333234	-.20185E-02	4.68750	-7.82025	-4.11028
3500.0	6.835426	-.19961E-02	4.55000	-7.79712	-4.22176
3250.0	7.329909	-.19570E-02	4.38750	-7.76778	-4.35126
3000.0	7.812645	-.19023E-02	4.20000	-7.73270	-4.49928
2750.0	8.279911	-.18335E-02	3.98750	-7.69229	-4.66633
2500.0	8.728336	-.17518E-02	3.75000	-7.64699	-4.85286
2250.0	9.154912	-.16589E-02	3.48750	-7.59717	-5.05932
2000.0	9.556998	-.15562E-02	3.20000	-7.54322	-5.28612
1750.0	9.932308	-.14449E-02	2.88750	-7.48547	-5.53365
1500.0	10.278889	-.13265E-02	2.55000	-7.42425	-5.80228
1250.0	10.595081	-.12020E-02	2.18750	-7.35984	-6.09232
1000.0	10.879505	-.10725E-02	1.80000	-7.29252	-6.40409
750.0	11.131001	-.93881E-03	1.38750	-7.22254	-6.73786
500.0	11.348622	-.80161E-03	.95000	-7.15010	-7.09387
250.0	11.531571	-.66154E-03	.48750	-7.07541	-7.47234
.0	11.679196	-.51907E-03	-.00000	-6.99864	-7.87347

LBAR= .47279037E+01 GM/M**3

Figure D-1. Steady state profiles of precipitation and motion parameters based on Runge-Kutta calculations with a simplified numerical model.

```
C     SOLUTION OF PRECIPITATION CONTENT FROM THE STEADY STATE EQUATION
C     NSSL NO. 71-18
C     WRITTEN FOR IBM 1620
C     VERSION 3
C     MODIFICATION TO INCLUDE K5*M (29 JUL 1970)
C     VERSION 2 - COMPUTES LBAR - ALLOWS PRTING OF EVERY IP H
C     SSW 2 ON STEPPING IS STOPPED AND NEW DATA READ
C     DATA CARD
C       HTOP    TOP OF COLUMN
C       WMAX    VERTICAL VELOCITY
C       XMO     STARTING PERTURBATION OF M
C       XNO     DROP DISTRIBUTION PARAMETER
C       DELH    HEIGHT INCREMENT
C       IVP     IF NON ZERO. V IS HELD CONSTANT AT CK1*EXP(CK2*Z)
C       IP      OUTPUT EVERY IPTH LEVEL
C       XK5     I/P PARAMETER
C       IC      IF NON ZERO READS A SECOND CARD FOR SPECIAL RESTART
      DIMENSION Y(4),DV(4)
      PLNP=-1.E-4
      CK2= 0.5*PLNP
      XMOU=0.1
    1 READ 700,HTOP,WMAX,XMO,XNO,DELH,IVP,IP,XK5,IC
  700 FORMAT(5F10.0,2I5,F10.0,I5)
  600 FWMAX=4.0*WMAX/HTOP
      XM=XMO
      CK1= 38.6*XNO**(-.125)
      H=HTOP
      DH=-DELH
      IPX=0
      PUNCH 800,WMAX,XNO,XMO,DH,XK5
  800 FORMAT(79X,1H9,/5HWMAX=,F10.2,5HM/SEC,/5H  NO=,E15.8,
     1/5H  MO=,E15.8,7HGM/M**3,/5H  DH=,F9.3,1HM,
     2/5H  K5=,E15.8,/)
      IF(IVP)3,4,3
    3 PUNCH 803,CK1,CK2
  803 FORMAT(18HV HELD CONSTANT AT,F10.2,5H*EXP(,E9.2,3H*Z))
    4 PUNCH 804
  804 FORMAT(6X,1HZ,12X,1HM,8X,5HDM/DZ,10X,1HW,10X,1HV,8X,9HW+1.125*V)
      IF(IC)10,11,10
   10 READ 700,XM,H
   11 DH2=DH*0.5
      CPTS=-H/DH
      CP=CPTS
      XL=0.0
      LB=1
C     COMPUTE FIRST 3 PTS. BY 4TH ORDER RUNGE-KUTTA.
      EXECUTE PROCEDURE 200
      X=XM
      Z=H
      EXECUTE PROCEDURE 100
      EXECUTE PROCEDURE 300
      Y(1)=XM
      DO 2 I=2,4
      XK1=DH2*FUN
      Z=H+DH2
      X=XM XK1
      EXECUTE PROCEDURE 100
      XK2=DH2*FUN
      X=XM XK2
      EXECUTE PROCEDURE 100
      XK3=DH*FUN
      Z=H+DH
      X=XM XK3
      EXECUTE PROCEDURE 100
      XK4=DH*FUN
      XM=XM+(2.0*(XK1+XK3)+4.0*XK2+XK4)/6.0
```

Figure D-2a. List of program used to calculate the vertical profiles shown in figure D-1. The parameter CK2 in this program is $k_7/2$ elsewhere in this report and the parameter CK1 is k_o elsewhere.

```
      EXECUTE PROCEDURE 200
      H=H+DH
      Z=H
      X=XM
      EXECUTE PROCEDURE 100
      EXECUTE PROCEDURE 300
      Y(I)=XM
      DV(I)=FUN
    2 CONTINUE
C     USE MILNE'S METHOD FOR THE REMAINING POINTS.
      CPTS=CPTS-3.0
      CI=0.0
      H3=DH/3.0
      FH3=4.*H3
   20 H=H+DH
      T=DV(4)+DV(2)
      X=Y(1)+FH3*(T+T-DV(3))
      Z=H
      EXECUTE PROCEDURE 100
      X=Y(3)+H3*(DV(3)+4.*DV(4)+FUN)
      XM=X
      EXECUTE PROCEDURE 200
      EXECUTE PROCEDURE 100
      EXECUTE PROCEDURE 300
      Y(1)=Y(2)
      Y(2)=Y(3)
      Y(3)=Y(4)
      Y(4)=X
      DV(2)=DV(3)
      DV(3)=DV(4)
      DV(4)=FUN
      CI=CI+1.0
      IF(CI-CPTS)20,30,30
   30 LB=3
      EXECUTE PROCEDURE 200
      XL=XL/CP
      PUNCH 806,XL
  806 FORMAT(/,5HLBAR=,E17.8,8H GM/M**3)
      GO TO 1
C**PROC. TO CALCULATE FUNCTION**
      BEGIN PROCEDURE 100
      W=FWMAX*Z*(1.0-Z/HTOP)
      G=3.E-3-3.E-7*Z
      IF(IVP)101,102,101
  101 V=CK1*EXP(CK2*Z)
      IF(X)108,104,104
  102 IF(X)108,107,103
  107 V=0.0
      GO TO 110
  108 PRINT 900,Z,X
  900 FORMAT(8HM IS NEG,2E17.8)
      PUNCH 805,Z,X
  805 FORMAT(F10.1,F13.6,9H M IS NEG)
      XMO=XMO*10.0
      IF(XMO-XMOU)600,600,1
  103 V=CK1*(X**.125)*EXP(CK2*Z)
  110 IF(W)104,111,104
  111 IF(V)104,112,104
  112 FUN=G
      GO TO 105
  104 WV=W 1.125*V
      FUN=(W*(G+X*PLNP)-(CK2*V+XK5)*X)/WV
      IF(SENSE SWITCH 2) 106,105
  106 PAUSE
      GO TO 1
  105 CONTINUE
```

Figure D-2b. Continuation of figure D-2a.

```
      END PROCEDURE 100
C**PROC. TO COMPUTE LBAR**
      BEGIN PROCEDURE 200
      IF(XM)210,210,202
  202 GO TO (204,206,208),LB
  204 XL=XL+0.5*XM
      LB=2
      GO TO 210
  208 XL=XL-0.5*XM
      GO TO 210
  206 XL=XL+XM
  210 CONTINUE
      END PROCEDURE 200
C**PUNCH PROC.**
      BEGIN PROCEDURE 300
      IPX=IPX-1
      IF(IPX)302,302,304
  302 IPX=IP
      PUNCH 802,Z,X,FUN,W,V,WV
  802 FORMAT(F10.1,F13.6,E13.5,2F11.5,F14.5)
  304 CONTINUE
      END PROCEDURE 300
      END
```

Figure D-2c. Continuation of figure D-2a.

APPENDIX E

COMPUTER PROGRAM FOR THE COMPLETE NUMERICAL MODEL

E.1. Finite Difference Forms

The finite difference techniques employed are a logical extension of the program discussed by Newburg and Kessler (Kessler, 1969). Equations (1) and (2) are rewritten in the form

$$\frac{\partial M}{\partial t} = -(w+V)\frac{\partial M}{\partial z} + BCM \ , \tag{E-1}$$

$$\frac{\partial m}{\partial t} = -w\frac{\partial m}{\partial z} + BSM \ . \tag{E-2}$$

The finite difference forms for the interior points are:

$$M(z,t+k) = \overline{M}(z,t) + \frac{k}{2h}[(V(z-h,t) + w(z-h,t))\ M(z-h,t)$$
$$-(V(z+h,t) + w(z+h,t))\ M(z+h,t)]$$
$$+\frac{k}{2}[BCM(z+h,t) + BCM(z-h,t)], \tag{E-3}$$

$$m(z,t+k) = \overline{m}(z,t) + \frac{k}{2h}[w(z-h,t)\ m(z-h,t) - w(z+h,t)\ m(z-h,t)]$$
$$+\frac{k}{2}[BSM(z+h,t) + BSM(z-h,t)] \ , \tag{E-4}$$

where

$$\overline{M}(z,t) = \frac{1}{2}[M(z+h,t) + M(z-h,t)] \ , \tag{E-5}$$

$$\overline{m}(z,t) = \frac{1}{2}[m(z+h,t) + m(z-h,t)] \ . \tag{E-6}$$

At the lower boundary, the form is

$$M(o,t+k) = M(o,t) + \frac{k}{h}[M(o,t)V(o,t) - M(h,t)V(h,t)]$$
$$+ k[BCM(o) - M(o,t)PW(o)] \ ; \tag{E-7}$$

$$m(o,t+k) = m(o,t) + k[BSM(o) - m(o,t)PW(o)] \quad ; \qquad (E\text{-}8)$$

where $PW = \frac{\partial w}{\partial z}$. At the grid point adjacent to the upper boundary, the cloud equation is handled in a special manner if $\overline{w} \geq 0$ (see footnote, p. 78). There,

$$m(H-h,t+k) = m(H-h,t) + \frac{k}{h}[m(H-2h,t)\,w(H-2h,t)$$

$$-m(H-h,t)\,w(H-h,t)] + k\ BSM(H-h); \qquad (E\text{-}9)$$

and on the top boundary

$$M(H,t+k) = C_9; \quad m(H,t+k) = m(H,t) \quad . \qquad (E\text{-}10)$$

In the precipitation equations (E-3) and (E-5), the averaging procedure generally causes a "fictitious" leaking (effective diffusion) of precipitation boeht upward and downward. Upward leaks in the model are self-stabilizing and have a natural counterpart in the upward motion of small drops among size-distributed precipitation particles. However, downward leaks from the base of a precipitation column, in the presence of general upward motion of precipitation, must be prevented in the model, because these can be self-amplifying under certain conditions and radically alter the character of the solutions.

At each point in height and time, we calculate

$$-(V+w)\frac{\partial M}{\partial z} \equiv \Delta M \approx \frac{1}{2h}\,[(V(z-h)+w(z-h))\,M(z-h,t)$$

$$-(V(z+h) + w(z+h))\ M(z+h)] + BCM(z) \quad . \qquad (E\text{-}11)$$

Wherever ΔM is positive, then

$$M(z,t+k) = \overline{M}(z,t) + k\ \Delta M, \qquad (E\text{-}12)$$

where $\overline{M}$ is given by (E-5).

Where $M(z,t) = 0$ and ΔM is zero or negative, however, we check $M(z-k,t)$. If $M(z-k,t) = 0$, then $M(z,t+k)$ is set to zero. Also, if $M(z-h,t)$ is positive, but there is no cloud at z, i.e., if $m(z,t) \leq 0$, then $M(z,t+k)$ is set to zero.

The finite difference forms for the vertical velocity and buoyancy equations, (4) and (5), are the standard forward-differencing schemes without averaging.

In the difference equations, a condition is placed on the time step k to insure stability. At the beginning of each time step, the smallest k of the following four is chosen: Initial k (DELK1), $\frac{.8h}{|V + Wmax|_{max}}$, $\frac{.8h}{|Wmax|}$, $\frac{1}{|\frac{dw}{dt}|}$. If k becomes less than 1.0 sec, the calculations are terminated.

Since negative values of M are physically impossible, the program tests M at all grid points at each time step and any negative M is set to zero.

E.2. Options

A. The initial conditions, and the first 10 time steps are always printed out. All other time steps printed are multiples of any whole number, such as every 5th or every 7th.

B. Either of two equations can be used to define the fall speed of precipitation, viz., $V(z)=C_6+C_7z$, or $V(z,t) = k_0/\rho(z)N_0^{-.125}M^{E_0}$, where $\rho(z) = \exp(k_7z/2)$, where C_6, C_7, k_0, k_7, N_0, and E_0 are input parameters.

C. The initial values of m(z) can be read in from cards or can be computed by the program from the equation:

$$m(z) = C_0 + C_1z + C_2z^2 \ .$$

The initial values of M(z) are always zero for all z, except that M at z-H can be a specified positive constant.

D. It is possible to reenter the program at either one of two problem times, t_1, or t_2, if $t_1<t_2$. If $t_2=0$, the program terminates at t_1. If $t_2>t_1$, each time step beyond t_1 is printed until t_2 is reached. This option is used mainly for debugging.

E.3. Arrangement and Format of Input and Output Data Cards

A. Input data cards for initial run. The first card is blank and is used in the program for comparative purposes.

<u>Card 1</u>. Title card containing any alphanumeric information in columns 1-72. (If blank, it causes termination of execution.)

<u>Card 2.</u> Control card (Format is 5I6).

Column	Program Notation	Contents
1-6	IP	This value determines what time step multiples will be printed out.
7-12	IN	This value determines which fall velocity equation will be used. If 1; $V(z)=C_6 + C_7 z$ If 2; $V(z,t)= k_0/\rho\ (z)N_0{}^{-.125}M^{E_0}$
13-18	JN	This value allows for re-entry. If 1; initial run. If 2; re-entry run.
19-24	KN	This value determines whether m(z,0) will be read in or whether it will be calculated by the program. If 1; calculated by the program. If 2; read in.
25-30	NT	The starting time step, always zero on initial runs.

Cards 3-10. Data cards containing problem constants (format is 6E12.5). The order of the constants and parameters on the data input cards are shown below. The format for each data input value is $\pm$ x.xxxxxE $\pm$ xx, with the sign starting in columns 1, 13, 25, 37, 49, and 61.

Card 3 contains $h, k, H, w_{max}, t_1, t_2$.

Card 4 contains $C_0, C_1, C_2, C_4, C_5, C_6$.

Card 5 contains $C_7, C_8, C_9, C_{10}, C_{11}, C_3$.

Card 6 contains E_0, E_2, E_3.

Card 7 contains k_0, k_1, k_2, k_3, N_0.

Card 8 contains γ, t, AR, RP, k_7 (t,AR, and RP are used for continuation runs only).

Card 9 contains $S_o, k_8, k_9, k_4, k_5, k_6$.

Card 10 contains S_m, S_d, F_4, t_s.

Cards 11 on: Data cards containing initial values of m(z). These cards, the first of which is illustrated below are accepted as input only if the value in column 24 of the control card is 2. Of course, these cards are never used for a reentry.

Column	Contents
1-12	$m(0,0)$
13-24	$m(z_1,0)$
25-36	$m(z_2,0)$
37-48	$m(z_3,0)$
49-60	$m(z_4,0)$
61-72	$m(z_5,0)$

The format is 6E12.5 and the cards are continued until the values m(z,0) are exhausted, and finally, a blank terminator card.

B. Punched output: Every run produces punched output cards headed by a card with T1 repeated across it. These cards contain the program control values, the problem constants and values of m and M at the last computed time step.

C. Input Data Cards for a Continuation Run: The T1 header card is removed from the punched output and the two cards described below are added to the back of the deck:

(1) Title card with any alphanumeric information in columns 1-72.

(2) Data card, format 6E12.5, showing t, in columns 1-12.

E.4. Computational Products and Program Lists

Figure E-1 (a-e) are selections from the printed products of the computer program, whose output is also illustrated in figure 12. Program input parameters are listed and explained in table E-1. Tables E-2 and E-3 explain the headings of various columns of the printed computational products (figs. E-1 (b-e)). A listing of the complete program is given in figure E-2.

*Table E-1. Program Input Parameters (fig. E-1a).**

Input Parameter	Computer Notation	Typical Value or Range	Explanation
h	DELH	H/100	Vertical increment.
k	DELK1	$k = h/2w_{max}$	Time increment used if machine computed DELTA T<k. Used to insure smooth transition from cloud only to cloud plus precipitation.
H	H	10^3-10^4	Height of the updraft column.
w_{max}	WMAX	0.0	Initial vertical speed.
t_1	T1	3000-10,000	Time when printout of all time steps begins.
t_2	T2	3000-10,000	Time when computations stops.
C_0	C0	0 to -10	The initial value of m is
C_1	C1	$-2C_o \times 10^{-4}$	$m = C_0 + C_1z + C_2z^2$ unless m(z,0)
C_2	C2	$C_o \times 10^{-8}$	is input.
C_3	C3	0	Coefficient in alternative mixing law (not used in this study). This is not the same C_3 that appears in Eq. (8).
C_4	C4	3×10^{-3}	The generation condensation function is $G = C_4 + C_5z$.
C_5	C5	-3×10^{-7}	
C_6,C_7	C6,C7	0	The fall speed of precipitation can be $V=C_6 + C_7z$. (Not used in this study.)
C_8	C8	1	Divides first condensation products between precipitation and cloud; when there is unity, all condensation forms cloud.
C_9	C9	0	Value of M at z = H.
C_{10}	C10	.5	Coefficients in the equation $\alpha=C_{10} + C_{11}z$, which describes
C_{11}	C11	0	the height variation of the auto-conversion threshold.
E_0	E0	.875	Exponent to M in fall speed equation.
E_2	E2	.125	Exponent to M in accretion term.
E_3	E3	.65	Exponent to M in evaporation term.
k_0	XKO	-38.6	Fall speed can be $V = [k_0/\rho]N_o^{-.125}\ M^{E_0}$.

Table E-1. Program Input Parameters (fig. E-1a). (Cont'd.)

Input Parameter	Computer Notation	Typical Value or Range	Explanation
k_1	XK1	10^{-3} to 10^{-4}	Coefficient to cloud conversion ter
k_2	XK2	6.96×10^{-4}	Coefficient to cloud collection ter
k_3	XK3	1.93×10^{-6}	Coefficient to evaporation term.
k_4	XK4	1	Multiplier of first bracketed term in Eq. (5).
k_5	XK5	10^{-3} to 10^{-4}	Mixing rate.
k_6	XK6	0.1	Factor to convert evaporation rate to buoyancy tendency.
k_7	XK7	10^{-4}	$\frac{\partial(\ln\rho)}{\partial z}$ (ρ is time-independent, horizontally uniform air density.
k_8	XK8	10^{-8}	Factor to convert water load to equivalent acceleration.
k_9	XK9	1	Multiplier of evaporation-of-cloud term.
N_0	XN0	10^7	Drop distribution parameter.
S_o	SZER	10^{-3} to 10^{-1}	Starting perturbation buoyancy; A_o in text.
S_M	SMOIST	0 to 0.4	0 - moist ad lapse rate, 0.4 - dry ad lapse rate.
S_D	SDRY	$0.4 - S_m$	See S_m.
--	F4	--	Effect of subsiding storm environment on S_m. (Not used in this study
t_s	TSTEP	100.	Printing increment in seconds for summary tables.
γ	GAM	0	When $\gamma \neq 0$, the initial values of m are adjusted to reflect a vertical displacement of air in advance of marching calculations (see (Kessler, 1969, eq. 12.4, p. 43; $\gamma = 4\alpha$).

* The order of entries here is not the same as the order in which they are entered on input data cards or printed by the program. All of these entries are part of the computer program listed in figure E-2, though all are not repeated in figure E-1a.

Table E-2. Explanation of Printout Column Headers (fig. E-1b,c).

Title on Computer Printout	Quantity
CLD H2O	m
PRECIP H2O	M
SM*DIV(W)	$m \frac{\partial w}{\partial z}$
CM*DIV(W)	$M \frac{\partial w}{\partial z}$
CLDCNVRSN	$k_1(m-a)$
ACRTN + EVAP†	$[k_2/\rho(z)]N_0^{.125} M^{E_2} m$ $+ k_3 N_0^{.35} M^{E_3} m$.
CNDNSTN	wG
RR	3.6MV at (z=0) = rainfall rate in mm/hr.
AR	$\int_o^T 3.6MVdt$=accumulated rainfall in mm.

†The accretion term is calculated when m>o and the evaporation term is calculated when m<o.

Table E-3. Explanation of Column Labels in Printout Summary Tables (figs. E-1d,e).

Title on Computer Printout	Quantity
T, TIME	t in seconds
EVPRECIP	$\overline{(k_3 N_o^{.35} m M^{.65})}$ (column average)
F1	Condensation-evaporation parameter (See App. A)
RR	Rainfall rate in mm/hr.
EVCLOUD	$(k_5 + C_3 \lvert w_{max} \rvert) \frac{k_6 k_9}{H/h+1} \sum_{m<o} m(z,o)$
SDRY	S_d
-K5*SBAR	$-k_5 A$ (Diffusion of buoyancy)
DELTA S(M)	$+ \frac{k_4 \overline{w}}{H} F_1 (S_m - \overline{S} * \text{sign}(\overline{w}))$ ††
DELTA S(D)	$- \frac{k_4 \overline{w}}{H} (1-F_1)(S_d + \overline{S} * \text{sign}(\overline{w}))$ ††
WMAX	w_{max}
LBAR	L
DW/DT	$\frac{dw}{dt}$
M(O)	M(1) (Precipitation at ground)
AR	Accumulated rainfall in mm
SMOIST	S_m
SBAR	A

††The factor $\overline{w}$ in these terms is $\frac{1}{2}[w_{max}(t-k) + w_{max}(t)]$.

```
                                 CLOUD  VERSION 9 RUN 37
DELTA H = 250.
K       =  20.
H       = 10000.
WMAX    =  0.
T1      =  5000.
C0      = -4.C0000E+00
C1      =  8.00000E-04
C2      = -4.00000F-08
C4      =  3.00000E-03
C5      = -3.00000E-07
C6      =  0.
C7      =  0.
C8      =  1.00000E+00
C9      =  0.
C10     =  5.00000E-01
C11     =  0.
C3      =  0.
E0      =  1.25000E-01
E2      =  8.75000E-01
E3      =  6.50000F-01
K0      = -3.86000E+01
K1      =  1.00000E-04
K2      =  6.96000E-04
K3      =  1.93000E-06
K7      = -1.00000E-04
NO      =  1.00000E+07        NO**.125 =  7.49894E+00        NO**.35 =  2.81838E+02        NO**-.125 =  1.33352E-01
SZER    =  2.50000E-02
K8      =  1.00000E-02
K9      =  1.00000E+00
K4      =  1.00000E+00
K5      =  3.00000E-04
K6      =  1.00000E-01
SMOIST  =  2.00000E-01
SDRY    =  2.00000E-01
F4      =  0.
```

Figure E-1a. Table of input parameters prepared by the main computer program. The listed parameters have been applied in calculations whose results are illustrated in figure 12.

TIME STEP NUMBER = 40 DELTA T = 20. TIME = 782. SECONDS

HEIGHT	CLD H20	PRECIP H20	FALL SP V	V + W	B(CLD)	B(PRECIP)	SM*DIV(W)	CM*DIV(W)	CLD CNVRSN	ACRTN+EVAP	CNDNSTN
METERS	GRAMS/CUBIC METER		METERS PER SECOND		GRAMS PER CUBIC METER PER SECOND				GRAMS PER CUBIC METER PER SECOND		
10000.	-2.842E-14	0.	0.	0.	4.461E-17	0.	4.461E-17	0.	0.	0.	0.
9500.	3.000E-01	2.130E-03	-3.836E+00	-3.088E+00	-4.390E-04	7.764E-06	-4.239E-04	-3.009E-06	0.	1.157E-05	1.118E-04
9000.	6.306E-01	1.125E-02	-4.607E+00	-3.189E+00	-7.731E-04	9.573E-05	-7.919E-04	-1.413E-05	1.306E-05	1.018E-04	4.238E-04
8500.	9.576E-01	3.887E-02	-5.246E+00	-3.238E+00	-1.149E-03	4.296E-04	-1.052E-03	-4.271E-05	4.576E-05	4.460E-04	9.006E-04
8000.	1.238E+00	9.993E-02	-5.758E+00	-3.237E+00	-1.748E-03	1.209E-03	-1.166E-03	-9.412E-05	7.379E-05	1.285E-03	1.507E-03
7500.	1.442E+00	2.048E-01	-6.143E+00	-3.189E+00	-2.684E-03	2.546E-03	-1.132E-03	-1.607E-04	9.417E-05	2.734E-03	2.207E-03
7000.	1.570E+00	3.476E-01	-6.401E+00	-3.092E+00	-3.835E-03	4.282E-03	-9.858E-04	-2.182E-04	1.070E-04	4.612E-03	2.967E-03
6500.	1.648E+00	5.003E-01	-6.533E+00	-2.949E+00	-4.865E-03	6.044E-03	-7.760E-04	-2.356E-04	1.148E-04	6.494E-03	3.750E-03
6000.	1.704E+00	6.197E-01	-6.545E+00	-2.764E+00	-5.378E-03	7.405E-03	-5.350E-04	-1.946E-04	1.204E-04	7.898E-03	4.521E-03
5500.	1.752E+00	6.637E-01	-6.438E+00	-2.539E+00	-5.015E-03	7.975E-03	-2.750E-04	-1.042E-04	1.252E-04	8.410E-03	5.245E-03
5000.	1.781E+00	6.115E-01	-6.215E+00	-2.277E+00	-3.535E-03	7.465E-03	0.	0.	1.281E-04	7.760E-03	5.886E-03
4500.	1.755E+00	4.778E-01	-5.878E+00	-1.978E+00	-1.021E-03	5.882E-03	2.755E-04	7.500E-05	1.255E-04	6.010E-03	6.410E-03
4000.	1.629E+00	3.087E-01	-5.428E+00	-1.647E+00	1.933E-03	3.713E-03	5.113E-04	9.693E-05	1.129E-04	3.713E-03	6.781E-03
3500.	1.365E+00	1.579E-01	-4.868E+00	-1.284E+00	4.429E-03	1.744E-03	6.426E-04	7.436E-05	8.646E-05	1.687E-03	6.964E-03
3000.	9.479E-01	5.736E-02	-4.184E+00	-8.752E-01	5.817E-03	5.160E-04	5.952E-04	3.602E-05	4.479E-05	4.713E-04	6.922E-03
2500.	3.859E-01	1.057E-02	-3.303E+00	-3.489E-01	5.978E-03	4.462E-05	3.029E-04	8.297E-06	0.	4.261E-05	6.622E-03
2000.	-3.022E-01	0.	0.	2.521E+00	5.142E-03	0.	-2.846E-04	0.	0.	0.	6.028E-03
1500.	-1.099E+00	0.	0.	2.009E+00	3.579E-03	0.	-1.208E-03	0.	0.	0.	5.104E-03
1000.	-1.994E+00	0.	0.	1.418E+00	1.218E-03	0.	-2.504E-03	0.	0.	0.	3.814E-03
500.	-2.972E+00	0.	0.	7.483E-01	-2.043E-03	0.	-4.198E-03	0.	0.	0.	2.125E-03
0.	-4.000E+00	0.	0.	0.	-6.279E-03	0.	-6.279E-03	0.	0.	0.	0.

WMAX= 3.93865E+00 SBAR= 1.13435E-02 LBAR= 1.13198E+00 DW/DT= -1.43338E-03 WMEAN= 3.92431E+00

RAINFALL IN MILLIMETERS PER HOUR MILLIMETERS OF ACCUMULATED RAINFALL

3.6*RR = 0.

TIME STEP NUMBER = 90 DELTA T = 20. TIME = 1782. SECONDS

HEIGHT	CLD H20	PRECIP H20	FALL SP V	V + W	B(CLD)	B(PRECIP)	SM*DIV(W)	CM*DIV(W)	CLD CNVRSN	ACRTN+EVAP	CNDNSTN
METERS	GRAMS/CUBIC METER		METERS PER SECOND		GRAMS PER CUBIC METER PER SECOND				GRAMS PER CUBIC METER PER SECOND		
10000.	-2.842E-14	0.	0.	0.	-3.236E-17	0.	-3.236E-17	0.	0.	0.	0.
9500.	1.164E-01	3.938E-03	-4.143E+00	-4.659E+00	-1.171E-06	1.075E-05	1.193E-04	4.036E-06	0.	7.685E-06	-8.113E-05
9000.	1.828E-01	1.302E-02	-4.692E+00	-5.671E+00	-2.225E-04	4.283E-05	1.665E-04	1.186E-05	0.	3.354E-05	-3.074E-04
8500.	1.837E-01	2.989E-02	-5.077E+00	-6.464E+00	-6.303E-04	8.718E-05	1.464E-04	2.382E-05	0.	6.798E-05	-6.533E-04
8000.	1.353E-01	5.679E-02	-5.365E+00	-7.106E+00	-1.150E-03	1.177E-04	9.243E-05	3.880E-05	0.	8.562E-05	-1.093E-03
7500.	6.173E-02	9.622E-02	-5.589E+00	-7.629E+00	-1.707E-03	1.069E-04	3.515E-05	5.478E-05	0.	6.044E-05	-1.601E-03
7000.	-2.049E-02	1.519E-01	-5.772E+00	-8.056E+00	-2.265E-03	5.667E-05	-9.331E-06	6.919E-05	0.	-3.274E-06	-2.152E-03
6500.	-1.038E-01	2.301E-01	-5.929E+00	-8.403E+00	-2.876E-03	4.744E-05	-3.547E-05	7.859E-05	0.	-2.173E-05	-2.720E-03
6000.	-1.844E-01	3.382E-01	-6.068E+00	-8.678E+00	-3.459E-03	1.840E-05	-4.200E-05	7.703E-05	0.	-4.959E-05	-3.279E-03
5500.	-2.590E-01	4.845E-01	-6.190E+00	-8.882E+00	-3.984E-03	-4.161E-05	-2.949E-05	5.517E-05	0.	-8.797E-05	-3.805E-03
5000.	-3.251E-01	6.773E-01	-6.295E+00	-9.015E+00	-4.428E-03	-1.477E-04	0.	0.	0.	-1.373E-04	-4.270E-03
4500.	-3.812E-01	9.244E-01	-6.383E+00	-9.075E+00	-4.766E-03	-3.191E-04	4.341E-05	-1.053E-04	0.	-1.970E-04	-4.650E-03
4000.	-4.280E-01	1.232E+00	-6.453E+00	-9.064E+00	-4.975E-03	-5.801E-04	9.747E-05	-2.806E-04	0.	-2.666E-04	-4.919E-03
3500.	-4.721E-01	1.603E+00	-6.504E+00	-8.979E+00	-5.029E-03	-9.621E-04	1.613E-04	-5.475E-04	0.	-3.489E-04	-5.051E-03
3000.	-5.327E-01	2.032E+00	-6.535E+00	-8.819E+00	-4.875E-03	-1.508E-03	2.426E-04	-9.254E-04	0.	-4.594E-04	-5.021E-03
2500.	-6.454E-01	2.500E+00	-6.540E+00	-8.580E+00	-4.419E-03	-2.276E-03	3.674E-04	-1.423E-03	0.	-6.368E-04	-4.804E-03
2000.	-8.544E-01	2.962E+00	-6.516E+00	-8.256E+00	-3.515E-03	-3.314E-03	5.837E-04	-2.023E-03	0.	-9.413E-04	-4.372E-03
1500.	-1.198E+00	3.338E+00	-6.451E+00	-7.837E+00	-2.001E-03	-4.605E-03	9.552E-04	-2.661E-03	0.	-1.427E-03	-3.702E-03
1000.	-1.697E+00	3.517E+00	-6.332E+00	-7.311E+00	2.329E-04	-5.989E-03	1.546E-03	-3.203E-03	0.	-2.091E-03	-2.767E-03
500.	-2.342E+00	3.384E+00	-6.146E+00	-6.663E+00	3.166E-03	-7.113E-03	2.400E-03	-3.467E-03	0.	-2.814E-03	-1.541E-03
0.	-3.084E+00	2.913E+00	-5.884E+00	-5.884E+00	6.597E-03	-7.552E-03	3.511E-03	-3.317E-03	0.	-3.361E-03	0.

WMAX= -2.71933E+00 SBAR= 9.00811E-04 LBAR= 1.29129E+00 DW/DT= -1.27318E-02 WMEAN= -2.84665E+00

RAINFALL IN MILLIMETERS PER HOUR MILLIMETERS OF ACCUMULATED RAINFALL

3.6*RR = 6.17074E+01 AR = 3.31273E+00

Figure E-1b. Profiles of moisture and motion parameters at selected times, from the same results illustrated in figure 12.

TIME STEP NUMBER = 150 DELTA T = 20. TIME = 2982. SECONDS

HEIGHT METERS	CLD H2O	PRECIP H2O	FALL SP V	V + W	B(CLD)	B(PRECIP)	SM*DIV(W)	CM*DIV(W)	CLD CNVRSN	ACRTN+EVAP	CNDNSTN
	GRAMS/CUBIC METER		METERS PER SECOND		GRAMS PER CUBIC METER PER SECOND				GRAMS PER CUBIC METER PER SECOND		
10000.	-2.842E-14	0.	0.	0.	-1.037E-17	0.	-1.037E-17	0.	0.	0.	0.
9500.	-8.255E-02	2.419E-06	-1.644E+00	-1.807E+00	-3.275E-05	-9.927E-09	-2.710E-05	7.941E-10	0.	-1.004E-08	-2.599E-05
9000.	-1.731E-01	4.666E-06	-1.740E+00	-2.049E+00	-1.147E-04	-3.215E-08	-5.052E-05	1.362E-09	0.	-3.226E-08	-9.850E-05
8500.	-2.769E-01	5.550E-06	-1.735E+00	-2.172E+00	-2.368E-04	-5.776E-08	-7.072E-05	1.417E-09	0.	-5.777E-08	-2.093E-04
8000.	-3.976E-01	4.529E-06	-1.649E+00	-2.198E+00	-3.891E-04	-7.278E-08	-8.703E-05	9.914E-10	0.	-7.268E-08	-3.502E-04
7500.	-5.370E-01	2.280E-06	-1.476E+00	-2.119E+00	-5.615E-04	-6.295E-08	-9.795E-05	4.160E-10	0.	-6.284E-08	-5.130E-04
7000.	-6.948E-01	4.510E-07	-1.176E+00	-1.896E+00	-7.436E-04	-2.839E-08	-1.014E-04	6.580E-11	0.	-2.835E-08	-6.895E-04
6500.	-8.680E-01	0.	0.	-7.798E-01	-9.251E-04	0.	-9.499E-05	0.	0.	0.	-8.714E-04
6000.	-1.051E+00	0.	0.	-8.226E-01	-1.096E-03	0.	-7.668E-05	0.	0.	0.	-1.051E-03
5500.	-1.237E+00	0.	0.	-8.483E-01	-1.248E-03	0.	-4.512E-05	0.	0.	0.	-1.219E-03
5000.	-1.417E+00	0.	0.	-8.569E-01	-1.372E-03	0.	0.	0.	0.	0.	-1.368E-03
4500.	-1.586E+00	0.	0.	-8.483E-01	-1.462E-03	0.	5.784E-05	0.	0.	0.	-1.490E-03
4000.	-1.735E+00	0.	0.	-8.226E-01	-1.513E-03	0.	1.266E-04	0.	0.	0.	-1.576E-03
3500.	-1.862E+00	0.	0.	-7.798E-01	-1.518E-03	0.	2.038E-04	0.	0.	0.	-1.618E-03
3000.	-1.964E+00	0.	0.	-7.198E-01	-1.471E-03	0.	2.866E-04	0.	0.	0.	-1.609E-03
2500.	-2.044E+00	0.	0.	-6.427E-01	-1.368E-03	0.	3.729E-04	0.	0.	0.	-1.539E-03
2000.	-2.106E+00	2.489E-05	-1.512E+00	-2.060E+00	-1.198E-03	-1.177E-06	4.610E-04	-5.447E-09	0.	-1.165E-06	-1.401E-03
1500.	-2.155E+00	2.273E-04	-1.944E+00	-2.381E+00	-9.513E-04	-5.137E-06	5.504E-04	-5.804E-08	0.	-5.022E-06	-1.186E-03
1000.	-2.198E+00	9.002E-04	-2.252E+00	-2.561E+00	-6.175E-04	-1.303E-05	6.414E-04	-2.627E-07	0.	-1.253E-05	-8.865E-04
500.	-2.237E+00	2.409E-03	-2.484E+00	-2.647E+00	-1.860E-04	-2.565E-05	7.344E-04	-7.908E-07	0.	-2.417E-05	-4.939E-04
0.	-2.275E+00	4.834E-03	-2.643E+00	-2.643E+00	3.508E-04	-4.188E-05	8.298E-04	-1.764E-06	0.	-3.866E-05	0.

WMAX= -8.56878E-01 SBAR= -4.41257E-03 LBAR= 3.43176E-04 DW/DT= -5.51281E-03 WMEAN= -9.12006E-01

RAINFALL IN MILLIMETERS PER HOUR MILLIMETERS OF ACCUMULATED RAINFALL

3.6*RR = 4.60029E-02 AR = 1.03277E+01

TIME STEP NUMBER = 220 DELTA T = 20. TIME = 4382. SECONDS

HEIGHT METERS	CLD H2O	PRECIP H2O	FALL SP V	V + W	B(CLD)	B(PRECIP)	SM*DIV(W)	CM*DIV(W)	CLD CNVRSN	ACRTN+EVAP	CNDNSTN
	GRAMS/CUBIC METER		METERS PER SECOND		GRAMS PER CUBIC METER PER SECOND				GRAMS PER CUBIC METER PER SECOND		
10000.	-2.842E-14	0.	0.	0.	-5.423E-18	0.	-5.423E-18	0.	0.	0.	0.
9500.	-1.040E-01	0.	0.	-9.768E-02	-4.200E-06	0.	-1.785E-05	0.	0.	0.	-1.359E-05
9000.	-2.157E-01	0.	0.	-1.851E-01	-3.543E-05	0.	-3.293E-05	0.	0.	0.	-5.151E-05
8500.	-3.396E-01	0.	0.	-2.622E-01	-8.821E-05	0.	-4.535E-05	0.	0.	0.	-1.095E-04
8000.	-4.770E-01	0.	0.	-3.290E-01	-1.572E-04	0.	-5.460E-05	0.	0.	0.	-1.832E-04
7500.	-6.279E-01	0.	0.	-3.856E-01	-2.373E-04	0.	-5.989E-05	0.	0.	0.	-2.683E-04
7000.	-7.911E-01	0.	0.	-4.319E-01	-3.233E-04	0.	-6.038E-05	0.	0.	0.	-3.606E-04
6500.	-9.651E-01	0.	0.	-4.678E-01	-4.104E-04	0.	-5.524E-05	0.	0.	0.	-4.558E-04
6000.	-1.147E+00	0.	0.	-4.935E-01	-4.936E-04	0.	-4.377E-05	0.	0.	0.	-5.495E-04
5500.	-1.334E+00	0.	0.	-5.090E-01	-5.687E-04	0.	-2.546E-05	0.	0.	0.	-6.375E-04
5000.	-1.523E+00	0.	0.	-5.141E-01	-6.312E-04	0.	0.	0.	0.	0.	-7.155E-04
4500.	-1.710E+00	0.	0.	-5.090E-01	-6.774E-04	0.	3.262E-05	0.	0.	0.	-7.791E-04
4000.	-1.890E+00	0.	0.	-4.935E-01	-7.036E-04	0.	7.213E-05	0.	0.	0.	-8.242E-04
3500.	-2.062E+00	0.	0.	-4.678E-01	-7.063E-04	0.	1.180E-04	0.	0.	0.	-8.464E-04
3000.	-2.222E+00	0.	0.	-4.319E-01	-6.823E-04	0.	1.696E-04	0.	0.	0.	-8.414E-04
2500.	-2.368E+00	0.	0.	-3.856E-01	-6.283E-04	0.	2.259E-04	0.	0.	0.	-8.049E-04
2000.	-2.499E+00	0.	0.	-3.290E-01	-5.411E-04	0.	2.861E-04	0.	0.	0.	-7.326E-04
1500.	-2.614E+00	0.	0.	-2.622E-01	-4.177E-04	0.	3.491E-04	0.	0.	0.	-6.203E-04
1000.	-2.712E+00	0.	0.	-1.851E-01	-2.548E-04	0.	4.139E-04	0.	0.	0.	-4.636E-04
500.	-2.794E+00	0.	0.	-9.768E-02	-4.873E-05	0.	4.797E-04	0.	0.	0.	-2.583E-04
0.	-2.865E+00	0.	0.	0.	2.062E-04	0.	5.467E-04	0.	0.	0.	0.

WMAX= -5.14111E-01 SBAR= 2.13504E-03 LBAR= 0. DW/DT= 3.71312E-03 WMEAN= -4.76980E-01

RAINFALL IN MILLIMETERS PER HOUR MILLIMETERS OF ACCUMULATED RAINFALL

3.6*RR = 0. AR = 1.03284E+01

Figure E-1c. Continuation of figure E-1b.

CLOUD VERSION 9 RUN 37

	T	EVPRECIP	F1	RR	EVCLOUD	SDRY	-K5*SBAR	DELTA S(M)	DELTA S(D)
6	102.	0.	0.	0.	0.	2.00000E-01	-6.08080E-06	0.	-7.67846E-05
11	202.	0.	7.35609E-02	0.	-9.16463E-07	2.00000E-01	-3.20982E-06	6.87911E-06	-9.64302E-05
16	302.	0.	4.53675E-01	0.	-7.90976E-06	2.00000E-01	-1.38179E-06	4.57131E-05	-5.76439E-05
21	402.	0.	6.29606E-01	0.	-1.26768E-05	2.00000E-01	-1.22415E-06	6.10709E-05	-3.74242E-05
26	502.	0.	7.17070E-01	0.	-1.56494E-05	2.00000E-01	-1.70169E-06	6.56404E-05	-2.74113E-05
31	602.	0.	7.59258E-01	0.	-1.72957E-05	2.00000E-01	-2.31420E-06	6.39960E-05	-2.19197E-05
36	702.	0.	7.59258E-01	0.	-1.72957E-05	2.00000E-01	-2.93453E-06	5.91397E-05	-2.06803E-05
41	802.	-5.80537E-09	7.99800E-01	0.	-1.90537E-05	2.00000E-01	-3.52395E-06	5.86242E-05	-1.65057E-05
46	902.	-1.32119E-07	7.99800E-01	0.	-1.90537E-05	2.00000E-01	-4.07172E-06	5.55604E-05	-1.59325E-05
51	1002.	-6.02771E-07	7.99800E-01	6.71518E-06	-1.90537E-05	2.00000E-01	-4.52614E-06	5.28593E-05	-1.53905E-05
56	1102.	-2.14936E-06	7.99800E-01	6.66939E-04	-1.90537E-05	2.00002E-01	-4.88269E-06	5.04817E-05	-1.48753E-05
61	1202.	-5.95755E-06	7.99800E-01	4.10167E-02	-1.90537E-05	2.00028E-01	-5.10547E-06	4.82235E-05	-1.43204E-05
66	1302.	-1.27423E-05	7.59258E-01	6.40831E-01	-1.72957E-05	2.00206E-01	-5.09915E-06	4.22141E-05	-1.59044E-05
71	1402.	-2.19422E-05	7.59258E-01	4.18235E+00	-1.72957E-05	2.00861E-01	-4.67776E-06	3.37081E-05	-1.26043E-05
76	1502.	-3.17923E-05	7.59258E-01	1.42734E+01	-1.72957E-05	2.02422E-01	-3.78693E-06	1.94764E-05	-7.18020E-06
81	1602.	-4.06766E-05	6.73706E-01	3.12767E+01	-1.41110E-05	2.05086E-01	-2.34477E-06	-3.72252E-07	1.75435E-07
86	1702.	-5.03338E-05	1.93800E-01	5.02425E+01	-2.73659E-06	2.08647E-01	-8.10988E-07	-6.28935E-06	2.77661E-05
91	1802.	-5.99254E-05	5.80078E-02	6.35590E+01	-7.04268E-07	2.12606E-01	-2.21923E-07	-3.37142E-06	6.16554E-05
96	1902.	-6.24261E-05	2.25750E-02	6.50653E+01	-2.56098E-07	2.16390E-01	-3.89418E-07	-1.63399E-06	8.22952E-05
101	2002.	-5.63549E-05	5.15625E-03	5.45660E+01	-5.48780E-08	2.19546E-01	-1.08400E-06	-3.88099E-07	8.78428E-05
106	2102.	-4.48350E-05	0.	3.83898E+01	0.	2.21862E-01	-2.04342E-06	0.	7.76322E-05
111	2202.	-3.19180E-05	0.	2.34561E+01	0.	2.23355E-01	-2.79687E-06	0.	4.91388E-05
116	2302.	-2.07789E-05	0.	1.29903E+01	0.	2.24169E-01	-2.96445E-06	0.	1.58386E-05
121	2402.	-1.26798E-05	0.	6.78323E+00	0.	2.24486E-01	-2.47122E-06	0.	-1.34681E-05
126	2502.	-7.41451E-06	0.	3.41732E+00	0.	2.24459E-01	-1.43998E-06	0.	-3.17314E-05
131	2602.	-4.23540E-06	0.	1.66666E+00	0.	2.24204E-01	-1.94849E-07	0.	-3.62807E-05
136	2702.	-2.38984E-06	0.	7.75634E-01	0.	2.23797E-01	9.24126E-07	0.	-2.82506E-05
141	2802.	-1.32836E-06	0.	3.32925E-01	0.	2.23291E-01	1.59505E-06	0.	-1.08123E-05
146	2902.	-6.81845E-07	0.	1.23391E-01	0.	2.22723E-01	1.66863E-06	0.	8.37221E-06
151	3002.	-2.83807E-07	0.	3.44369E-02	0.	2.22116E-01	1.19389E-06	0.	2.29444E-05
156	3102.	-7.09707E-08	0.	4.89540E-03	0.	2.21490E-01	3.91559E-07	0.	2.88772E-05
161	3202.	-1.03776E-11	0.	0.	0.	2.20860E-01	-4.63918E-07	0.	2.60276E-05
166	3302.	0.	0.	0.	0.	2.20241E-01	-1.10023E-06	0.	1.46239E-05
171	3402.	0.	0.	0.	0.	2.19641E-01	-1.32755E-06	0.	-1.66670E-08
176	3502.	0.	0.	0.	0.	2.19059E-01	-1.11918E-06	0.	-1.32997E-05
181	3602.	0.	0.	0.	0.	2.18494E-01	-5.84938E-07	0.	-2.09230E-05
186	3702.	0.	0.	0.	0.	2.17946E-01	7.91428E-08	0.	-2.18835E-05
191	3802.	0.	0.	0.	0.	2.17414E-01	6.69242E-07	0.	-1.58367E-05
196	3902.	0.	0.	0.	0.	2.16898E-01	9.98329E-07	0.	-5.25952E-06
201	4002.	0.	0.	0.	0.	2.16397E-01	9.89232E-07	0.	5.89601E-06
206	4102.	0.	0.	0.	0.	2.15911E-01	6.76444E-07	0.	1.41275E-05
211	4202.	0.	0.	0.	0.	2.15439E-01	1.86282E-07	0.	1.73848E-05
216	4302.	0.	0.	0.	0.	2.14982E-01	-3.24579E-07	0.	1.53971E-05
221	4402.	0.	0.	0.	0.	2.14538E-01	-6.97481E-07	0.	8.49856E-06
226	4502.	0.	0.	0.	0.	2.14107E-01	-8.24242E-07	0.	-3.38973E-07
231	4602.	0.	0.	0.	0.	2.13688E-01	-6.88735E-07	0.	-8.32804E-06
236	4702.	0.	0.	0.	0.	2.13283E-01	-3.55966E-07	0.	-1.30288E-05
241	4802.	0.	0.	0.	0.	2.12889E-01	5.79982E-08	0.	-1.36805E-05
246	4902.	0.	0.	0.	0.	2.12507E-01	4.27894E-07	0.	-1.00283E-05
251	5002.	0.	0.	0.	0.	2.12136E-01	6.38612E-07	0.	-3.51005E-06

Figure E-1d. Summary table of the same results illustrated in figure 12.

CLOUD VERSION 9 RUN 37

STEP	TIME	WMAX	LBAR	DW/DT	M(0)	AR	SMOIST	SBAR
6	102.	3.26133E+00	0.	2.24608E-02	0.	0.	2.00000E-01	2.02693E-02
11	202.	4.86996E+00	1.81437E-03	7.01125E-03	0.	0.	2.00000E-01	1.06994E-02
16	302.	5.16726E+00	1.29246E-01	-1.04158E-03	0.	0.	2.00000E-01	4.60596E-03
21	402.	4.97509E+00	3.55971E-01	-2.41437E-03	0.	0.	2.00000E-01	4.08049E-03
26	502.	4.74050E+00	5.94131E-01	-2.99195E-03	0.	0.	2.00000E-01	5.67230E-03
31	602.	4.41650E+00	8.13164E-01	-3.30521E-03	0.	0.	2.00000E-01	7.71402E-03
36	702.	4.12007E+00	1.00131E+00	-2.52289E-03	0.	0.	2.00000E-01	9.78175E-03
41	802.	3.90998E+00	1.16255E+00	-1.63658E-03	0.	0.	2.00000E-01	1.17465E-02
46	902.	3.74247E+00	1.30454E+00	-1.62095E-03	0.	0.	2.00000E-01	1.35724E-02
51	1002.	3.58845E+00	1.43450E+00	-1.42968E-03	1.88285E-06	4.92096E-08	2.00000E-01	1.50871E-02
56	1102.	3.44925E+00	1.56174E+00	-1.37485E-03	1.12190E-04	3.87438E-06	1.99998E-01	1.62756E-02
61	1202.	3.30917E+00	1.69007E+00	-1.35454E-03	4.36580E-03	3.22218E-04	1.99972E-01	1.70182E-02
66	1302.	3.08387E+00	1.81518E+00	-4.22892E-03	5.02577E-02	6.97944E-03	1.99794E-01	1.69972E-02
71	1402.	2.50144E+00	1.91165E+00	-8.26373E-03	2.66293E-01	6.31109E-02	1.99139E-01	1.55925E-02
76	1502.	1.51026E+00	1.93082E+00	-1.23330E-02	7.92929E-01	3.02240E-01	1.97578E-01	1.26231E-02
81	1602.	1.30524E-01	1.81755E+00	-1.57779E-02	1.59247E+00	9.23192E-01	1.94914E-01	7.81590E-03
86	1702.	-1.51004E+00	1.55359E+00	-1.62300E-02	2.42689E+00	2.05913E+00	1.91353E-01	2.70329E-03
91	1802.	-2.97397E+00	1.22089E+00	-1.15341E-02	2.99096E+00	3.66069E+00	1.87394E-01	7.39745E-04
96	1902.	-3.86552E+00	8.64407E-01	-4.88973E-03	3.05389E+00	5.47684E+00	1.83610E-01	1.29806E-03
101	2002.	-4.09986E+00	5.49920E-01	1.07181E-03	2.61167E+00	7.15973E+00	1.80454E-01	3.61335E-03
106	2102.	-3.70892E+00	3.18767E-01	9.89726E-03	1.91064E+00	8.45464E+00	1.78138E-01	6.81139E-03
111	2202.	-2.44928E+00	1.72092E-01	1.53410E-02	1.23308E+00	9.30548E+00	1.76645E-01	9.32290E-03
116	2302.	-8.89258E-01	8.93636E-02	1.50132E-02	7.29238E-01	9.80103E+00	1.75831E-01	9.88151E-03
121	2402.	4.69631E-01	4.56672E-02	1.09088E-02	4.09300E-01	1.00677E+01	1.75514E-01	8.23740E-03
126	2502.	1.33307E+00	2.31461E-02	5.10126E-03	2.22522E-01	1.02046E+01	1.75541E-01	4.79994E-03
131	2602.	1.61597E+00	1.15596E-02	-2.44025E-04	1.17540E-01	1.02726E+01	1.75796E-01	6.49496E-04
136	2702.	1.34229E+00	5.56957E-03	-6.23441E-03	5.95531E-02	1.03052E+01	1.76203E-01	-3.08042E-03
141	2802.	5.84317E-01	2.47268E-03	-8.82820E-03	2.80806E-02	1.03199E+01	1.76709E-01	-5.31682E-03
146	2902.	-2.87251E-01	9.29987E-04	-7.94933E-03	1.16208E-02	1.03259E+01	1.77277E-01	-5.56211E-03
151	3002.	-9.67135E-01	2.55350E-04	-4.76767E-03	3.73735E-03	1.03279E+01	1.77884E-01	-3.97963E-03
156	3102.	-1.28739E+00	3.45764E-05	-8.74347E-04	6.59881E-04	1.03284E+01	1.78510E-01	-1.30520E-03
161	3202.	-1.22084E+00	3.27370E-09	3.40596E-03	0.	1.03284E+01	1.79140E-01	1.54639E-03
166	3302.	-7.39181E-01	0.	6.39435E-03	0.	1.03284E+01	1.79759E-01	3.66742E-03
171	3402.	-6.64969E-02	0.	6.72407E-03	0.	1.03284E+01	1.80359E-01	4.42518E-03
176	3502.	5.47661E-01	0.	4.92985E-03	0.	1.03284E+01	1.80941E-01	3.73060E-03
181	3602.	9.28819E-01	0.	2.03084E-03	0.	1.03284E+01	1.81506E-01	1.94979E-03
186	3702.	1.01477E+00	0.	-9.47377E-04	0.	1.03284E+01	1.82054E-01	-2.63809E-04
191	3802.	7.77262E-01	0.	-4.13006E-03	0.	1.03284E+01	1.82586E-01	-2.23081E-03
196	3902.	2.99675E-01	0.	-5.34086E-03	0.	1.03284E+01	1.83102E-01	-3.32776E-03
201	4002.	-2.21484E-01	0.	-4.68894E-03	0.	1.03284E+01	1.83603E-01	-3.29744E-03
206	4102.	-6.20013E-01	0.	-2.75460E-03	0.	1.03284E+01	1.84089E-01	-2.25481E-03
211	4202.	-8.00709E-01	0.	-3.91908E-04	0.	1.03284E+01	1.84561E-01	-6.20940E-04
216	4302.	-7.41941E-01	0.	2.21155E-03	0.	1.03284E+01	1.85018E-01	1.08193E-03
221	4402.	-4.39849E-01	0.	3.93748E-03	0.	1.03284E+01	1.85462E-01	2.32494E-03
226	4502.	-2.58616E-02	0.	4.14930E-03	0.	1.03284E+01	1.85893E-01	2.74747E-03
231	4602.	3.54763E-01	0.	3.08227E-03	0.	1.03284E+01	1.86312E-01	2.29578E-03
236	4702.	5.94549E-01	0.	1.29427E-03	0.	1.03284E+01	1.86717E-01	1.18655E-03
241	4802.	6.49399E-01	0.	-6.20252E-04	0.	1.03284E+01	1.87111E-01	-1.93327E-04
246	4902.	5.00828E-01	0.	-2.57344E-03	0.	1.03284E+01	1.87493E-01	-1.42631E-03
251	5002.	2.01065E-01	0.	-3.39253E-03	0.	1.03284E+01	1.87864E-01	-2.12871E-03

Figure E-1e. Continuation of figure E-1d.

```
C****ONE DIMENSIONAL CLOUD MODEL  KESSLER/BUMGARNER****
C     NSSL NO 71-19
C     VERSION 9 - 11 SEP 1970
C     MODIFICATION  11 MAR 1971
C         ALLOWS FOR INCREASING H TO ABOVE 10000 METERS
C       SUPM NOW A FUNCTION OF M(O,T) AND MDBAR
C     VERSION 8A - 03 AUG 1970
C       ADDED PRINTED COLUMNS AND NEW LABELING.
C     VERSION 8 - 15 JUL 1970
C         DELK AS FUNCTION OF DW/DT
C     VERSION 7 - 13 JUL 1970
C        WEIGHTING FUNCTION USED IN CALCULATION OF F1
C     VERSION 6 - 18 JUN 1970
C         CONTROLS AVERAGING OF PRECIP.
C     VERSION 5 - 02 JUN 1970
C     VERSION 5A - 08 JUN 1970
C     IN DS/DT EQN WMEAN REPLACED BY 1.5*WMEAN
C     VERSION 5B - 10 JUN 1970
C     VERSION 5B RESTORED TO VERSION 5 LEVEL PLUS
C       ADDING 1.5 TO THE DW/DT EQN
C     CORRECTION MADE  20 MAY 1970
C       SDZER IS NOW NEGATIVE ON INPUT AND IN THE COMPUTATION
C     MODIFCATION OF DS/DT EQUATION TO ACCOUNT FOR BOTH POSITIVE AND
C       NEGATIVE BUOYANCY
C        MEAN WMAX BETWEEN TWO STEPS REVISION MADE 26 SEP 1969
C     INTRODUCES A DYNAMICAL CONSTRAINT ON THE VERTICAL VELOCITY
C         MODIFIED 22 SEP 1969
C     REVISION OF KESSLER/NEWBURG 9157 CLOUDS AND RAIN PROGRAM
C         MODIFICATION STARTED  19 SEP 1969
C
      COMMON CMP(201),SMP(201),BCM(201),BSM(201),TCM1(201),TSM1(201),
     1TM2(201),TM34(201),TM(201),V(201),VW(201),Z(201),XM0(201),
     2XM1(201),ICOM(18)
      COMMON DELH,DELK,H,WMAX,T,T1,NT,L2,L3,X,RR,AR,IH,DELK1,IHP,XH,
     1XLBAR,SBAR,SMOIST,SDRY,SZER,F4,WMEAN,DWDT,INFILE,OUTFLE,CARDP,
     2C0,C1,C2,C3,C4,C5,C6,C7,C8,C9,C10,C11,C12,E0,E2,E3,SN0,SN1,SN2,
     3SN3,XK0,XK1,XK2,XK3,XK4,XK5,XK6,XK7,XK8,XK9
      DIMENSION G(201),PW(201),W(201),CMF(201),SMF(201),CME0(201),
     1CME2(201),CME3(201),ZHOF(201),THOF(201),SV(700,9),
     2SMPSV(201),CFF(201)
      INTEGER OUTFLE,CARDP,PRTTBL
C
C     LOGICAL UNITS FOR I/O
C       INFILE   I/P CARDS
C       OUTFLE   MAIN PRINTER O/P
C       CARDP    PUNCHED O/P
C       PRTTBL   AUXILIARY PRINTER O/P
C
      INFILE=5
      OUTFLE=6
      CARDP=8
      PRTTBL=10
C     THE FIRST NTLIM TIME STEPS ARE PRINTED
      NTLIM=10
      LTDIM=700
      LTSWCH=1
C     READ A BLANK CARD
      READ(INFILE,100) LANK
   90 READ(INFILE,100) ICOM
      DO 97 I=1,18
      IF(ICOM(I)-LANK) 98,97,98
   97 CONTINUE
      CALL EXIT
C     IP - TIME STEP PRT INCREMENT
C     IN - VELOCITY TYPE
C     JN - =1 INITIAL RUN, =2 REENTRY
```

Figure E-2a. List of the complete program for marching calculations.

```
C       KN - =1 CALCULATE M(Z,0), =2 READ IN
C       NT - INITIAL TIME STEP NO.
   98 READ (INFILE,120) IP,IN,JN,KN,NT
      READ (INFILE,110) DELH,DELK1,H,WMAX,T1,T2
      READ (INFILE,110) C0,C1,C2,C4,C5,C6
      READ (INFILE,110) C7,C8,C9,C10,C11,C3
      READ (INFILE,110) E0,E2,E3
      READ (INFILE,110) XK0,XK1,XK2,XK3,SN0
      READ (INFILE,110) GAM,T,AR,RP,XK7
      READ (INFILE,110) SZER,XK8,XK9,XK4,XK5,XK6
      READ (INFILE,110) SMOIST,SDRY,F4,TSTEP
      IH = H/DELH+1.0
      GO TO (81,80),JN
   80 READ (INFILE,110) (CMP(I),I=1,IH)
      READ (INFILE,110) (SMP(I),I=1,IH)
      READ (INFILE,110) (SMPSV(I),I=1,IH)
      READ (INFILE,110) SBAR,SUPM,SDWD,BARMD
C     NEW HEADER FOR REENTRY
      READ (INFILE,100) ICOM
      READ (INFILE,110) T1
      DO 2  I=1,IH
      CME0(I) = CMP(I) ** E0
      CME2(I) = CMP(I) ** E2
    2 CME3(I) = CMP(I) ** E3
   81 DELK2 = 0.
      WRITE(PRTTBL,9001) ICOM
 9001 FORMAT(1H1,18A4,//1H ,12X,1HT,5X,8HEVPRECIP,10X,2HF1,12X,2HRR,
     1  8X,7HEVCLOUD,9X,4HSDRY,9X,8H-K5*SBAR,5X,10HDELTA S(M),4X,
     2  10HDELTA S(D))
      DELK2=0.0
      TEN3 = 1000.
      TH6 = 3600.
      HLIM=10000.
      IHLIM=HLIM/DELH+1.0
      IHLIMP=IHLIM+1
      IONE = 1
      ITWO = 2
      L2 = 1
      L3 = 1
      KT1 = DELK1
      IH1 = IH-1
      IHS2=IH/2+1
      X=IH1
      X = X/20.
      IHP = IH1/20
      XH = IHP
      IF(SN0)4,5,4
    4 SN1= SN0**(.125)
      SN2 = SN0 **(.35)
      SN3 = 1.0 / SN1
      GO TO 6
    5 SN1=0.0
      SN2=0.0
      SN3=0.0
    6 HKKK=DELK1/DELH
C     CONSTANT REDUCED FACTORS
      XK3SN2=XK3*SN2
      SMSD=SMOIST+SDRY
      GRDPT=IH
      XK4H=XK4/H
      XK6GRD=XK6/GRDPT
      XK95G=XK6GRD*XK9
      Z1 = 0.0
      LT=0
      TVH=2./H
      FVH=4./H
```

Figure E-2b. Continuation of figure E-2a.

```
      DWDT=0.4
      TLIM=TSTEP
      TVTH=1./(2.*DELH)
      CON4=FVH*WMAX
      DO 20  I=1,IH
      IF(I IHLIM)450,450,452
  452 G(I)=0.0
      GO TO 454
  450 G(I)=C4+C5*Z1
  454 PW(I)=(1.0-TVH*Z1)*CON4
      W(I)=CON4*(Z1*(1.0-Z1/H))
      Z(I) = Z1
      RHOF=EXP(XK7*Z1*0.5)
      THOF(I)=XK2/RHOF*SN1
      ZHOF(I)=XK0/RHOF*SN3
      XM0(I)=C10 + C11*Z1
      XM1(I)=XM0(I)
      GO TO (82,19),JN
   82 CME0(I) = 0.0
      CME2(I) = 0.0
      CME3(I) = 0.0
      CMP(I) = 0.0
   19 Z1 = Z1+DELH
   20 CONTINUE
C     CALCULATE PARTIAL FI
      IF(H HLIM)460,460,464
  464 CON1=1./(HLIM*(C4/2.+(C5-C4/H)*HLIM/3.-(HLIM**2*C5)/(4.*H))*
     1  (HLIM/DELH))
      DO 466 I=IHLIMP,IH
  466 CFF(I)=0.0
      GO TO 468
  460 CON1=6./(H*(C4+C5*H/2.)*(H/DELH))
  468 DO 462 I=1,IH
  462 CFF(I)=CON1*(Z(I)*(1.-Z(I)/H))*G(I)
      IF(GAM)61,8,61
   61 EXL=EXP(GAM)
      DO 62  I=1,IH
      ALF = Z(I) * H / ((H-Z(I)) * EXL + Z(I))
      Z2 = Z(I) ** 2
      ALF2 = ALF**2
      TX = Z(I) - ALF
      TY = Z2 - ALF2
   62 SMP(I) = C0 + C1*ALF + C2*ALF2 + C4*TX + .5*C5*TY
      GO TO 3
    8 GO TO (9,7),KN
    7 READ (INFILE,110) (SMP(I),I=1,IH)
      GO TO 3
    9 GO TO (89,603),JN
   89 DO 1 I=1,IHLIM
    1 SMP(I)=(Z(I)*C2+C1)*Z(I)+C0
      IF(IHLIM-IH)456,3,3
  456 DO 457 I=IHLIMP,IH
  457 SMP(I)=0.0
C     CALCULATE MEAN INITIAL CLOUD VALUE
    3 SUPM=SMOIST
      SDWD=SDRY
      SBAR=SZER
      ZC=-340.*SMP(1)
      BARMD=0.0
      DO 600 I=1,IH
      IF(ZC-Z(I))600,602,602
  602 IF(SMP(I))604,600,600
  604 BARMD=BARMD+SMP(I)
  600 SMPSV(I)=SMP(I)
      IF(SMP(1))606,605,606
  605 BARMD=0.0
```

Figure E-2c. Continuation of figure E-2a.

```
      GO TO 603
  606 BARMD=BARMD*XK6GRD/SMP(1)
  603 GO TO (21,23),IN
   21 DO 22  I=1,IH
   22 V(I) = C6+C7*Z(I)
      GO TO 25
C     REITERATE ENTRY POINT
   23 DO 24  I=1,IH
   24 V(I)=ZHOF(I)*CMEO(I)
   25 IF(T T1)16,13,13
   13 WRITE(CARDP,130)
      WRITE(CARDP,100) ICOM
      WRITE(CARDP,120) IP,IN,ITWO,IONE,NT
      WRITE(CARDP,110) DELH,DELK1,H,WMAX,T1
      WRITE(CARDP,110) C0,C1,C2,C4,C5,C6
      WRITE(CARDP,110) C7,C8,C9,C10,C11,C3
      WRITE(CARDP,110) E0,E2,E3
      WRITE(CARDP,110) XK0,XK1,XK2,XK3,SNO
      WRITE(CARDP,110) GAM,T,AR,RP,XK7
      WRITE(CARDP,110) SZER,XK8,XK9,XK4,XK5,XK6
      WRITE(CARDP,110) SMOIST,SDRY,F4,TSTEP
      WRITE(CARDP,110) (CMP(I),I=1,IH)
      WRITE(CARDP,110) (SMP(I),I=1,IH)
      WRITE(CARDP,110) (SMPSV(I),I=1,IH)
      WRITE(CARDP,110) SBAR,SUPM,SDWD,BARMD
C     COMPUTE RAINFALL IN MM/HR
   16 VW(1) = W(1) + V(1)
      RF=ABS(CMP(1)*VW(1)/TEN3)
      RR = RF * TH6
      RA=(RF+RP)*0.5*DELK2
      AR = AR + RA
C     COMPUTE NEW DELK (TIME STEP)
      AB1 = ABS(VW(1))
      DELK = DELK1
      HK=HKKK
      DKK=10000.
      IF(DWDT)680,681,680
  680 DKK=1.0/ABS(DWDT)
  681 DO 27 I=2,IH
      VW(I) = W(I) + V(I)
      GO TO (27,17),IN
   17 AB2 = ABS(VW(I))
      IF (AB1-AB2) 26,27,27
   26 AB1 = AB2
   27 CONTINUE
      IF(WMAX - AB1) 92,92,91
   91 AB1 = WMAX
   92 GO TO (9029,18),IN
   18 IF (AB1) 29,29,10
   10 KT = (.8*DELH)/AB1
      IF (KT-1) 14,11,11
   14 L3 = 2
      CALL PRT
   11 IF (KT-KT1) 28,29,29
   28 DELK = KT
      HK = DELK / DELH
   29 IF(DELK-DKK)9029,9029,9030
 9030 DELK=DKK
      HK=DELK/DELH
C     COMPUTE WATER LOAD (XLBAR)
 9029 XLBAR=0.0
      DO 220 I=1,IH
      IF(SMP(I))200,200,201
  200 XLBAR=XLBAR+CMP(I)
      GO TO 220
  201 XLBAR=XLBAR+CMP(I)+SMP(I)
```

Figure E-2d. Continuation of figure E-2a.

```
  220 CONTINUE
      XLBAR=XLBAR/GRDPT
      XK5C3=XK5+C3*ABS(WMAX)
      XK59=XK5C3*XK9
C     CALCULATE DW/DT
      BETA=SBAR-XK8*XLBAR
      ZK1=SQRT(ABS(BETA)/H)
      DWDT=1.5*(BETA-ZK1*WMAX)-XK59*WMAX
C     CALCULATE NEW WMAX AND WMEAN.
      WMAXP=WMAX+DELK*DWDT
      WMEAN=0.5*(WMAXP+WMAX)
      CON4=FVH*WMEAN
C     CALCULATE DW/DZ AND W USING WMEAN
      DO 207 I=1,IH
      PW(I)=(1.0-TVH*Z(I))*CON4
  207 W(I)=CON4*Z(I)*(1.0-Z(I)/H)
C     COMPUTE B(CLOUD),B(PRECIP)
      AEVAP=0.0
      CLEV=0.0
      CF1=0.0
      DO 44 I=1,IH
      IF(SMP(I)-XMO(I))30,30,31
   30 TM2(I)=0.0
      GO TO 34
   31 TM2(I)=XK1*(SMP(I)-XMO(I))
   34 IF(SMP(I))35,37,36
C     EVAP IS NEG
   35 EVAP=XK3SN2*CME3(I)*SMP(I)
      AEVAP=AEVAP+EVAP
      TM34(I)=EVAP
      GO TO 49
   37 TM34(I)=0.0
      GO TO 9449
   36 TM34(I)=THOF(I)*CME2(I)*SMP(I)
      CLEV=CLEV+SMPSV(I)
 9449 CF1=CF1+CFF(I)
   49 TCM1(I) = CMP(I) * PW(I)
      TSM1(I)=SMP(I)*PW(I)
      TM(I)=W(I)*G(I)
      TSM5=C8*TM(I)
      TCM5 = TM(I)-TSM5
      TTT=XK7*W(I)
      TSM6=TTT*SMP(I)
      TCM6=TTT*CMP(I)
      BCM(I)=TCM1(I)+TM2(I)+TM34(I)+TCM5+TCM6-XK5C3*CMP(I)
   44 BSM(I)=TSM1(I)-TM2(I)-TM34(I)+TSM5+TSM6+XK5C3*(SMPSV(I)-SMP(I))
      AEVAP=AEVAP*XK6GRD
      CLEV=XK5C3*CLEV*XK95G
C     COMPUTE NEW SBAR BUT HOLD AS HSBAR
C       DO NOT OPTIMIZE - SPLIT FOR PRINTING PURPOSES
      SK5= XK5C3*SBAR
      S4W=XK4H*WMEAN
      SSGW=SBAR
      IF(WMEAN)674,673,673
  674 SSGW=-SBAR
  673 SDELSM=S4W*CF1*(SUPM-SSGW)
      SDELSD=-S4W*(1.0-CF1)*(SDWD+SSGW)
      SUM=SK5+(SDELSM+SDELSD)
      IF(SBAR+SUPM)676,675,675
  675 SUM=SUM+(AEVAP+CLEV)
  676 HSBAR=SBAR+DELK*SUM
      IF(IP-1)500,500,503
  503 IF(T TLIM)404,400,400
  400 TLIM=TLIM+TSTEP
      GO TO (500,404),LTSWCH
  500 IF(LT-LTDIM)501,501,502
```

Figure E-2e. Continuation of figure E-2a.

```
  502 LTSWCH=2
      GO TO 404
  501 LT=LT+1
      SV(LT,1)=T
      SV(LT,2)=WMAX
      SV(LT,3)=XLBAR
      SV(LT,4)=DWDT
      SV(LT,5)=CMP(1)
      SV(LT,6)=AR
      SV(LT,7)=SUPM
      SV(LT,8)=SBAR
      SV(LT,9)=NT
      WRITE(PRTTBL,9000)NT,T,AEVAP,CF1,RR,CLEV,SDWD,SK5,SDELSM,SDELSD
 9000 FORMAT(1H ,I6,F8.0,8(1PE14.5))
  404 IF(T T1)48,58,58
   48 IF(NT-NTLIM)54,54,51
   51 IF(NT-(NT/IP)*IP)55,54,55
   54 CALL PRT
   55 IF(IP-1)655,655,656
  655 WRITE(OUTFLE,800) NT,DELK,T
  800 FORMAT (1H127X,19HTIME STEP NUMBER = ,I5,7X,10HDELTA T = ,F4.0,7X,
     17HTIME = ,F6.0,8H SECONDS)
      WRITE(OUTFLE,801)
  801 FORMAT (7HOHEIGHT,3X,19HCLD H20  PRECIP H20,3X, 9HFALL SP V,4X,5HV
     1 + W,6X,6HB(CLD),4X,9HB(PRECIP),3X,42HSM*DIV(W)  CM*DIV(W) CLD CNV
     2RSN ACRTN+EVAP,3X,7HCNDNSTN/7H METERS,4X,17HGRAMS/CUBIC METER,6X,1
     37HMETERS PER SECOND,8X,32HGRAMS PER CUBIC METER PER SECOND,5X,32HG
     4RAMS PER CUBIC METER PER SECOND)
      DO 657 K=1,IH
      J=IH 1-K
  657 WRITE(OUTFLE,802) Z(J),SMP(J),CMP(J),V(J),VW(J),BSM(J),BCM(J),TSM1
     1(J),TCM1(J),TM2(J),TM34(J),TM(J)
  802 FORMAT (1H ,F6.0,1X,1PE10.3,1X,1PE10.3,3X,1PE10.3,1X,1PE10.3,2X,1P
     1E10.3,1X,1PE10.3,1X,5(1X,1PE10.3))
  656 NT=NT+1
      T=T+DELK
C     COMPUTE NEW VW (V+W) FOR MIDPOINT
      DO 208 I=1,IH
  208 VW(I)=V(I)+W(I)
C     COMPUTE  M(CLOUD) AND M(PRECIP)
      CMF(1)=CMP(1)+HK*(CMP(1)*V(1)-CMP(2)*V(2)+DELH*(BCM(1)-CMP(1)*
     1PW(1)))
      SMF(1)=SMP(1)+HK*(DELH*(BSM(1)-SMP(1)*PW(1)))
      DO 60  I=2,IH1
      DELVW=(VW(I-1)*CMP(I-1)-VW(I+1)*CMP(I+1))*TVTH
      IF(WMEAN)9470,9470,9472
 9472 IF(I IHS2)9473,9470,9470
 9473 IF(CMP(I))9462,9462,9470
 9462 DELM=DELVW+BCM(I)
      IF(DELM)9463,9463,9471
 9463 IF(CMP(I-1))9464,9464,9480
 9480 IF(SMP(I))9464,9464,9471
 9464 CMF(I)=0.0
      GO TO 60
 9471 CMF(I)=0.5*(CMP(I+1)+CMP(I-1))+DELK*DELM
      GO TO 60
 9470 CMF(I)=0.5*(CMP(I+1)+CMP(I-1)+DELK*(BCM(I+1)+BCM(I-1)))+DELK*DELVW
   60 SMF(I)=0.5*(SMP(I+1)+SMP(I-1)+HK*(W(I-1)*SMP(I-1)-
     1W(I+1)*SMP(I+1)+DELH*(BSM(I+1)+BSM(I-1))))
      IF(WMEAN)9460,9461,9461
 9461 SMF(IH-1)=SMP(IH-1)+HK*(SMP(IH-2)*W(IH-2)-SMP(IH-1)*W(IH-1)+
     1DELH*BSM(IH-1))
 9460 CMF(IH)=C9
      SMF(IH) = SMP(IH)
      DO 65  I=1,IH
      IF(CMF(I))70,70,72
```

Figure E-2f. Continuation of figure E-2a.

```
   70 CMP(I)=0.0
      CME0(I)=0.0
      CME2(I) = 0.0
      CME3(I) = 0.0
      GO TO 73
   72 CME0(I) = CMF(I) **E0
      CME2(I) = CMF(I) **E2
      CME3(I) = CMF(I) **E3
      CMP(I)=CMF(I)
   73 SMP(I)=SMF(I)
   65 CONTINUE
      IF(IHLIM-IH)471,71,71
  471 DO 472 I=IHLIMP,IH
      IF(SMP(I))473,472,472
  473 SMP(I)=0.0
  472 CONTINUE
   71 DELK2=DELK
      RP = RF
C     COMPUTE W FOR NEXT TIME STEP
      WMAX=WMAXP
      CON4=FVH*WMAX
      DO 206 I=1,IH
  206 W(I)=CON4*Z(I)*(1.0-Z(I)/H)
C     SET NEW SBAR,SUPM,SDWD
      SBAR=HSBAR
      SUPM=SMOIST+BARMD*(SMPSV(1)-SMP(1))
      SDWD=SMSD-SUPM
      GO TO (25,23),IN
C     OUT PUT INFORMATION FOR EACH TIME STEP
   58 CALL PRT
      IF(T1-T2)661,660,660
  661 T1=T2
      IP=1
      GO TO 655
  660 NC=0
      DO 300 L=1,LT
      NC=NC-1
      IF(NC)302,302,304
  302 WRITE(OUTFLE,900)  ICOM
  900 FORMAT(1H1,18A4,//1H ,6H  STEP,4X,4HTIME,6X,4HWMAX,10X,4HLBAR,
     1  10X,5HDW/DT,9X,4HM(0),12X,2HAR,10X,6HSMOIST,10X,4HSBAR,/)
      NC=56
  304 NT=SV(L,9)
      WRITE(OUTFLE,902) NT,(SV(L,K),K=1,8)
  902 FORMAT(1H ,I6,F8.0,7(1PE14.5))
  300 CONTINUE
      WRITE(PRTTBL,140)
  140 FORMAT(////)
      GO TO 90
  100 FORMAT(18A4)
  110 FORMAT (6(1PE12.5))
  120 FORMAT (10I6)
  130 FORMAT (30HT1T1T1T1T1T1T1T1T1T1T1T1T1T1T1)
      END
```

Figure E-2g. Continuation of figure E-2a.

```
      SUBROUTINE PRT
C   PRINT ROUTINE FOR I/P DATA AND SELECTED TIME STEPS
      COMMON CMP(201),SMP(201),BCM(201),BSM(201),TCM1(201),TSM1(201),
     1TM2(201),TM34(201),TM(201),V(201),VW(201),Z(201),XM0(201),
     2XM1(201),ICOM(18)
      COMMON DELH,DELK,H,WMAX,T,T1,NT,L2,L3,X,RR,AR,IH,DELK1,IHP,XH,
     1XLBAR,SBAR,SMOIST,SDRY,SZER,F4,WMEAN,DWDT,INFILE,OUTFLE,CARDP,
     2C0,C1,C2,C3,C4,C5,C6,C7,C8,C9,C10,C11,C12,E0,E2,E3,SN0,SN1,SN2,
     3SN3,XK0,XK1,XK2,XK3,XK4,XK5,XK6,XK7,XK8,XK9
      INTEGER OUTFLE,CARDP
      WRITE(OUTFLE,400)
      GO TO (1,38),L3
    1 GO TO (2,4),L2
    2 L2 = 2
      IF (XH-X) 36,3,36
    3 WRITE(OUTFLE,100) ICOM
      WRITE(OUTFLE,155) DELH,DELK1,H,WMAX,T1
      WRITE(OUTFLE,210) C0,C1,C2,C4,C5,C6,C7,C8,C9,C10,C11,C3
      WRITE(OUTFLE,255) E0,E2,E3,XK0,XK1,XK2,XK3,XK7
      WRITE(OUTFLE,305) SN0,SN1,SN2,SN3
      WRITE(OUTFLE,350) SZER,XK8,XK9
      WRITE(OUTFLE,360) XK4,XK5,XK6,SMOIST,SDRY,F4
      WRITE(OUTFLE,400)
    4 J = IH
    5 WRITE(OUTFLE,550) NT,DELK,T
      WRITE(OUTFLE,600)
   10 WRITE(OUTFLE,650) Z(J),SMP(J),CMP(J),V(J),VW(J),BSM(J),BCM(J),TSM1
     1(J),TCM1(J),TM2(J),TM34(J),TM(J)
      J=J-IHP
      IF (J) 40,40,10
   36 WRITE(OUTFLE,700)
      T=T1
      GO TO 99
   38 WRITE(OUTFLE,850)
      T=T1
      GO TO 99
   40 WRITE(OUTFLE,1000) WMAX,SBAR,XLBAR,DWDT,WMEAN
      WRITE(OUTFLE,800)
      WRITE(OUTFLE,900)
      WRITE(OUTFLE,950) RR,AR
   99 RETURN
  100 FORMAT(1H ,29X,18A4)
  155 FORMAT (11H0DELTA H = ,F4.0/2H0K,7X,2H= ,F4.0/2H0H,7X,2H= ,F6.0/11
     1H0WMAX     = ,1PE8.1/3H0T1,6X,2H= ,0PF6.0)
  210 FORMAT (3H0C0,6X,2H= ,1PE12.5/3H0C1,6X,2H= ,1PE12.5/3H0C2,6X,2H= ,
     11PE12.5/3H0C4,6X,2H= ,1PE12.5/3H0C5,6X,2H= ,1PE12.5/3H0C6,6X,2H= ,
     21PE12.5/3H0C7,6X,2H= ,1PE12.5/3H0C8,6X,2H= ,1PE12.5/3H0C9,6X,2H= ,
     31PE12.5/4H0C10,5X,2H= ,1PE12.5/4H0C11,5X,2H= ,1PE12.5,
     4/3H0C3,6X,2H= ,1PE12.5)
  255 FORMAT (3H0E0,6X,2H= ,1PE12.5/3H0E2,6X,2H= ,1PE12.5/3H0E3,6X,2H= ,
     11PE12.5/3H0K0,6X,2H= ,1PE12.5/3H0K1,6X,2H= ,1PE12.5/3H0K2,6X,2H= ,
     21PE12.5/3H0K3,6X,2H= ,1PE12.5/3H0K7,6X,2H= ,1PE12.5)
  305 FORMAT (3H0N0,6X,2H= ,1PE12.5,10X,11HN0**.125 = ,1PE12.5,10X,10HN0
     1**.35 = ,1PE12.5,10X,12HN0**-.125 = ,1PE12.5)
  350 FORMAT(5H0SZER,4X,2H= ,1PE12.5,/3H0K8,6X,2H= ,1PE12.5,
     1/3H0K9,6X,2H= ,1PE12.5)
  360 FORMAT(3H0K4,6X,2H= ,1PE12.5,/3H0K5,6X,2H= ,1PE12.5,/3H0K6,6X,
     12H= ,1PE12.5,/7H0SMOIST,2X,2H= ,1PE12.5,/5H0SDRY,4X,2H= ,
     21PE12.5,/3H0F4,6X,2H= ,1PE12.5)
  400 FORMAT (1H1)
  550 FORMAT (1H027X,19HTIME STEP NUMBER = ,I5,7X,10HDELTA T = ,F4.0,7X,
     17HTIME = ,F6.0,8H SECONDS)
  600 FORMAT (7H0HEIGHT,3X,19HCLD H20  PRECIP H20,3X, 9HFALL SP V,4X,5HV
     1 + W,6X,6HB(CLD),4X,9HB(PRECIP),3X,42HSM*DIV(W)  CM*DIV(W) CLD CNV
     2RSN ACRTN+EVAP,3X,7HCNDNSTN/7H METERS,4X,17HGRAMS/CUBIC METER,6X,1
     37HMETERS PER SECOND,8X,32HGRAMS PER CUBIC METER PER SECOND,5X,32HG
```

Figure E-2h. Continuation of figure E-2a.

```
     4RAMS PER CUBIC METER PER SECOND)
 650 FORMAT (1H ,F6.0,1X,1PE10.3,1X,1PE10.3,3X,1PE10.3,1X,1PE10.3,2X,1P
    1E10.3,1X,1PE10.3,1X,5(1X,1PE10.3))
 700 FORMAT (1H1,47HNO EXECUTION. H/DELTA H IS NOT DIVISIBLE BY 20.)
 800 FORMAT(/1H0)
 850 FORMAT (1H0,52HEXECUTION STOPPED.  DELTA-T COMPUTATION LESS THAN 1
    1.)
 900 FORMAT (1H0,22X,32HRAINFALL IN MILLIMETERS PER HOUR,11X,35HMILLIME
    1TERS OF ACCUMULATED RAINFALL)
 950 FORMAT (1H0,26X,12H 3.6*RR   =   ,1PE12.5,22X,7HAR   =   ,1PE12.5)
1000 FORMAT(/1H0,5HWMAX=,1PE13.5,6X,5HSBAR=,1PE13.5,6X,5HLBAR=,
    11PE13.5,6X,6HDW/DT=,1PE13.5,6X,6HWMEAN=,1PE13.5)
     END
```

Figure E-2i. Continuation of figure E-2a.

E.5. Machine Requirements and Timing

This program is coded in full USASI standard FORTRAN IV and has been run without modification on an IBM 7090, IBM 360/50, and CDC 6400. The core requirements are a 112 K partition on the 360/50 and a 60 K octal partition on the 6400. The running time on the 360/50 is about 30 sec CPU time per 100 steps with every 10th step printed. Required logical unit numbers for input/output files are unit 5, card input; unit 6, printer; unit 8, card-punched output; unit 10, auxiliary print file.

NATIONAL SEVERE STORMS LABORATORY

The NSSL Technical Memoranda, beginning with No. 28, continue the sequence established by the U. S. Weather Bureau National Severe Storms Project, Kansas City, Missouri. Numbers 1-22 were designated NSSP Reports. Numbers 23-27 were NSSL Reports, and 24-27 appeared as subseries of Weather Bureau Technical Notes. These reports are available from the National Technical Information Service, Operations Division, Springfield, Virginia 22151, for $3.00, and a microfiche version for $0.95. NTIS numbers are given below in parentheses.

No. 1 National Severe Storms Project Objectives and Basic Design. Staff, NSSP. March 1961. (PB-168207)

No. 2 The Development of Aircraft Investigations of Squall Lines from 1956-1960. B. B. Goddard. (PB-168208)

No. 3 Instability Lines and Their Environments as Shown by Aircraft Soundings and Quasi-Horizontal Traverses. D. T. Williams. February 1962. (PB-168209)

No. 4 On the Mechanics of the Tornado. J. R. Fulks. February 1962. (PB-168210)

No. 5 A Summary of Field Operations and Data Collection by the National Severe Storms Project in Spring 1961. J. T. Lee. March 1962. (PB-165095)

No. 6 Index to the NSSP Surface Network. T. Fujita. April 1962. (PB-168212)

No. 7 The Vertical Structure of Three Dry Lines as Revealed by Aircraft Traverses. E. L. McGuire. April 1962. (PB-168213)

No. 8 Radar Observations of a Tornado Thunderstorm in Vertical Section. Ralph J. Donaldson, Jr. April 1962. (PB-174859)

No. 9 Dynamics of Severe Convective Storms. Chester W. Newton. July 1962. (PB-163319)

No. 10 Some Measured Characteristics of Severe Storms Turbulence. Roy Steiner and Richard H. Rhyne. July 1962. (N62-16401)

No. 11 A Study of the Kinematic Properties of Certain Small-Scale Systems. D. T. Williams. October 1962. (PB-168216)

No. 12 Analysis of the Severe Weather Factor in Automatic Control of Air Route Traffic. W. Boynton Beckwith. December 1962. (PB-168217)

No. 13 500-Kc./Sec. Sferics Studies in Severe Storms. Douglas A. Kohl and John E. Miller. April 1963. (PB-168218)

No. 14 Field Operations of the National Severe Storms Project in Spring 1962. L. D. Sanders. May 1963. (PB-168219)

No. 15 Penetrations of Thunderstorms by an Aircraft Flying at Supersonic Speeds. G. P. Roys. Radar Photographs and Gust Loads in Three Storms of 1961 Rough Rider. Paul W. J. Schumacher. May 1963. (PB-168220)

No. 16 Analysis of Selected Aircraft Data from NSSP Operations, 1962. T. Fujita. May 1963. (PB-168221)

No. 17 Analysis of Methods for Small-Scale Surface Network Data. D. T. Williams. August 1963. (PB-168222)

No. 18 The Thunderstorm Wake of May 4, 1961. D. T. Williams. August 1963. (PB-168223)

No. 19 Measurements by Aircraft of Condensed Water in Great Plains Thunderstorms. George P. Roys and Edwin Kessler. July 1966. (PB-173048)

No. 20 Field Operations of the National Severe Storms Project in Spring 1963. J. T. Lee, L. D. Sanders and D. T. Williams. January 1964. (PB-168224)

No. 21 On the Motion and Predictability of Convective Systems as Related to the Upper Winds in a Case of Small Turning of Wind with Height. James C. Fankhauser. January 1964. (PB168225)

No. 22 Movement and Development Patterns of Convective Storms and Forecasting the Probability of Storm Passage at a Given Location. Chester W. Newton and James C. Fankhauser. January 1964. (PB-168226)

No. 23 Purposes and Programs of the National Severe Storms Laboratory, Norman, Oklahoma. Edwin Kessler. December 1964. (PB-166675)

No. 24 Papers on Weather Radar, Atmospheric Turbulence, Sferics, and Data Processing. August 1965. (AD-621586)

No. 25 A Comparison of Kinematically Computed Precipitation with Observed Convective Rainfall. James C. Fankhauser. September 1965. (PB-168445).

No. 26 Probing Air Motion by Doppler Analysis of Radar Clear Air Returns. Roger M. Lhermitte. May 1966. (PB-170636)

No. 27 Statistical Properties of Radar Echo Patterns and the Radar Echo Process. Larry Armijo. May 1966. The Role of the Kutta-Joukowski Force in Cloud Systems with Circulation. J. L. Goldman. May 1966. (PB-170756)

No. 28 Movement and Predictablity of Radar Echoes. James Warren Wilson. November 1966. (PB-173972)

No. 29 Notes on Thunderstorm Motions, Heights, and Circulations. T. W. Harrold, W. T. Roach, and Kenneth E. Wilk. November 1966. (AD-644899)

No. 30 Turbulence in Clear Air Near Thunderstorms. Anne Burns, Terence W. Harrold, Jack Burnham, and Clifford S. Spavins. December 1966. (PB-173992)

No. 31 Study of a Left-Moving Thunderstorm of 23 April 1964. George R. Hammond. April 1967. (PB-174681)

No. 32 Thunderstorm Circulations and Turbulence from Aircraft and Radar Data. James C. Fankhauser and J. T. Lee. April 1967. (PB-174860)

No. 33 On the Continuity of Water Substance. Edwin Kessler. April 1967. (PB-175840)

No. 34 Note on the Probing Balloon Motion by Doppler Radar. Roger M. Lhermitte. July 1967. (PB-175930)

No. 35 A Theory for the Determination of Wind and Precipitation Velocities with Doppler Radars. Larry Armijo. August 1967. (PB-176376)

No. 36 A Preliminary Evaluation of the F-100 Rough Rider Turbulence Measurement System. U. O. Lappe. October 1967. (PB-177037)

No. 37 Preliminary Quantitative Analysis of Airborne Weather Radar. Lester P. Merritt. December 1967. (PB-177188)

No. 38 On the Source of Thunderstorm Rotation. Stanley L. Barnes. March 1968. (PB-178990)

No. 39 Thunderstorm - Environment Interactions Revealed by Chaff Trajectories in the Mid-Troposphere. James C. Fankhauser. June 1968. (PB-179659)

No. 40 Objective Detection and Correction of Errors in Radiosonde Data. Rex L. Inman. June 1968. (PB-180284)

No. 41 Structure and Movement of the Severe Thunderstorms of 3 April 1964 as Revealed from Radar and Surface Mesonetwork Data Analysis. Jess Charba and Yoshikazu Sasaki. October 1968. (PB-183310)

No. 42 A Rainfall Rate Sensor. Brian E. Morgan. November 1968. (PB-183979)

No. 43 Detection and Presentation of Severe Thunderstorms by Airborne and Ground-Based Radars: A Comparative Study. Kenneth E. Wilk, John K. Carter, and J. T. Dooley. February 1969. (PB-183572)

No. 44 A Study of a Severe Local Storm of 16 April 1967. George Thomas Haglund. May 1969. (PB-184-970)

No. 45 On the Relationship Between Horizontal Moisture Convergence and Convective Cloud Formation. Horace R. Hudson. March 1970. (PB-191720)

No. 46 Severe Thunderstorm Radar Echo Motion and Related Weather Events Hazardous to Aviation Operations. Peter A. Barclay and Kenneth E. Wilk. June 1970. (PB-192498)

No. 47 Evaluation of Roughness Lengths at the NSSL-WKY Meteorological Tower. Leslie D. Sanders and Allen H. Weber. August 1970. (PB-194587)

No. 48 Behavior of Winds in the Lowest 1500 ft in Central Oklahoma: June 1966 - May 1967. Kenneth C. Crawford and Horace R. Hudson. August 1970.

No. 49 Tornado Incidence Maps. Arnold Court. August 1970. (COM-71-00019)

No. 50 The Meteorologically Instrumented WKY-TV Tower Facility. John K. Carter. September 1970. (COM-71-00108)

No. 51 Papers on Operational Objective Analysis Schemes at the National Severe Storms Forecast Center. Rex L. Inman. November 1970. (COM-71-00136)

No. 52 The Exploration of Certain Features of Tornado Dynamics Using a Laboratory Model. Neil B. Ward. November 1970. (COM-71-00139)

No. 53 Rawinsonde Observation and Processing Techniques at the National Severe Storms Laboratory. Stanley L. Barnes, James H. Henderson and Robert J. Ketchum. April 1971.

GPO 836-576